

UiO : **University of Oslo**

Francesco Patrizi

# **Refinement strategies and linear independence for LR B-splines**

**Thesis submitted for the degree of Philosophiae Doctor**

Department of Mathematics  
Faculty of Mathematics and Natural Sciences

Department of Mathematics and Cybernetics  
SINTEF



**2020**

© **Francesco Patrizi, 2020**

*Series of dissertations submitted to the Faculty of Mathematics and Natural Sciences, University of Oslo*

ISSN ISSN

All rights reserved. No part of this publication may be reproduced or transmitted, in any form or by any means, without permission.

Cover: Hanne Baadsgaard Utigard.

Print production: Representralen, University of Oslo.

*To my family, Cristina and Ercole*



# Preface

This thesis is submitted in partial fulfillment of the requirements for the degree of *Philosophiae Doctor* at the University of Oslo. The research presented here is conducted under the supervision of Professor Arne B. Sletsjøe and Doctors Tor Dokken, Georg Muntingh, Oliver Barrowclough and Heidi E.I. Dahl.

The work presented is connected to the Innovative Training Network ARCADES (Algebraic Representations in Computer-Aided Design for complex Shapes), which is part of the European Union's Horizon 2020 research and innovation programme under the Marie Skłodowska-Curie grant agreement No. 675789. The ARCADES project aims to disrupt the traditional paradigm in Computer-Aided Design (CAD) to build the next generation of CAD software relying on strong foundations from algebraic geometry, differential geometry, scientific computing, and algorithm design.

The thesis is a collection of three papers. The common theme to them is the investigation and deepening of all the aspects needed to efficiently employ the Locally Refined (LR) B-splines in simulations and approximations: from the study of linear independence to the construction of local and adaptive refinement strategies and the analysis of the mesh parametrization problem. The papers are preceded by an introductory chapter that relates them together and provides background information and motivation for the work. The first paper is a joint work with Doctor Tor Dokken. The second paper is a joint work with Professors Carla Manni, Francesca Pelosi and Hendrik Speleers. The last paper is a joint work with Professor Michael S. Floater.



# Acknowledgements

First and foremost, I wish to thank Tor Dokken for his precious guidance, his enthusiasm and his help throughout my PhD studies. Despite his numerous commitments, he was never too busy for talking with me.

A special thanks goes to Georg Muntingh, for his advice and his support during the most difficult times of these three years.

I wish to thank also Oliver Barrowclough and Heidi E.I. Dahl, your doors were always open for discussion.

I am also grateful to Johan S. Seland, Morten Ofstad and Stein Pedersen, for your kindness and patience. You made me feel immediately part of your fantastic team at Bluware inc.

I gratefully acknowledge Michael S. Floater. It has been a pleasure to work together and I hope there will be other occasions to do it again.

I would also like to express my deep gratitude to Carla Manni, Francesca Pelosi and Hendrik Speleers, as you have encouraged and supported me to apply for this PhD position. I have been so lucky in finding kind people like you in my Master's to guide me during my first steps in the academic world. I would not be here if it was not for you.

Last, but absolutely not least, I want to thank my parents and my girlfriend Cristina. You have always believed in me.

## • Francesco Patrizi

Oslo, September 2020



Marie Skłodowska-Curie  
Actions

This thesis was funded by the European Union's Horizon 2020 research and innovation programme under the Marie Skłodowska-Curie grant agreement No. 675789.



# List of Papers

## Paper I

F. Patrizi, and T. Dokken ‘Linear dependence of bivariate Minimal Support and Locally Refined B-splines over LR-meshes’. Accepted for publication on *Computer Aided Geometric Design*.

## Paper II

F. Patrizi, C. Manni, F. Pelosi, and H. Speleers ‘Adaptive refinement with locally linearly independent LR B-splines: Theory and applications’. *Submitted for publication*.

## Paper III

M. S. Floater, and F. Patrizi ‘Transfinite mean value interpolation over polygons’. In press on *Numerical Algorithms*, DOI: 10.1007/s11075-019-00849-w.



# Contents

|   |           |
|---|-----------|
| Preface   | iii       |
| Acknowledgements  | v         |
| List of Papers  | vii       |
| Contents  | ix        |
| <b>1 Introduction</b>   | <b>1</b>  |
| 1.1 Spline spaces . . . . .   | 3         |
| 1.2 Minimal Support and Locally Refined B-splines . . . . .   | 10        |
| 1.3 Generalized barycentric coordinates and mesh parametrization                                      | 22        |
| 1.4 Summary of Papers . . . . .   | 27        |
| References . . . . .  | 28        |
| <b>Papers</b>   | <b>32</b> |
| <b>I Linear dependence of bivariate Minimal Support and Locally Refined B-splines over LR-meshes</b>  | <b>33</b> |
| I.1 Introduction . . . . .  | 33        |
| I.2 Box-partitions and LR-meshes . . . . .  | 36        |
| I.3 Spline spaces . . . . .   | 39        |
| I.4 Univariate B-splines and bivariate B-splines . . . . .  | 42        |
| I.5 Minimal Support B-splines and Locally Refined B-splines .   | 44        |
| I.6 Hand-in-hand principle . . . . .  | 46        |
| I.7 Characterization of linear dependence in $\mathcal{B}^{MS}(\mathcal{N})$ . . . . .                | 48        |
| I.8 Minimal number of LR B-splines for a linear dependence relation . . . . .                         | 60        |
| I.9 Improvement of the Peeling Algorithm . . . . .  | 65        |
| I.10 Conclusions, conjectures and future work . . . . .   | 66        |
| References . . . . .  | 67        |
| <b>II Adaptive refinement with locally linearly independent LR B-splines: Theory and applications</b> | <b>69</b> |
| II.1 Introduction . . . . .   | 69        |
| II.2 Locally refined B-splines . . . . .  | 71        |
| II.3 $N_2S$ structured mesh refinement strategy . . . . .   | 78        |
| II.4 Application I: Quasi-interpolation . . . . .   | 85        |
| II.5 Application II: Isogeometric analysis . . . . .  | 89        |
| II.6 Conclusion . . . . .   | 91        |

## Contents

---

|   |            |
|---|------------|
| References . . . . .  | 92         |
| <b>III Transfinite mean value interpolation over polygons</b> | <b>95</b>  |
| III.1 Introduction . . . . .                                  | 95         |
| III.2 Definitions . . . . .                                   | 96         |
| III.3 Interpolation on an edge . . . . .                      | 97         |
| III.4 Interpolation at a vertex . . . . .                     | 99         |
| III.5 Numerical examples . . . . .                            | 101        |
| References . . . . .  | 104        |
| <b>Appendices</b>   | <b>105</b> |
| <b>A Dimension of the spline spaces</b>                       | <b>107</b> |
| References . . . . .  | 112        |
| <b>B B-splines</b>  | <b>113</b> |
| References . . . . .  | 117        |

# Chapter 1

## Introduction

Since the '70s, curves and surfaces in engineering have been usually expressed by means of Computer Aided Design (CAD) technologies, such as B-splines and Non-Uniform Rational B-splines (NURBS). These have numerous properties that allow to easily control and modify the geometries they describe:

- positivity,
- local supports,
- piecewise (rational) polynomials,
- partition of unity and convex hull property.

These properties make B-splines and NURBS useful tools to engineer objects with complex shapes. Furthermore, the introduction of Isogeometric Analysis (IgA) [19] has integrated such technologies into the Finite Element Analysis (FEA) as well, unifying the geometric description of the problem with its numerical resolution, in order to expedite the simulation process and gaining in accuracy. In addition to the properties listed above, B-splines and NURBS feature other qualities appreciated in this context, such as (local) linear independence and high global smoothness.

Nevertheless, the constantly increasing demand for higher precision in simulations and reverse engineering processes requires the possibility to refine only where large variations occur, in order to reduce the approximation error while retaining feasible computational costs. In order to achieve this adaptivity, new formulations of B-splines and NURBS have been established [3, 6, 7, 9, 15, 16, 31]. These new classes of functions are defined on locally refined meshes, in which T-vertices in the interior of the domain are allowed, as opposed to classical B-splines and NURBS for which tensor meshes, with no internal T-vertices, are required.

Locally Refined B-splines, or in short LR B-splines [7], are one of these new formulations, and their definition is inspired by the knot insertion refinement process of B-splines. These latter are defined on global knot sequences, one per direction. In 2D, the insertion of a new knot in a knot sequence corresponds to a line segment in the mesh crossing the entire domain. This refines all the B-splines whose supports are crossed by the inserted segment. Instead, LR B-splines are defined on local knot vectors and the insertion of a new knot is always performed with respect to a particular LR B-spline. This means that in addition to the knot, one also decides which LR B-spline supports the corresponding line segment in the mesh is traversing, i.e., which LR B-splines have to be refined by the knot insertion. As a consequence, the LR B-spline definition is consistent with

## 1. Introduction

---

the B-spline definition when the underlying mesh at the end of the process is a tensor mesh, and the formulation of LR B-splines remains broadly similar to the standard B-splines even though they address local refinements. This makes them one of the most elegant extensions to achieve the adaptivity of the mesh and worthy of investigation.

LR B-splines satisfy the same properties of classical B-splines except the local linear independence for which a particular structure of the mesh is required. Even though such a characterization for the local linear independence of the LR B-splines in terms of meshing constraints is provided in [2], an adaptive refinement strategy to produce meshes with this structure was missing in the literature. To the best of my knowledge, the only mesh construction that leads to a locally linearly independent collection of LR B-splines is proposed in [2] as well. However, such a process cannot be recorded as an adaptive refinement because the regions to be refined and the maximal resolution, i.e., the sizes of the smallest cells in the domain induced by the mesh, have to be chosen a priori. The purpose of Paper 2 is to describe the first fully adaptive refinement ensuring the local linear independence of the LR B-splines. Such a property allows, *inter alia*, to design efficient quasi-interpolation schemes and to bound the band-width in the matrices produced by the numerical discretization of PDEs.

More generally, the set of LR B-splines can even be linearly dependent if no assumptions on the locally refined mesh are established. Although linear dependence is not a major issue for geometric design, it constitutes a difficulty when performing simulations in the IgA context, as it requires the resolution of singular linear systems to assemble the numerical approximation. As of today, there is no known characterization of the linear independence for LR B-splines. Paper 1 starts this analysis by looking at geometric necessary conditions for the mesh to have a linear dependence relation among the LR B-splines. In particular, it relates the linear dependence to the position of the T-vertices in the mesh and to the LR B-spline support inclusions. These observations allow also the computation of the minimal number of LR B-splines that can form a linear dependence relation. Such a lower bound (8 functions) turns out to be independent of the polynomial bidegree used to define the LR B-splines and it is sharp, as shown by the examples contained in the paper where a linear dependence relation with exactly 8 LR B-splines is provided for any bidegree  $(p_1, p_2) \neq (0, 0), (1, 0), (0, 1), (1, 1)$ .

For some applications, e.g., reservoir modeling and biomedical engineering, the geometry of the problem is not directly established within the CAD system but it has to be modeled from the scanning of a physical object. A fundamental step to generate a spline surface approximation of the acquired data is what is called mesh parametrization. This establishes a bijective map between a triangular surface, which represents a first approximation of the data, and a parameter domain. Mesh parametrizations almost always introduce distortions in either the angles or the areas, which affect the quality of the final spline surface approximation. Therefore, it is crucial to define mesh parametrizations as similar as possible to isometries in order to reduce such distortions. For piecewise linear surfaces, such as the triangular surfaces, a strategy that has proved to be

efficient for this purpose consists of expressing the image of the interior vertices of the triangulation in terms of the images of the surrounding vertices using generalized barycentric coordinates. In particular, the mean value coordinates turned out to be a successful and popular choice thanks to their simple and closed formula and the smoothness of the resulting mesh parametrization.

Generalized barycentric coordinates allow the construction of smooth functions that interpolate piecewise linear continuous data prescribed at the boundary of a polygon. One can then consider the more general problem of finding a smooth function that interpolates the value of any given continuous function at the boundary of a closed domain. The mean value coordinates have been extended to a transfinite mean value interpolant to address this problem in [8]. However, a proof of interpolation is provided in [8] only under strong conditions on the shape of the boundary, which exclude polygonal domains. Paper 3 provides an alternative proof for these cases that relies on the continuity of the given data.

The remainder of this Chapter yields the background knowledge to understand the content of the papers. The LR B-splines are elements of spline spaces, that is, spaces of piecewise polynomials of some bidegree defined on a partition in boxes of a rectangular domain with prescribed continuity constraints on the line segments forming the mesh. Section 1.1 defines these spaces and studies the stability of their dimension formula. Section 1.2 introduces the notion of Minimal Support B-splines, or in short MS B-splines, and LR B-splines. As one can guess from their name, MS B-splines are the B-splines with minimal support, i.e., without superfluous line segments crossing their support, identifiable on the locally refined mesh. The LR B-splines are a subset of the MS B-splines. The difference between the two is that the latter are not always the result of a knot insertion. For a given bidegree, they depend only on the mutual position of the line segments in the mesh. We then explain under which conditions the MS and LR B-spline sets form a basis of the spline space. Moreover, Section 1.2 introduces the linear dependence problem for the LR B-splines, illustrates the current tools used to detect and solve it in most configurations and explains the motivation for Paper 1. Furthermore, the local linear independence is characterized at the end of the section and the motivation for Paper 2 is provided. Finally, Section 1.3 briefly describes a procedure to define mesh parametrizations by using generalized barycentric coordinates. Then it recalls the mean value coordinates, their numerous properties, shows their extension to transfinite interpolation and the motivation for Paper 3.

The Chapter terminates with a Summary of Papers, which constitutes a more technical description of the results achieved in each of the papers.

## 1.1 Spline spaces

In this section we define the univariate spline space over a knot sequence and the bivariate spline space over an arbitrary axis-aligned partition of a rectangular domain in  $\mathbb{R}^2$ , with given polynomial degrees and continuity constraints. In

particular we provide the dimension formula for such spaces. The formula for the bivariate space can be divided into two parts. One part is a combinatorial term that only depends on the topological structure of the partition, polynomial bidegree and continuity constraints. The second part is an alternating sum of dimensions of homological terms. Such terms make the dimension of the spline space unstable, that is, dependent also on the size of the partition elements [22]. Therefore, we present sufficient conditions to nullify such homological terms in order to reduce the computation of the dimension to a combinatorial counting.

### 1.1.1 Univariate spline space

**Definition 1.1.1.** Given an increasing sequence  $\boldsymbol{\tau} = (\tau_1, \dots, \tau_n)$  of real numbers, a positive integer  $p$  and a function  $\mu : \boldsymbol{\tau} \rightarrow \mathbb{N}$  such that  $1 \leq \mu(\tau_i) \leq p + 1$  for all  $i$ , we define the corresponding **spline sequence** as the triple  $\boldsymbol{\tau}_p^\mu = (\boldsymbol{\tau}, \mu, p)$ .

Given a spline sequence  $\boldsymbol{\tau}_p^\mu$ , we say that  $\tau_i \in \boldsymbol{\tau}$  has **full multiplicity** if  $\mu(\tau_i) = p + 1$  and we say that  $\boldsymbol{\tau}_p^\mu$  is **open** if  $\tau_1$  and  $\tau_n$  have full multiplicity.

Sometimes it is more convenient to write a spline sequence, in the equivalent way, as the pair  $\mathbf{t}_p = (\mathbf{t}, p)$  where  $\mathbf{t}$  is a non-decreasing sequence  $\mathbf{t} = (t_1, \dots, t_\ell)$  with  $\ell = \sum_{i=1}^n \mu(\tau_i)$  and

$$\underbrace{t_1 = \dots = t_{\mu(\tau_1)}}_{=\tau_1} < \underbrace{t_{\mu(\tau_1)+1} = \dots = t_{\mu(\tau_1)+\mu(\tau_2)}}_{=\tau_2} < \dots$$

We use bold Greek letters with the multiplicity function in superscript in the first way of expression and bold Latin letters for the second way.

Given a degree  $p$ , we denote as  $\Pi_p \subset \mathbb{R}[t]$  the vector space spanned by the monomials  $t^j$  such that  $0 \leq j \leq p$ .

**Definition 1.1.2.** Given a spline sequence  $\boldsymbol{\tau}_p^\mu = (\boldsymbol{\tau}, \mu, p)$  with  $\boldsymbol{\tau} = (\tau_1, \dots, \tau_n)$ , we define the **univariate spline space** on  $\boldsymbol{\tau}_p^\mu$ , denoted  $\mathbb{S}(\boldsymbol{\tau}_p^\mu)$  or equivalently  $\mathbb{S}(\mathbf{t}_p)$ , as the set of all functions  $f : \mathbb{R} \rightarrow \mathbb{R}$  such that

1.  $f$  is zero outside  $[\tau_1, \tau_n]$ ,
2. the restrictions of  $f$  to the intervals  $[\tau_i, \tau_{i+1})$  for  $1 \leq i < n-1$  and  $[\tau_{n-1}, \tau_n]$  are polynomials in  $\Pi_p$ ,
3.  $f$  is  $C^{p-\mu(\tau_i)}$ -continuous at  $\tau_i$ .

**Theorem 1.1.3** ([30, Theorem 4.4]). *Given a spline sequence  $\boldsymbol{\tau}_p^\mu$ , the corresponding spline space  $\mathbb{S}(\boldsymbol{\tau}_p^\mu)$  has dimension*

$$\dim \mathbb{S}(\boldsymbol{\tau}_p^\mu) = \max \left\{ \left( \sum_{i=1}^n \mu(\tau_i) \right) - (p + 1), 0 \right\}. \quad (1.1)$$

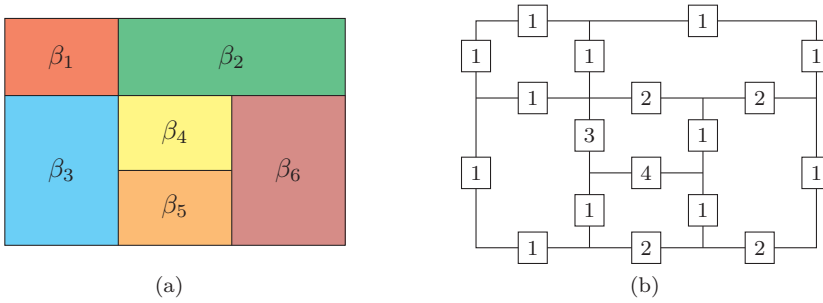


Figure 1.1: Example of box-partition and corresponding mesh.

### 1.1.2 Spline space over a box-partition

**Definition 1.1.4.** Given an axis-aligned rectangle  $\Omega \subseteq \mathbb{R}^2$ , a **box-partition** of  $\Omega$  is a finite collection  $\mathcal{E}$  of axis-aligned rectangles in  $\Omega$  such that:

1.  $\beta_1 \cap \beta_2 = \emptyset$  for any  $\beta_1, \beta_2 \in \mathcal{E}$ , with  $\beta_1 \neq \beta_2$ .
2.  $\bigcup_{\beta \in \mathcal{E}} \beta = \Omega$ .

**Definition 1.1.5.** Given a box partition  $\mathcal{E}$ , we define the **vertices** of  $\mathcal{E}$  as the vertices of its elements. In particular, a vertex of  $\mathcal{E}$  is called a **T-vertex** if it is the intersection of edges of three elements. We call  $\mathcal{V}$  the **set of vertices** of  $\mathcal{E}$ .

**Definition 1.1.6.** Given a box-partition  $\mathcal{E}$  of a rectangle  $\Omega \in \mathbb{R}^2$ , a **meshline** of  $\mathcal{E}$  is a segment contained in an edge of an element  $\mathcal{E}$ , connecting two, and only two, vertices of  $\mathcal{V}$  at its end-points. The collection of all the meshlines of the box-partition is called the **mesh**,  $\mathcal{M}$ .

We further define a multiplicity function  $\mu : \mathcal{M} \rightarrow \mathbb{N}^*$  that associates a positive integer to every meshline, called the **multiplicity** of the meshline.

When the T-vertices of  $\mathcal{E}$  occur only on  $\partial\Omega$  and all collinear meshlines have the same multiplicity, the corresponding mesh is called a **tensor mesh**.

Finally, if all the meshlines of a box-partition  $\mathcal{E}$  have the same multiplicity  $m$  we say that the corresponding mesh  $\mathcal{M}$  has multiplicity  $m$ .

Figure 1.1 shows an example of (a) a box-partition  $\mathcal{E}$  and (b) a corresponding mesh  $\mathcal{M}$ . The meshlines are identified by squares reporting the associated multiplicities.

A meshline can be expressed as the Cartesian product of a point in  $\mathbb{R}$  and a finite interval. Let  $a \in \mathbb{R}$  be the value of such a point and let  $k \in \{1, 2\}$  be its position in the Cartesian product. If  $k = 1$  the meshline is vertical and if  $k = 2$  the meshline is horizontal. We sometimes write  $k$ -meshline to specify the direction of the meshline and  $(k, a)$ -meshline to specify on exactly what axis-parallel line in  $\mathbb{R}^2$  the meshline lies.

## 1. Introduction

---

**Definition 1.1.7.** A **spline mesh** in  $\mathbb{R}^2$  is a triple  $\mathcal{N} = (\mathcal{M}, \mu, \mathbf{p})$  where  $\mathcal{M}$  is a mesh from a box-partition  $\mathcal{E}$ ,  $\mathbf{p} = (p_1, p_2)$  is a pair of positive integers and  $\mu : \mathcal{M} \rightarrow \mathbb{N}$  is a multiplicity function such that  $1 \leq \mu(\gamma) \leq p_k + 1$  for every  $k$ -meshline  $\gamma \in \mathcal{M}$ . In particular, if a  $k$ -meshline  $\gamma$  has multiplicity  $p_k + 1$  we say that  $\gamma$  has **full multiplicity**. A spline mesh  $\mathcal{N}$  is **open** if every boundary meshline has full multiplicity. A spline mesh  $\mathcal{N} = (\mathcal{M}, \mu, \mathbf{p})$  is called a **tensor spline mesh** if  $\mathcal{M}$  is a tensor mesh.

*Remark 1.1.8.*  $\mathcal{N} = (\mathcal{M}, \mu, \mathbf{p})$  is a tensor spline mesh if and only if there exist two spline sequences  $\boldsymbol{\tau}_{1,p_1}^{\mu_1}, \boldsymbol{\tau}_{2,p_2}^{\mu_2}$  such that every  $k$ -meshline  $\gamma$  in  $\mathcal{M}$  is a  $(k, \tau_i)$ -meshline for some  $\tau_i \in \boldsymbol{\tau}_k$  and  $\mu(\gamma) = \mu_k(\tau_i)$ . Therefore, we sometimes write  $\mathcal{N}[\boldsymbol{\tau}_{1,p_1}^{\mu_1}, \boldsymbol{\tau}_{2,p_2}^{\mu_2}] = (\mathcal{M}[\boldsymbol{\tau}_{1,p_1}^{\mu_1}, \boldsymbol{\tau}_{2,p_2}^{\mu_2}], \mu[\boldsymbol{\tau}_{1,p_1}^{\mu_1}, \boldsymbol{\tau}_{2,p_2}^{\mu_2}], \mathbf{p})$  to specify from what spline sequences the tensor spline mesh  $\mathcal{N}$  can be generated from.

Given a bidegree  $\mathbf{p} = (p_1, p_2)$ , we denote as  $\Pi_{\mathbf{p}} \subset \mathbb{R}[x, y]$  the vector space spanned by the monomials  $x^{i_1}y^{i_2}$  such that  $0 \leq i_k \leq p_k$  for  $k = 1, 2$ .

**Definition 1.1.9.** Given a spline mesh  $\mathcal{N} = (\mathcal{M}, \mu, \mathbf{p})$  corresponding to a box-partition  $\mathcal{E}$  of a rectangle  $\Omega = [a_1, b_1] \times [a_2, b_2]$ , for any element  $\beta \in \mathcal{E}$ ,  $\beta = J_1 \times J_2$  with  $J_k = [a_{\beta,k}, b_{\beta,k}]$ , we set

$$\tilde{\beta} = \tilde{J}_1 \times \tilde{J}_2 \text{ with } \tilde{J}_k = \begin{cases} [a_{\beta,k}, b_{\beta,k}) & \text{if } b_{\beta,k} < b_k \\ [a_{\beta,k}, b_{\beta,k}] & \text{if } b_{\beta,k} = b_k. \end{cases} \quad (1.2)$$

The **spline space on  $\mathcal{N}$** , denoted by  $\mathbb{S}(\mathcal{N})$ , is the set of all functions  $f : \mathbb{R}^2 \rightarrow \mathbb{R}$  such that

1.  $f$  is zero outside  $\Omega$ ,
2. for each element  $\beta \in \mathcal{E}$ , the restriction of  $f$  to  $\tilde{\beta}$  is a bivariate polynomial function in  $\Pi_{\mathbf{p}}$ ,
3. for each  $k$ -meshline  $\gamma \in \mathcal{M}$ ,  $f \in C^{p_k - \mu(\gamma)}$ -continuous across  $\gamma$ .

Before stating the dimension formula of the spline space, we formalize the mesh refinement, that is, we describe how a mesh changes when new segments are inserted.

**Definition 1.1.10.** Given a box-partition  $\mathcal{E}$  and an axis-aligned segment  $\gamma$ , we say that  $\gamma$  **traverses**  $\beta \in \mathcal{E}$  if  $\gamma \subseteq \beta$  and the interior of  $\beta$  is divided into two parts by  $\gamma$ , i.e.,  $\beta \setminus \gamma$  is not connected.

A **split** is a finite union of contiguous and collinear axis-aligned segments  $\gamma = \cup_i \gamma_i$  such that every  $\gamma_i$  either is a meshline of the box-partition or  $\gamma_i$  traverses some  $\beta \in \mathcal{E}$ .

We say that a spline mesh  $\mathcal{N} = (\mathcal{M}, \mu, \mathbf{p})$  has **constant splits** if any split  $\gamma$  in  $\mathcal{M}$  is made of meshlines of the same multiplicity.

In this work we consider only spline meshes with constant splits.

As for meshlines, we sometimes write  $k$ -split with  $k \in \{1, 2\}$  to specify the direction of the split or  $(k, a)$ -split to specify on what axis-parallel line the split lies.

When a split  $\gamma$  is inserted in a box-partition  $\mathcal{E}$ , any traversed  $\beta \in \mathcal{E}$  is replaced by the two subrectangles  $\beta_1, \beta_2$  given by the closures of the connected components of  $\beta \setminus \gamma$ . The resulting new box-partition is indicated as  $\mathcal{E} + \gamma$  and its corresponding mesh as  $\mathcal{M} + \gamma$ . Assigning a positive integer  $\mu_\gamma$  to  $\gamma$ , the multiplicities of the meshlines in  $\mathcal{M} \cap (\mathcal{M} + \gamma)$  not contained in  $\gamma$  are unchanged, while the multiplicities of those that are in  $\gamma$  are increased by  $\mu_\gamma$ . The new meshlines contained in  $(\mathcal{M} + \gamma) \setminus \mathcal{M}$  have multiplicity equal to  $\mu_\gamma$ . If  $\mu$  was the multiplicity function associated to  $\mathcal{M}$ , the multiplicity function on the refined mesh  $\mathcal{M} + \gamma$  is denoted as  $\mu + \mu_\gamma$ .

The spline meshes used in applications are often the result of a mesh refinement process. That is, given an initial coarse tensor spline mesh  $\mathcal{N}_0$  and a sequence of splits  $\gamma_i$  with associated integers  $\mu_{\gamma_i}$  for  $i = 1, \dots, N - 1$ , the spline mesh considered is the final entry of a sequence of spline meshes of the form  $\mathcal{N}_i = \mathcal{N}_{i-1} + \gamma_i$  where  $\mathcal{N}_{i-1} + \gamma_i = (\mathcal{M}_i + \gamma_i, \mu_{i-1} + \mu_{\gamma_i}, \mathbf{p})$ . However, not every mesh is obtained in this way. For example, there is no sequence of splits that can generate the mesh depicted in Figure 1.2 from the tensor mesh equal to the domain boundary.

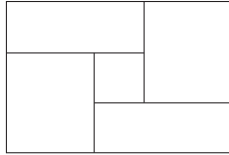


Figure 1.2: A mesh that cannot be obtained by a mesh refinement process.

In this introduction we will provide the dimension formula only for those spline space that can be built through a mesh refinement process. In Appendix A we treat the more general case. We also assume some conditions on the splits inserted during the process. The next definitions introduce the notations needed for these conditions.

**Definition 1.1.11.** Given a mesh  $\mathcal{M}$  corresponding to a box-partition  $\mathcal{E}$ , for any vertex  $\mathbf{v}$  of  $\mathcal{E}$  we define

$$\begin{aligned} \mu_1(\mathbf{v}) &= \max\{\mu(\gamma) : \mathbf{v} \in \gamma \text{ and } \gamma \text{ 1-meshline of } \mathcal{M}\} \\ \mu_2(\mathbf{v}) &= \max\{\mu(\gamma) : \mathbf{v} \in \gamma \text{ and } \gamma \text{ 2-meshline of } \mathcal{M}\} \end{aligned}$$

$\mu_1(\mathbf{v})$  is called **vertical multiplicity** and  $\mu_2(\mathbf{v})$  **horizontal multiplicity** of vertex  $\mathbf{v}$ .

Note that for meshes with constant splits, each maximum in Definition 1.1.11 is taken over identical multiplicities.

**Example 1.1.12.** Figure 1.3 shows an example of the computation of horizontal and vertical multiplicities for two vertices of a box-partition. The meshlines

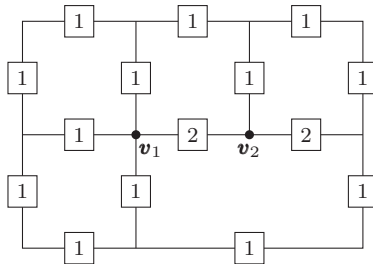


Figure 1.3: Example of the computation of vertical and horizontal multiplicities.

on the left and right hand side of  $\mathbf{v}_1$  have multiplicity 1 and 2 respectively. So  $\mu_2(\mathbf{v}_1) = \max\{1, 2\} = 2$ . The meshlines above and below  $\mathbf{v}_1$  have both multiplicity 1, so that  $\mu_1(\mathbf{v}_1) = 1$ . Concerning  $\mathbf{v}_2$ , we have  $\mu_2(\mathbf{v}_2) = 2$ , whereas  $\mu_1(\mathbf{v}_2) = \max\{1\} = 1$  since there is no meshline below  $\mathbf{v}_2$ .

**Definition 1.1.13.** Given a  $(k, a)$ -split  $\gamma$  in a spline mesh  $\mathcal{N} = (\mathcal{M}, \mu, \mathbf{p})$ , all the vertices where  $\gamma$  intersects meshlines of  $\mathcal{M}$  have  $k$ th coordinate equal to  $a$  and different  $(3 - k)$ th coordinate. We define the **spline sequence on  $\gamma$**  as  $\boldsymbol{\tau}_{p_{3-k}}^{\mu_{3-k}}$ , where the elements of  $\boldsymbol{\tau}$  are given by such  $(3 - k)$ th coordinates and the multiplicity function of this spline sequence is the  $\mu_{3-k}$  multiplicity function of the corresponding vertices.

**Definition 1.1.14.** When a spline mesh  $\mathcal{N} = (\mathcal{M}, \mu, \mathbf{p})$  is refined by inserting a  $k$ -split  $\gamma$ , we define the **expanded spline sequence on  $\gamma$** ,  $\boldsymbol{\tau}_{p_{3-k}}^{\mu_{3-k}}$ , as the spline sequence on  $\gamma$ ,  $\boldsymbol{\tau}_{p_{3-k}}^{\mu_{3-k}}$ , as split of  $\mathcal{N} + \gamma := (\mathcal{M} + \gamma, \mu + \mu_\gamma, \mathbf{p})$ , except that, in case  $\gamma$  is an extension of a split of  $\mathcal{M}$ , the point in  $\boldsymbol{\tau}$  corresponding to the joint vertex has full multiplicity.

As an example, when  $\gamma$  is an extension of two splits of  $\mathcal{M}$ , i.e., it connects them, then the expanded spline sequence on  $\gamma$  is open, that is,  $\tau_1$  and  $\tau_n$  have both full multiplicity.

The dimension formula for the spline space is presented in [28] and consists of two parts. The first part is a combinatorial counting, easy and direct to compute by looking at the topology of the mesh, meshline multiplicities and bidegree. The second part is a sum of homology terms. This is harder to calculate and the value can depend not only on the topology of the mesh but also on its geometrical representation [22]. This means that the spline dimension is unstable under slight changes of the size of the box-partition elements. As a consequence, spline spaces on meshes with the same topological structure, the same meshline multiplicities and the same bidegree, might have different dimension. An example is shown in Figure 1.4. We consider two open spline meshes with  $\mathbf{p} = (2, 2)$ , meshes as in Figure 1.4(a) and Figure 1.4(b) with interior meshlines of multiplicity 1. One can show that the combinatorial part of the spline dimension formula is equal to 36 in both cases, while the homological part is equal to 1 in (a) and 0 in (b). Therefore the corresponding spline space has dimension 37 in (a) and 36 in (b).

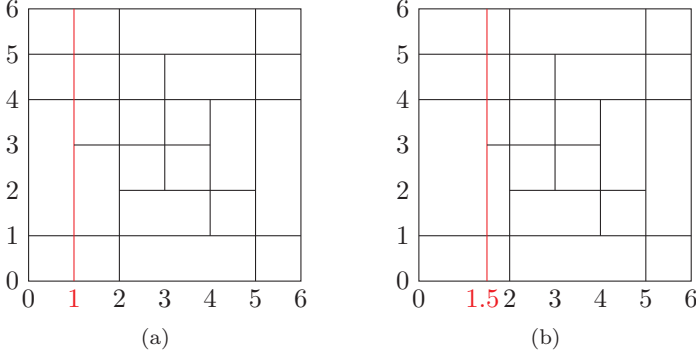


Figure 1.4: Two meshes with same topology and different geometry.

However, if we restrict our attention to a spline mesh  $\mathcal{N}$  resulting from mesh refinement process,  $\mathcal{N} = \mathcal{N}_N$  for some  $N \in \mathbb{N}$ , such that

- **LR-rule 1:** The spline space  $\mathbb{S}(\mathcal{N}_0)$  over the initial tensor spline mesh  $\mathcal{N}_0$  is nontrivial, i.e.,  $\mathbb{S}(\mathcal{N}_0) \neq \{0\}$ ,
- **LR-rule 2:** The spline space  $\mathbb{S}(\tau_{p_{3-k}}^{\tilde{\mu}_{3-k}})$  over the expanded spline sequence  $\tau_{p_{3-k}}^{\tilde{\mu}_{3-k}}$  on any  $k$ -split inserted during the refinement process is nontrivial,

then the spline space  $\mathbb{S}(\mathcal{N})$  defined on the spline mesh  $\mathcal{N} = (\mathcal{M}, \mu, \mathbf{p})$ , corresponding to a box-partition  $\mathcal{E}$ , has dimension given by the following combinatoric counting:

$$\begin{aligned} \dim \mathbb{S}(\mathcal{N}) &= \sum_{\mathbf{q} \in \mathcal{V}} [(p_1 - \mu_1(\mathbf{q}) + 1)(p_2 - \mu_2(\mathbf{q}) + 1)] \\ &\quad - (p_2 + 1) \sum_{\gamma \in \mathcal{M}^1} (p_1 - \mu(\gamma) + 1) - (p_1 + 1) \sum_{\gamma \in \mathcal{M}^2} (p_2 - \mu(\gamma) + 1) \\ &\quad + |\mathcal{E}|(p_1 + 1)(p_2 + 1), \end{aligned} \tag{1.3}$$

where  $|\mathcal{E}|$  is the cardinality of  $\mathcal{E}$ ,  $\mu_1, \mu_2$  are respectively the vertical and horizontal multiplicities of the box-partition vertices and  $\mathcal{M}^1, \mathcal{M}^2 \subset \mathcal{M}$  are the collections of 1-meshlines and 2-meshlines in  $\mathcal{M}$ .

We will always assume the LR-rules when performing a mesh refinement process. Note that the LR-rule 2 is not verified in the mesh refinement process that leads to the meshes in Figure 1.4 and, as a consequence, the dimension of the corresponding spline space is unstable. A more deep analysis of the spline space dimension can be found in Appendix A.

The next Theorem 1.1.15 is called **dimension increasing formula** and it describes the consequential increase in the spline space dimension due to a mesh refinement. It relates the dimension of the refined spline space to the dimensions

## 1. Introduction

---

of the old spline space and of the univariate spline space on the expanded spline sequence on the split inserted. This result can be proved from the dimension formula (1.3) by looking at the local change in the topology when a split is inserted in a mesh.

**Theorem 1.1.15** ([7, Theorem 5.5]). *When a spline mesh  $\mathcal{N} = (\mathcal{M}, \mu, \mathbf{p})$  is refined by inserting a  $k$ -split  $\gamma$ , the dimension of the spline space on the resulting new spline mesh  $\mathcal{N} + \gamma$  is given by*

$$\dim \mathbb{S}(\mathcal{N} + \gamma) = \dim \mathbb{S}(\mathcal{N}) + \dim \mathbb{S}(\boldsymbol{\tau}_{p_3-k}^{\tilde{\mu}_{3-k}}), \quad (1.4)$$

where  $\boldsymbol{\tau}_{p_3-k}^{\tilde{\mu}_{3-k}}$  is the expanded spline sequence on  $\gamma$ .

We rather use the dimension increasing formula to compute the spline space dimension when the underlying mesh can be built through a mesh refinement process from a coarse tensor mesh.

## 1.2 Minimal Support and Locally Refined B-splines

In this section we define the bivariate Minimal Support B-splines, or in short MS B-splines, and their subcollection of Locally Refined B-splines, or in short LR B-splines. The former can be defined on any spline mesh, as their definition depends on the topological structure of the box-partition, bidegree and meshline multiplicities. The latter can be defined only on spline meshes that are the result of a mesh refinement process, as they are generated while performing such a mesh refinement process, by means of the so-called knot insertion procedure.

Both the definitions are generalizations of the concept of bivariate B-splines. Univariate and bivariate B-splines, their basic properties and the knot insertion procedure are briefly recalled in Appendix B. We denote the bivariate B-spline defined on the knot vectors  $\mathbf{x} = (x_1, \dots, x_{p_1+2})$  and  $\mathbf{y} = (y_1, \dots, y_{p_2+2})$  as  $B[\mathbf{x}, \mathbf{y}]$ . The bidegree of  $B[\mathbf{x}, \mathbf{y}]$  is  $\mathbf{p} = (p_1, p_2)$  and it is implicitly expressed by the number of entries in  $\mathbf{x}$  and  $\mathbf{y}$ . Given a bivariate B-spline  $B[\mathbf{x}, \mathbf{y}]$ , its knot vectors  $\mathbf{x}$  and  $\mathbf{y}$  identify a tensor spline mesh  $\mathcal{N}[\mathbf{x}, \mathbf{y}] = (\mathcal{M}[\mathbf{x}, \mathbf{y}], \mu[\mathbf{x}, \mathbf{y}], \mathbf{p})$  in  $\text{supp } B[\mathbf{x}, \mathbf{y}]$ . In fact, let  $x_{i_1}, \dots, x_{i_r}$  and  $y_{j_1}, \dots, y_{j_s}$  be the distinct knots in  $\mathbf{x}$  and  $\mathbf{y}$ , respectively. Any knot  $x_{i_\ell}$  defines a 1-split of  $\mathcal{M}[\mathbf{x}, \mathbf{y}]$  as

$$\gamma = \bigcup_{n=1}^s \gamma_n \quad \text{with } \gamma_n = \{x_{i_\ell}\} \times [y_{j_n}, y_{j_{n+1}}] \quad (1.5)$$

where the multiplicities  $\mu[\mathbf{x}, \mathbf{y}](\gamma_n)$  are equal to the multiplicity of  $x_{i_\ell}$  in  $\mathbf{x}$ , for all  $n = 1, \dots, s$ . In the same way, the knots  $y_{j_\ell}$ , for  $\ell = 1, \dots, s$ , define the 2-splits in  $\mathcal{M}[\mathbf{x}, \mathbf{y}]$  and the multiplicities assigned to the 2-meshlines.

**Definition 1.2.1.** Given a spline mesh  $\mathcal{N} = (\mathcal{M}, \mu, \mathbf{p})$  and a B-spline  $B[\mathbf{x}, \mathbf{y}]$  of bidegree  $\mathbf{p}$ , we say that  $B[\mathbf{x}, \mathbf{y}]$  **has support on**  $\mathcal{N}$  if the meshlines in  $\mathcal{M}[\mathbf{x}, \mathbf{y}]$  can be obtained as unions of meshlines in  $\mathcal{M}$ , and their multiplicities are less than or equal to the multiplicities of the corresponding meshlines in  $\mathcal{M}$ .

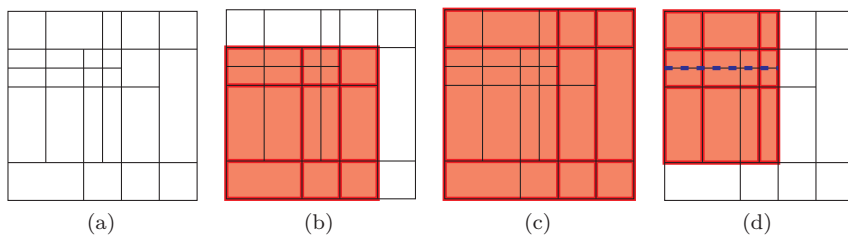


Figure 1.5: Support of B-splines of bidegree  $(2, 2)$  on a spline mesh  $\mathcal{N} = (\mathcal{M}, 1, (2, 2))$ . The mesh  $\mathcal{M}$  is shown in (a). The B-splines whose supports are depicted in (b) and (c) have minimal support on  $\mathcal{M}$ . The tensor meshes defined by their knots in their supports are highlighted with thicker lines. On the other hand, the B-spline in (d) does not have minimal support on  $\mathcal{N}$ : the split highlighted by the dashed line disconnects the support.

**Definition 1.2.2.** Given a spline mesh  $\mathcal{N} = (\mathcal{M}, \mu, \mathbf{p})$ , a B-spline  $B[\mathbf{x}, \mathbf{y}]$  of bidegree  $\mathbf{p}$  with support on  $\mathcal{N}$  and a split  $\gamma \subseteq \mathcal{M}$ , we say that  $\gamma$  **traverses**  $B[\mathbf{x}, \mathbf{y}]$  if the interior of  $\text{supp } B[\mathbf{x}, \mathbf{y}]$  is divided into two parts by  $\gamma$ , i.e.,  $\text{supp } B[\mathbf{x}, \mathbf{y}] \setminus \gamma$  is not connected and either  $\gamma$  is in  $\mathcal{M} \setminus \mathcal{M}[\mathbf{x}, \mathbf{y}]$  or  $\gamma \subseteq \mathcal{M}[\mathbf{x}, \mathbf{y}]$  but the multiplicities of its meshlines are higher in  $\mathcal{N}$  than in  $\mathcal{N}[\mathbf{x}, \mathbf{y}]$ . Then a B-spline  $B[\mathbf{x}, \mathbf{y}]$  is said to have **minimal support on  $\mathcal{N}$**  if it has support on  $\mathcal{N}$  and there is no split  $\gamma$  in  $\mathcal{M}$  traversing  $B[\mathbf{x}, \mathbf{y}]$ . The collection of all the minimal support B-splines, or MS B-splines, on  $\mathcal{N}$  is denoted by  $\mathcal{B}^{\text{MS}}(\mathcal{N})$ .

Figure 1.5 shows examples of B-splines of bidegree  $(2, 2)$  with support on a spline mesh  $\mathcal{N} = (\mathcal{M}, 1, (2, 2))$ . In particular, in (a) is reported the mesh  $\mathcal{M}$ , the B-splines considered in (b)–(c) have minimal support, while the support of the B-spline in (d) can be disconnected by the split  $\gamma$ , visualized by the dashed line in the figure.

Given a spline mesh  $\mathcal{N}$  and a B-spline  $B[\mathbf{x}, \mathbf{y}]$  with support on  $\mathcal{N}$ , assume that it has not minimal support on  $\mathcal{N}$ . Then, there exists a  $(k, a)$ -split  $\gamma$ , for some  $k \in \{1, 2\}$  and  $a \in \mathbb{R}$ , traversing  $B[\mathbf{x}, \mathbf{y}]$ . Either  $\gamma$  is in  $\mathcal{M} \setminus \mathcal{M}[\mathbf{x}, \mathbf{y}]$  or  $\gamma \subseteq \mathcal{M}[\mathbf{x}, \mathbf{y}]$ , i.e.,  $a$  is an internal knot of  $\mathbf{x}$  for  $k = 1$  or  $\mathbf{y}$  for  $k = 2$ , but the multiplicities of its meshlines are higher in  $\mathcal{N}$  than in  $\mathcal{N}[\mathbf{x}, \mathbf{y}]$ . Assume that the meshlines in  $\gamma$  have multiplicity  $m$  in  $\mathcal{N}$ . One could consider such  $a$  as an extra knot, of multiplicity  $m$  if  $\gamma \subseteq \mathcal{M} \setminus \mathcal{M}[\mathbf{x}, \mathbf{y}]$  and of multiplicity  $m - \mu(a)$  if  $\gamma \subseteq \mathcal{M}[\mathbf{x}, \mathbf{y}]$ , with respect to the knot vector of  $B[\mathbf{x}, \mathbf{y}]$  on the  $k$ th direction (in  $\mathbf{x}$  if the  $k = 1$  and in  $\mathbf{y}$  if  $k = 2$ ) and perform the knot insertion on  $B[\mathbf{x}, \mathbf{y}]$ . In the second case, since  $a$  was already a knot in the knot vector, this means raising its multiplicity by  $m - \mu(a)$ . The resulting generated B-splines would still have support on  $\mathcal{N}$  and eventually they would also have minimal support on  $\mathcal{N}$ . As an example, the split  $\gamma$  highlighted with dashed lines in Figure 1.5(d) is made of  $(2, a)$ -meshlines, for some  $a \in \mathbb{R}$ , of multiplicity 1. Such a  $a$  can be inserted as a new knot of multiplicity 1 in the knot vector on the  $y$ -direction of

## 1. Introduction

---

the considered B-spline to refine it in two B-splines via knot insertion.

The LR B-splines are generated by means of the above procedure. We start by considering a coarse tensor spline mesh, defining at least one B-spline, and we refine it by inserting splits, one at a time. On the initial mesh we consider the collection of bivariate B-splines and whenever a B-spline in our collection has no longer minimal support during the mesh refinement process, we refine it by using the knot insertion procedure. The LR B-splines will be the final set of B-splines produced by this algorithm.

**Definition 1.2.3.** Given a bidegree  $\mathbf{p}$ , let  $\mathcal{N}_0 = (\mathcal{M}_0, \mu_0, \mathbf{p})$  be a tensor spline mesh and let  $\mathcal{B}_0$  be the set of bivariate B-splines of bidegree  $\mathbf{p}$  on  $\mathcal{N}_0$ . We then define a sequence of spline meshes  $\mathcal{N}_1, \mathcal{N}_2, \dots$  and corresponding function sets  $\mathcal{B}_1, \mathcal{B}_2, \dots$  as follows. For  $i = 0, 1, \dots$ , let  $\gamma_i$  be a split such that the support of at least one B-spline in  $\mathcal{B}_i$  is traversed by a split of  $\mathcal{N}_{i+1} := \mathcal{N}_i + \gamma_i$ . On this refined spline mesh  $\mathcal{N}_{i+1}$ , the new set of B-splines  $\mathcal{B}_{i+1}$  is constructed by the following algorithm:

1. Initialize the set by  $\mathcal{B}_{i+1} \leftarrow \mathcal{B}_i$ .
2. As long as there exists  $B[\mathbf{x}^j, \mathbf{y}^j] \in \mathcal{B}_{i+1}$  with no minimal support on  $\mathcal{N}_{i+1}$ :
  - a) apply knot insertion:

$$\exists B[\mathbf{x}_1^j, \mathbf{y}_1^j], B[\mathbf{x}_2^j, \mathbf{y}_2^j] : B[\mathbf{x}^j, \mathbf{y}^j] = \alpha_1 B[\mathbf{x}_1^j, \mathbf{y}_1^j] + \alpha_2 B[\mathbf{x}_2^j, \mathbf{y}_2^j]$$

for  $\alpha_1, \alpha_2 \in (0, 1]$ ,

- b) update the set:  $\mathcal{B}_{i+1} \leftarrow (\mathcal{B}_{i+1} \setminus \{B[\mathbf{x}^j, \mathbf{y}^j]\}) \cup \{B[\mathbf{x}_1^j, \mathbf{y}_1^j], B[\mathbf{x}_2^j, \mathbf{y}_2^j]\}$ .

The spline mesh produced at each step is called an **LR-mesh** and the corresponding function set is called an **LR B-spline set** and it is denoted by  $\mathcal{B}^{\mathcal{LR}}(\mathcal{N}_{i+1})$ .

In general, the mesh refinement process producing a given LR-mesh  $\mathcal{N} = \mathcal{N}_N$  is not unique. Indeed, the split insertion ordering can often be changed. However, the collection of LR B-splines on  $\mathcal{N}$  is well defined because it is independent of such insertion order, as proved in [7, Theorem 3.4].

Given an LR-mesh  $\mathcal{N}$ , since an LR B-spline is also a MS B-spline, we have  $\mathcal{B}^{\mathcal{LR}}(\mathcal{N}) \subseteq \mathcal{B}^{\mathcal{MS}}(\mathcal{N})$ . However, the two sets can be different. An example is reported in Figure 1.6. In Figure 1.6(a) we have an LR-mesh  $\mathcal{N} = (\mathcal{M}, 1, (2, 2))$ . This is obtained by inserting two 2-splits and two 1-splits in a tensor mesh  $\mathcal{N}_0$ . In Figure 1.6(b) we see the supports of the LR B-splines on  $\mathcal{N}$ , i.e., the elements of  $\mathcal{B}^{\mathcal{LR}}(\mathcal{N})$ , obtained by refining the B-splines with no minimal support during the insertion of the splits. However if we look at the final mesh  $\mathcal{M}$  in Figure 1.6(a), we see that there is one MS B-spline, whose support is depicted in Figure 1.6(c), not in  $\mathcal{B}^{\mathcal{LR}}(\mathcal{N})$ , defined on  $\mathcal{N}$ .

Both the MS B-splines and the LR B-splines have desirable properties for applications, inherited by the standard bivariate B-splines, as positivity and compact support. However, in general both the collections do not sum to one.

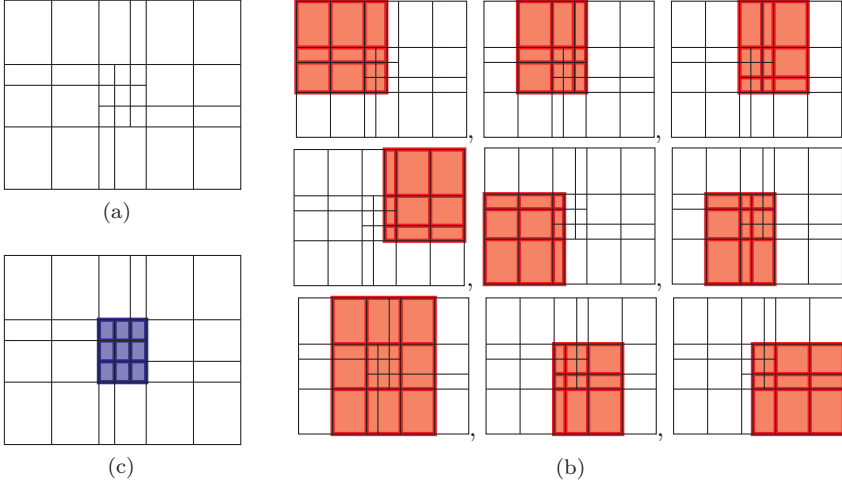


Figure 1.6: (a) an LR-mesh  $\mathcal{N} = (\mathcal{M}, 1, (2, 2))$ . (b) Supports of the LR B-splines defined on  $\mathcal{N}$ . (c) Support of a MS B-spline on the LR-mesh not in  $\mathcal{B}^{\mathcal{LR}}(\mathcal{N})$ .

Indeed, this happens only when the collections are locally linearly independent as we will see later. Nevertheless, the following Proposition 1.2.4 provides positive scaling weights to make the LR B-spline set form a partition of unity over any open LR-mesh. Given an LR-mesh  $\mathcal{N}$ , the corresponding LR B-spline set  $\mathcal{B}^{\mathcal{LR}}(\mathcal{N}) = \mathcal{B}_N$  is the final element of a sequence of B-spline sets  $\{\mathcal{B}_i\}_{i=1}^N$  described in Definition 1.2.3. However,  $\{\mathcal{B}_i\}_{i=1}^N$  is a subsequence of  $\{\tilde{\mathcal{B}}_i\}_i$ , whose final element is still  $\mathcal{B}^{\mathcal{LR}}(\mathcal{N})$ , given by

$$\tilde{\mathcal{B}}_{i+1} = (\tilde{\mathcal{B}}_i \setminus \{B_0\}) \cup \{B_1, B_2\}$$

where  $B_0 \in \tilde{\mathcal{B}}_i$  is an LR B-spline that has no longer minimal support on the LR-mesh and that therefore can be refined via knot insertion in  $B_1$  and  $B_2$ :

$$B_0 = \alpha_1 B_1 + \alpha_2 B_2 \quad \text{for } \alpha_1, \alpha_2 \in (0, 1]. \quad (1.6)$$

Note that  $B_1$  and/or  $B_2$  could already belong to  $\tilde{\mathcal{B}}_i$ .

**Proposition 1.2.4** (Partition of unity, [7, Lemma 7.1]). *Suppose  $\sum_{B \in \tilde{\mathcal{B}}_i} \gamma_{i,B} B = 1$  for some strictly positive numbers  $\gamma_{i,B}$ . Then  $\sum_{B \in \tilde{\mathcal{B}}_{i+1}} \gamma_{i+1,B} B = 1$  where  $\gamma_{i+1,B}$  are all strictly positive, and more precisely  $\gamma_{i+1,B} = \gamma_{i,B}$  if  $B \in \tilde{\mathcal{B}}_i \setminus \{B_0, B_1, B_2\}$  and*

$$\gamma_{i+1,B_\ell} = \begin{cases} \gamma_{i,B_0} \alpha_\ell & \text{if } B_\ell \notin \tilde{\mathcal{B}}_i \\ \gamma_{i,B_\ell} + \gamma_{i,B_0} \alpha_\ell & \text{if } B_\ell \in \tilde{\mathcal{B}}_i \end{cases} \quad \text{for } \ell = 1, 2 \quad (1.7)$$

where  $B_0, B_1, B_2, \alpha_1, \alpha_2$  are given by (1.6).

Since on the initial open tensor spline mesh  $\mathcal{N}_0$  the standard bivariate B-splines sum to one, Proposition 1.2.4 provides a constructive procedure to define

the weights to make the LR B-splines defined on the final LR-mesh  $\mathcal{N} = \mathcal{N}_N$  a partition on unity.

### 1.2.1 Spanning properties: the hand-in-hand principle

Given an LR-mesh  $\mathcal{N}$ , we have  $\text{span } \mathcal{B}^{\mathcal{LR}}(\mathcal{N}) \subseteq \text{span } \mathcal{B}^{\mathcal{MS}}(\mathcal{N}) \subseteq \mathbb{S}(\mathcal{N})$ .  $\mathcal{N} = \mathcal{N}_N$  is the final element of an LR-mesh sequence defined from an initial tensor spline mesh  $\mathcal{N}_0$ . On  $\mathcal{N}_0$ ,  $\mathcal{B}^{\mathcal{LR}}(\mathcal{N}_0) = \mathcal{B}^{\mathcal{MS}}(\mathcal{N}_0)$  and they are nothing more than the standard bivariate B-splines defined on  $\mathcal{N}_0$ . By the Curry-Schoenberg Theorem [5, page 97],  $\text{span } \mathcal{B}^{\mathcal{LR}}(\mathcal{N}_0) = \text{span } \mathcal{B}^{\mathcal{MS}}(\mathcal{N}_0) = \mathbb{S}(\mathcal{N}_0)$ . The purpose of this section is to investigate what are the conditions to satisfy during the mesh refinement process that produces  $\mathcal{N}$  to preserve these equalities. In this way, we maximize the approximation power of the MS and LR B-splines as the full spline space is spanned on the final LR-mesh  $\mathcal{N}$ .

Therefore, assume that on a given LR-mesh  $\mathcal{N} = (\mathcal{M}, \mu, \mathbf{p})$  we have  $\text{span } \mathcal{B}^{\mathcal{MS}}(\mathcal{N}) = \mathbb{S}(\mathcal{N})$ , or  $\text{span } \mathcal{B}^{\mathcal{LR}}(\mathcal{N}) = \mathbb{S}(\mathcal{N})$  respectively. Suppose we refine  $\mathcal{N}$  with the insertion of a split  $\gamma$ . We look for the conditions on  $\gamma$  in order to have  $\text{span } \mathcal{B}^{\mathcal{MS}}(\mathcal{N} + \gamma) = \mathbb{S}(\mathcal{N} + \gamma)$ , or  $\text{span } \mathcal{B}^{\mathcal{LR}}(\mathcal{N} + \gamma) = \mathbb{S}(\mathcal{N} + \gamma)$  respectively. If this happens, we say that  $\mathcal{N} + \gamma$  **goes MS-wise, or LR-wise respectively, hand-in-hand with  $\mathcal{N}$** . Note that if  $\mathcal{N} + \gamma$  goes LR-wise hand-in-hand with  $\mathcal{N}$ , then it also goes MS-wise hand-in-hand with  $\mathcal{N}$ , as  $\mathcal{B}^{\mathcal{LR}}(\mathcal{N} + \gamma) \subseteq \mathcal{B}^{\mathcal{MS}}(\mathcal{N} + \gamma)$ .

Therefore, in order for the MS, or the LR, B-splines to span the full spline space on the final LR-mesh provided by a mesh refinement process, we have to ensure that all the intermediate LR-meshes go MS-wise, or LR-wise, hand-in-hand.

**Theorem 1.2.5** ([7, Theorem 5.10]). *Let  $\mathcal{N} = (\mathcal{M}, \mu, \mathbf{p})$  be an LR-mesh. Assume that  $\text{span } \mathcal{B}^{\mathcal{MS}}(\mathcal{N}) = \mathbb{S}(\mathcal{N})$ , or  $\text{span } \mathcal{B}^{\mathcal{LR}}(\mathcal{N}) = \mathbb{S}(\mathcal{N})$  respectively. Let  $\gamma$  be a new  $k$ -split to insert and  $\tau_{p_{3-k}}^{\mu_{3-k}}$  be the expanded spline sequence on it. Let  $\mathcal{B}^{\mathcal{MS}}(\gamma)$ , or  $\mathcal{B}^{\mathcal{LR}}(\gamma)$  respectively, be the collections of the new B-splines created in the MS, or LR, B-spline set after the insertion of  $\gamma$ . For any  $B \in \mathcal{B}^{\mathcal{MS}}(\gamma)$ , or  $B \in \mathcal{B}^{\mathcal{LR}}(\gamma)$  respectively,  $B = B[\mathbf{x}, \mathbf{y}] = B[\mathbf{x}]B[\mathbf{y}]$  where  $B[\mathbf{x}]$  and  $B[\mathbf{y}]$  are the univariate B-splines in the  $x$  and  $y$  variable respectively, defined on the knot vectors  $\mathbf{x}$  and  $\mathbf{y}$ . Let  $B_\gamma$  be the univariate B-spline in the  $y$  variable if  $k = 1$  or in the  $x$  variable if  $k = 2$ , in the expression of  $B$ . Then  $\mathcal{N} + \gamma$  goes MS-wise, or LR-wise respectively, hand-in-hand with  $\mathcal{N}$  if and only if*

$$\text{span } \{B_\gamma\}_{B \in \mathcal{B}^{\mathcal{MS}}(\gamma) \text{ (or } \mathcal{B}^{\mathcal{LR}}(\gamma) \text{ resp.)}} = \mathbb{S}(\tau_{p_{3-k}}^{\mu_{3-k}}).$$

Theorem 1.2.5 allows to verify the hand-in-hand of the LR-meshes by looking at the span of univariate B-splines. Note that, since all the  $B_\gamma$  are contained in  $\mathbb{S}(\tau_{p_{3-k}}^{\mu_{3-k}})$ , we always have

$$\dim \text{span } \{B_\gamma\}_{B \in \mathcal{B}^{\mathcal{MS}}(\gamma) \text{ (or } \mathcal{B}^{\mathcal{LR}}(\gamma) \text{ resp.)}} \leq \dim \mathbb{S}(\tau_{p_{3-k}}^{\mu_{3-k}}).$$

We distinguish two cases when this is a strict inequality:

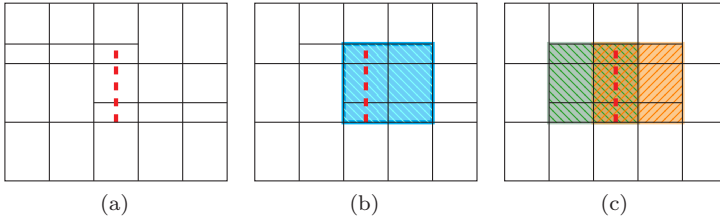


Figure 1.7: 3 different LR-meshes and a new split (dashed) to insert. In (a), after the insertion, the new LR-mesh does not go MS-wise (and so LR-wise) hand-in-hand, in (b) it goes MS-wise, but not LR-wise, hand-in-hand and in (c) it goes LR-wise (and so MS-wise) hand-in-hand.

1. The cardinality of  $\mathcal{B}^{\mathcal{MS}}(\gamma)$ , or  $\mathcal{B}^{\mathcal{LR}}(\gamma)$  respectively, is less than  $\dim \mathbb{S}(\tau_{p_3-k}^{\mu_{3-k}})$ ,
2. the cardinality of  $\mathcal{B}^{\mathcal{MS}}(\gamma)$ , or  $\mathcal{B}^{\mathcal{LR}}(\gamma)$  respectively, is at least equal to  $\dim \mathbb{S}(\tau_{p_3-k}^{\mu_{3-k}})$  but the linearly independent univariate B-splines  $B_\gamma$  are less than such dimension.

The cardinality of  $\mathcal{B}^{\mathcal{MS}}(\gamma)$ , or  $\mathcal{B}^{\mathcal{LR}}(\gamma)$ , depends on the mutual position of the splits in  $\mathcal{M}$ . This is explained in Figure 1.7. There we insert a new split  $\gamma$  (dashed line) in three different LR-meshes,  $\mathcal{N}^i = (\mathcal{M}^i, 1, (2, 2))$  for  $i = 1, 2, 3$ . Since the spline space on the expanded spline sequence on  $\gamma$  has dimension 1,  $\dim \mathbb{S}(\mathcal{N}^i + \gamma) = \dim \mathbb{S}(\mathcal{N}^i) + 1$  by Theorem 1.1.15. Therefore, a new MS, or LR, B-spline must be generated to have  $\mathcal{N}^i + \gamma$  going MS-wise or LR-wise hand-in-hand with  $\mathcal{N}^i$ .

Unfortunately, in the refined LR-mesh  $\mathcal{N}^1 + \gamma$  of Figure 1.7(a) no MS, or LR, B-splines are created after the insertion due to the splits mutual position. Thus  $\mathcal{B}^{\mathcal{MS}}(\mathcal{N}^1 + \gamma) = \mathcal{B}^{\mathcal{MS}}(\mathcal{N}^1)$ ,  $\mathcal{B}^{\mathcal{LR}}(\mathcal{N}^1 + \gamma) = \mathcal{B}^{\mathcal{LR}}(\mathcal{N}^1)$  and  $\mathcal{N}^1 + \gamma$  cannot go neither LR-wise nor MS-wise hand-in-hand with  $\mathcal{N}^1$ .

In Figure 1.7(b) a new MS B-spline is created when inserting  $\gamma$ , and its support is highlighted. This MS B-spline is not a result of a knot insertion procedure, it just appears on the new LR-mesh when  $\gamma$  is inserted. In this case,  $\mathcal{N}^2 + \gamma$  goes MS-wise hand-in-hand (but not LR-wise) with  $\mathcal{N}^2$ . In Figure 1.7(c), there is an LR B-spline on  $\mathcal{N}^3$  to refine via knot insertion after the insertion of  $\gamma$  and  $\mathcal{N}^3 + \gamma$  goes LR-wise (and so MS-wise) hand-in-hand with  $\mathcal{N}^3$ . The supports of the two generated LR B-splines are represented in the figure.

However, although the cardinality of such sets is sufficiently large, the linearly independent univariate B-splines  $B_\gamma$  can be insufficient for spanning the whole spline space  $\mathbb{S}(\tau_{p_3-k}^{\mu_{3-k}})$  on the expanded spline sequence  $\tau_{p_3-k}^{\mu_{3-k}}$  on  $\gamma$ . An example is reported in Figure 1.8. We consider an LR-mesh  $\mathcal{N} = (\mathcal{M}, 1, (2, 2))$  and a new 2-split  $\gamma$  as shown in Figure 1.8(a). The spline space on the expanded spline sequence  $\tau_2^{\mu_1}$  on  $\gamma$  has dimension 4 so that  $\dim \mathbb{S}(\mathcal{N} + \gamma) = \dim \mathbb{S}(\mathcal{N}) + 4$  by Theorem 1.1.15. Moreover, it is easy to verify that  $\mathcal{N}$  can be constructed

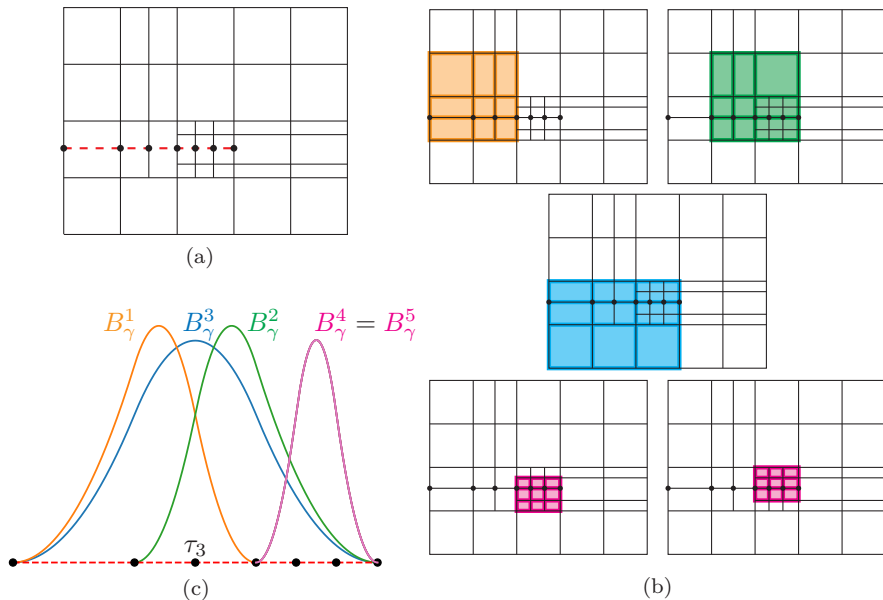


Figure 1.8: (a) LR-mesh  $\mathcal{N} = (\mathcal{M}, 1, (2, 2))$  and a new 2-split  $\gamma$  (dashed) with their intersections (black dots). In (b) the supports of the LR B-splines  $B^1, B^2$  (top),  $B^3$  (center),  $B^4, B^5$  (bottom) in  $\mathcal{B}^{\mathcal{LR}}(\gamma)$ . In (c) their corresponding univariate B-splines.

LR-wise hand-in-hand. Therefore,  $\mathcal{B}^{\mathcal{LR}}(\mathcal{N}) = \mathcal{B}^{\mathcal{MS}}(\mathcal{N})$  and they span the spline space  $\mathbb{S}(\mathcal{N})$ . When  $\gamma$  is inserted, there are 5 LR B-splines,  $B^1, B^2, B^3, B^4, B^5$ , in  $\mathcal{B}^{\mathcal{LR}}(\gamma)$ , whose support is depicted in Figure 1.8(b). The cardinalities  $|\mathcal{B}^{\mathcal{LR}}(\gamma)|, |\mathcal{B}^{\mathcal{MS}}(\gamma)|$  are large enough for  $\mathcal{N} + \gamma$  to go hand-in-hand with  $\mathcal{N}$ . However, if we look at the univariate B-splines  $B_\gamma$ , depicted in Figure 1.8(c), we can see that  $B_\gamma^4 = B_\gamma^5$  and  $B_\gamma^3$  can be expressed, via knot insertion of  $\tau_3$ , as a linear combination of  $B_\gamma^1, B_\gamma^2$ . Thus, there are only 3 linearly independent B-splines in  $\{B_\gamma\}_{B \in \mathcal{B}^{\mathcal{LR}}(\gamma)}$  and the spline mesh  $\mathcal{N} + \gamma$  cannot go neither LR-wise nor MS-wise hand-in-hand with  $\mathcal{N}$ .

Nevertheless, this phenomenon cannot happen if the spline space on the expanded spline sequence of the new  $k$ -split  $\gamma$  has dimension 1 or 2. Indeed, there exists at least one restriction  $B_\gamma$ , so it cannot happen if the univariate spline space has dimension 1. Similarly, if it has dimension 2, there are at least two different (and so linearly independent) univariate restrictions  $B_\gamma$ .

## 1.2.2 Linear dependence

The definition of LR-meshes leaves a lot of freedom in the refinement process. However, this can result in undesirable collections. Namely, the MS and LR B-splines obtained at the end of the refinement process may be linearly dependent. Figure 1.9 shows an example on an LR-mesh  $\mathcal{N} = (\mathcal{M}, 1, (2, 2))$  where the

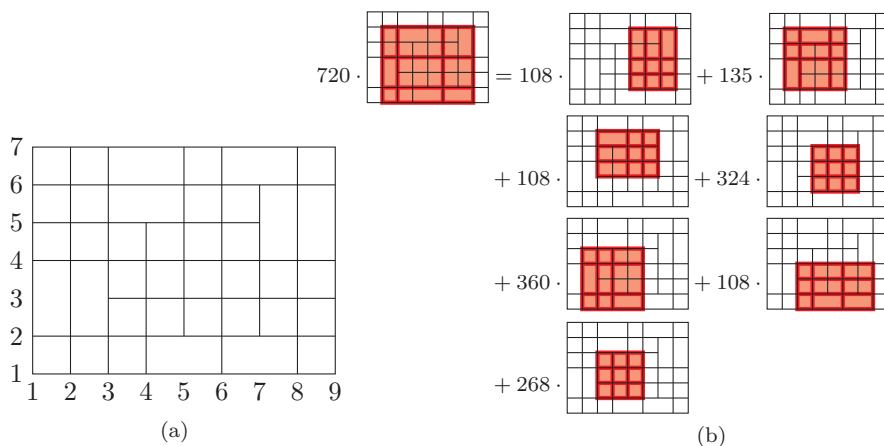


Figure 1.9: Example of linear dependence. The parametrization of an LR-mesh  $\mathcal{N} = (\mathcal{M}, 1, (2, 2))$  is considered in (a), and the linear dependence relation among some of the LR B-splines defined on  $\mathcal{N}$  is illustrated in (b). The LR B-splines are represented by means of their supports on the mesh and the tensor meshes generated by their knots are highlighted with thicker meshlines.

explicit relation is provided for a particular parametrization of the mesh  $\mathcal{M}$ . It is not yet known what are the precise conditions on the LR-mesh to ensure a linearly independent set of LR B-splines. In Paper 1, we start this analysis by looking at necessary geometrical conditions on the LR-mesh to encounter a linear dependence relation.

On the other hand, there are several ways to verify *a posteriori* if the MS and LR B-spline collections are linearly independent.

- **Hand-in-hand principle:** If the construction of the LR-mesh  $\mathcal{N}$  went MS-wise hand-in-hand then we can verify if the LR and MS B-spline collections are linearly independent or not by computing the spline space dimension, by using the dimension increasing formula (1.4) during the mesh refinement process or by using directly the dimension formula (1.3) on the final LR-mesh, and then counting the MS or LR B-splines defined on  $\mathcal{N}$ . If their number is higher than the dimension of the spline space, then the collection is linearly dependent. Otherwise, if it is equal to  $\dim \mathbb{S}(\mathcal{N})$ , then the collection is linearly independent. For example, consider again the LR-mesh  $\mathcal{N} = (\mathcal{M}, 1, (2, 2))$  of Figure 1.6(a). Since the dimension of the spline space on the underlying tensor spline mesh is 3 and, for equation (1.4), by inserting first the 2-splits and then the 1-splits, it increases by 1 twice and then by 2 twice, we have that

$$\dim \mathbb{S}(\mathcal{N}) = 3 + 1 + 1 + 2 + 2 = 9.$$

One can also easily check that the construction of  $\mathcal{N}$  went MS-wise hand-in-hand. Therefore, since the MS B-splines on the mesh are 10 and the

LR B-splines are 9, we conclude that the former are in linear dependence while the latter are linearly independent.

- **Tensor expansion:** This approach was proposed in [23, Theorem 1] for T-splines and extended to the LR B-spline context in [20]. Given an LR-mesh  $\mathcal{N} = (\mathcal{M}, \mu, \mathbf{p})$ , we prolong all the splits in  $\mathcal{M}$  to obtain a corresponding tensor spline mesh  $\mathcal{N}^T = (\mathcal{M}^T, \mu^T, \mathbf{p})$ . The MS and LR B-splines defined on  $\mathcal{N}$  can be expressed by the standard bivariate B-splines defined on  $\mathcal{N}^T$ , that is, there exist two rectangular matrices  $C_1$  and  $C_2$  that map the bivariate B-splines in the MS and LR B-splines respectively. We know that the bivariate B-splines are linearly independent. Therefore, the MS and LR B-splines are linearly independent if and only if the matrices  $C_1$  and  $C_2$  respectively have full rank.
- **Peeling algorithm:** This approach was proposed in [7, Algorithm 6.3]. An open LR-mesh  $\mathcal{N} = (\mathcal{M}, \mu, \mathbf{p})$  is defined through a mesh refinement process from an open tensor mesh  $\mathcal{N}_0$ . The standard bivariate B-spline defined on  $\mathcal{N}_0$  span the polynomial space  $\Pi_{\mathbf{p}}$  over every box-partition element of  $\mathcal{N}_0$ , that is, every box-partition element of  $\mathcal{N}_0$  is contained in  $(p_1 + 1)(p_2 + 1)$  bivariate B-spline supports. Consequentially, at each refinement step to produce  $\mathcal{N}$ , there will be at least  $(p_1 + 1)(p_2 + 1)$  LR B-splines with support covering each element, and the full polynomial space  $\Pi_{\mathbf{p}}$  is spanned on each element. If  $\mathcal{E}$  is the box-partition associated to  $\mathcal{M}$ , we say that an element of  $\mathcal{E}$  is **overloaded** if it is in the support of more LR B-splines than necessary for spanning the polynomial space  $\Pi_{\mathbf{p}}$ , that is, in more than  $(p_1 + 1)(p_2 + 1)$  supports. We call an LR B-spline overloaded if all the box-partition elements in its support are overloaded. Only the overloaded LR B-splines can be removed from the LR B-spline collection without changing the spanning properties over the box-partition elements in their supports. This implies that only overloaded LR B-splines occur in linear dependence relations. Moreover, a linear dependence relation has to involve at least two overloaded LR B-splines on every box-partition element. Therefore, if a box-partition element is contained only in one overloaded LR B-spline, this latter is just overloaded and cannot be in a linear dependence relation. This is the core of the Peeling algorithm (Algorithm 1.1).

However, the Peeling algorithm might end without answering whether the LR B-splines on  $\mathcal{N}$  are linearly independent or not. That is, it might happen that all the overloaded elements, collected in  $\mathcal{E}^O$ , are in the support of two overloaded LR B-splines but yet such LR B-splines are just overloaded and not in a linear dependence relation. Therefore, the Peeling algorithm can prove that the LR B-splines on an LR-mesh are linearly independent, but it cannot prove that they are linearly dependent.

The tensor expansion does not scale well, in terms of computational costs, with increasing problem sizes, but it has the advantage to handle all possible LR-meshes, as opposed to the hand-in-hand principle and Peeling algorithm.

**Algorithm 1.1:** Peeling Algorithm

- 1 From the set of LR splines  $\mathcal{B}^{\mathcal{LR}}(\mathcal{N})$  create the set  $\mathcal{B}^O$  of overloaded LR B-splines;
- 2 Let  $\mathcal{E}^O$  be the elements of  $\mathcal{E}$  in the supports of the LR B-splines in  $\mathcal{B}^O$ ;
- 3 Initialization of a subset  $\mathcal{B}_1^O$  of  $\mathcal{B}^O$  we are going to define,  $\mathcal{B}_1^O = \emptyset$ ;
- 4 **for every element  $\beta$  in  $\mathcal{E}^O$  do**
- 5     **if only one LR B-spline  $B$  of  $\mathcal{B}^O$  has  $\beta$  in its support then**
- 6          $\mathcal{B}_1^O = \mathcal{B}_1^O \cup \{B\}$
- 7 **if  $\mathcal{B}^O \setminus \mathcal{B}_1^O = \emptyset$  then**
- 8     linear independence.
- 9 **else**
- 10     **if  $\mathcal{B}_1^O = \emptyset$  then**
- 11         break, but might have linear dependence.
- 12      $\mathcal{B}^O = \mathcal{B}^O \setminus \mathcal{B}_1^O$ ;
- 13     Go to 2;

However, it is possible to combine these techniques. For example, one could narrow the possible areas of linear dependence down to only a subset of the LR-mesh using the Peeling algorithm and then apply tensor expansions only to these areas for a complete verification of the linear independence.

On the other hand, a characterization and/or a classification of the linearly dependent configurations would allow the creation of mesh refinement processes that guarantee the linear independence of the final MS and LR B-spline collections. This is the motivation for Paper 1.

### 1.2.3 Local linear independence and $N_2S$ property

The local linear independence is a strong property of bivariate B-splines and it is useful for many applications, such as quasi-interpolation and simulation. The generalization of it to LR B-splines context requires a particular displacement of the LR B-splines support.

**Definition 1.2.6.** Given an LR-mesh  $\mathcal{N}$ , let  $B[\mathbf{x}^1, \mathbf{y}^1], B[\mathbf{x}^2, \mathbf{y}^2]$  be two different MS B-splines defined on  $\mathcal{N}$ . We say that  $B[\mathbf{x}^2, \mathbf{y}^2]$  is **nested** in  $B[\mathbf{x}^1, \mathbf{y}^1]$ , and we write  $B[\mathbf{x}^2, \mathbf{y}^2] \preceq B[\mathbf{x}^1, \mathbf{y}^1]$ , if the multiplicities of  $z$  in  $\mathbf{x}^i$  and  $\mathbf{y}^i$  for  $i = 1, 2$ , called  $\mu_{\mathbf{x}^i}(z)$  and  $\mu_{\mathbf{y}^i}(z)$ , satisfy

$$\begin{aligned}
 1. \quad & \begin{cases} \mu_{\mathbf{x}^2}(z) \geq \mu_{\mathbf{x}^1}(z) & \forall z \in (x_1^2, x_{p_1+2}^2) \\ \mu_{\mathbf{y}^2}(z) \geq \mu_{\mathbf{y}^1}(z) & \forall z \in (y_1^2, y_{p_1+2}^2) \end{cases} \\
 2. \quad & \begin{cases} \mu_{\mathbf{x}^2}(z) \leq \mu_{\mathbf{x}^1}(z) & \forall z \in (-\infty, x_1^1] \cup [x_{p_1+2}^1, +\infty) \\ \mu_{\mathbf{y}^2}(z) \leq \mu_{\mathbf{y}^1}(z) & \forall z \in (-\infty, y_1^1] \cup [y_{p_1+2}^1, +\infty). \end{cases}
 \end{aligned}$$

## 1. Introduction

---

If  $z$  is not a knot in the considered knot vector, its multiplicity is assigned to be zero. An open LR-mesh  $\mathcal{N}$  where no LR B-spline is nested is said to have the **non-nested support property**, or in short the  $N_2S$  property.

Given an LR-mesh  $\mathcal{N}$ , we have locally linearly independent LR B-splines defined on  $\mathcal{N}$  if and only if  $\mathcal{N}$  has the  $N_2S$  property, as stated in the following Theorem.

**Theorem 1.2.7** ([2, Theorem 4]). *Given an open LR-mesh  $\mathcal{N} = (\mathcal{M}, \mu, \mathbf{p})$  with  $\mathcal{M}$  corresponding to a box-partition  $\mathcal{E}$ , let  $\mathcal{B}^{\mathcal{LR}}(\mathcal{N})$  be the set of LR B-splines defined on  $\mathcal{N}$ . The following statements are equivalent:*

1. *The elements of  $\mathcal{B}^{\mathcal{LR}}(\mathcal{N})$  are locally linearly independent.*
2.  *$\mathcal{N}$  has the  $N_2S$  property.*
3. *For any element  $\beta \in \mathcal{E}$ , the number of nonzero LR B-splines over  $\beta$  satisfies*

$$\#\{B \in \mathcal{B}^{\mathcal{LR}}(\mathcal{N}) : \text{supp } B \supseteq \beta\} = \dim \Pi_{\mathbf{p}} = (p_1 + 1)(p_2 + 1),$$

*that is, all the elements of the box-partition associated to  $\mathcal{M}$  are non-overloaded.*

4. *The LR B-splines form a partition of unity (without the use of scaling weights).*

Definition 1.2.6 of nested MS B-spline was formulated in [1]. In the following proposition we provide an equivalent definition, which is considered by the author to be easier to understand and to use in practice.

**Proposition 1.2.8.** *Given an LR-mesh  $\mathcal{N} = (\mathcal{M}, \mu, \mathbf{p})$ , let  $B^1 = B[\mathbf{x}^1, \mathbf{y}^1]$  and  $B^2 = B[\mathbf{x}^2, \mathbf{y}^2]$  be MS B-splines defined on  $\mathcal{N}$ . Then  $B^2 \preceq B^1$  if and only if*

1.  *$\text{supp } B^2 \subseteq \text{supp } B^1$ , and*
2.  *$\mu[\mathbf{x}^2, \mathbf{y}^2](\gamma) \leq \mu[\mathbf{x}^1, \mathbf{y}^1](\gamma)$  for all meshlines  $\gamma \subseteq \partial \text{supp } B^1 \cap \partial \text{supp } B^2$ .*

*Proof.* Suppose  $B^2 \preceq B^1$ . Let us first prove that  $\text{supp } B^2 \subseteq \text{supp } B^1$ . This means that  $[x_1^2, x_{p_1+2}^2] \subseteq [x_1^1, x_{p_1+2}^1]$  and  $[y_1^2, y_{p_2+2}^2] \subseteq [y_1^1, y_{p_2+2}^1]$ . Assume that  $x_1^2 < x_1^1$ . Then  $\mu_{\mathbf{x}^1}(x_1^2) = 0$  and  $\mu_{\mathbf{x}^2}(x_1^2) \geq \mu_{\mathbf{x}^1}(x_1^2)$ . This a contradiction of 2. in Definition 1.2.6. Therefore  $x_1^2 \geq x_1^1$ . Similarly one proves the other inequalities to have the interval inclusions. Let now  $\gamma \subseteq \partial \text{supp } B^1 \cap \partial \text{supp } B^2$ . Assume without loss of generality that it is a 1-meshline. Then  $\gamma$  is a  $(1, z)$ -meshlines for  $z \in \{x_1^1, x_{p_1+2}^1\}$ . For any choice of such  $z$ , we have  $\mu_{\mathbf{x}^2}(z) \leq \mu_{\mathbf{x}^1}(z)$ , by 2. of Definition 1.2.6, and therefore  $\mu[\mathbf{x}^2, \mathbf{y}^2](\gamma) \leq \mu[\mathbf{x}^1, \mathbf{y}^1](\gamma)$ .

Assume now that  $\text{supp } B^2 \subseteq \text{supp } B^1$  and  $\mu[\mathbf{x}^2, \mathbf{y}^2](\gamma) \leq \mu[\mathbf{x}^1, \mathbf{y}^1](\gamma)$  for all  $\gamma \subseteq \partial \text{supp } B^1 \cap \partial \text{supp } B^2$ . Let us prove that  $B^2 \preceq B^1$ . Let  $z \in (x_1^2, x_{p_1+2}^2)$ . Since  $\text{supp } B^2 \subseteq \text{supp } B^1$  we have  $(x_1^2, x_{p_1+2}^2) \subseteq (x_1^1, x_{p_1+2}^1)$ . If  $z \notin \mathbf{x}^1$ , then  $\mu_{\mathbf{x}^1}(z) = 0$  and therefore  $\mu_{\mathbf{x}^2}(z) \geq \mu_{\mathbf{x}^1}(z)$  for any value of  $\mu_{\mathbf{x}^2}(z)$ . If  $z \in \mathbf{x}^1$ , then it must be also in  $\mathbf{x}^2$ , otherwise the  $(1, z)$ -split  $\{z\} \times [y_1^1, y_{p_2+2}^1]$  would

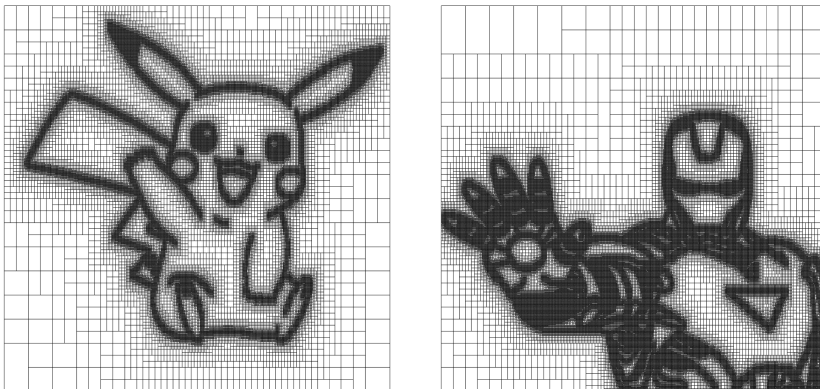


Figure 1.10: Example of LR-meshes with the  $N_2S$  property produced by the algorithm proposed in [2] with refinements localized in "random" regions.

traverse  $B^2$ , which would not have minimal support. For the same reason, it must also hold  $\mu_{\mathbf{x}^2}(z) = \mu_{\mathbf{x}^1}(z)$ . This proves 1. of Definition 1.2.6. Assume now  $z \in (-\infty, x_1^1) \cup (x_{p_2+2}^1, +\infty)$ . Since  $\text{supp } B^2 \subseteq \text{supp } B^1$ ,  $x_1^1 \leq x_1^2$  and  $x_{p_1+2}^2 \leq x_{p_1+2}^1$ . Therefore both  $\mu_{\mathbf{x}^1}(z) = \mu_{\mathbf{x}^2}(z) = 0$ . If  $z \in \{x_1^1, x_{p_1+2}^1\}$  but  $z \notin \mathbf{x}^2$ , then trivially  $\mu_{\mathbf{x}^2}(z) \leq \mu_{\mathbf{x}^1}(z)$ . If  $z \in \mathbf{x}^2$ , then  $z$  corresponds to  $(1, z)$ -meshlines in  $\partial\text{supp } B^1 \cap \partial\text{supp } B^2$ . By assumption, for any of such meshline  $\gamma$  it holds  $\mu[\mathbf{x}^2, \mathbf{y}^2](\gamma) \leq \mu[\mathbf{x}^1, \mathbf{y}^1](\gamma)$ , which means  $\mu_{\mathbf{x}^2}(z) \leq \mu_{\mathbf{x}^1}(z)$ . This proves 2. of Definition 1.2.6. ■

It is a hard task to define refinement strategies producing LR-meshes with the  $N_2S$  property. In [2] an algorithm to generate such LR-meshes is proposed. Although it creates nicely graded LR-meshes, see e.g. Figure 1.10, it has a relevant drawback for practical purposes: the regions to be refined and the maximal resolution, that is, the sides of the smallest box-partition elements on the final LR-mesh, have to be chosen a priori. Moreover, the algorithm cannot be stopped prematurely, before having inserted all the splits determined initially. In practice, one rarely knows in advance where the error will be large and how fine the mesh has to be in order to reduce it under a certain tolerance.

The purpose of Paper 2 is to provide the first truly adaptive refinement strategy that guarantees the  $N_2S$  property of the LR-meshes produced and therefore the local linear independence of the LR B-splines defined on them. This refinement strategy, which we refer to as  $N_2S$  structured mesh refinement, allows an easier implementation of the LR B-splines in quasi-interpolation methods and isogeometric analysis.

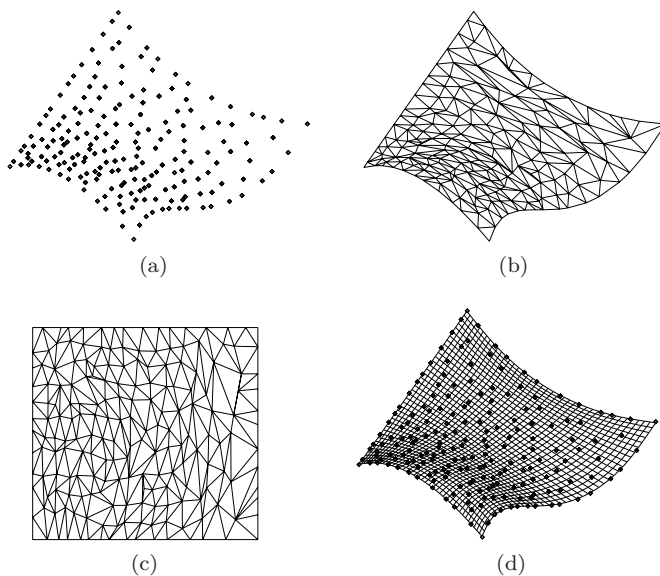


Figure 1.11: From a point cloud to its spline approximation. In (a) the point cloud. In (b) a first triangulation  $\mathcal{S}$  of the point cloud. In (c) a triangular mesh  $\mathcal{T}$  obtained from a mesh parametrization of  $\mathcal{S}$ . In (d) the final spline surface approximation. Pictures courtesy of Michael S. Floater.

### 1.3 Generalized barycentric coordinates and mesh parametrization

Many applications require the creation of a CAD model by approximating, via spline surfaces, a set of distinct points,  $\{\mathbf{x}_1, \dots, \mathbf{x}_n\} \subseteq \mathbb{R}^3$ , acquired e.g. by scanning an existing physical object. These points are often, at first, organized in a triangulation  $\mathcal{S}$ . Then, in order to obtain a spline surface, such a triangulation has to be "unfolded" to a triangular mesh  $\mathcal{T}$  on the plane. More precisely, this "unfolding process" is a mesh parametrization. Provided a mesh parametrization, there are several ways to approximate the vertices of  $\mathcal{S}$  by a spline surface relying on their parameter points, which are, the vertices of  $\mathcal{T}$ , e.g. [11, 17, 25]. The steps of this procedure are visually represented in Figure 1.11.

A general method to construct a mesh parametrization (homeomorphic to a disk) was first described in [32] and further analyzed in [11, 13]. Let  $V$  and  $E$  be the sets of vertices and edges of  $\mathcal{S}$ . Let also  $\Omega_{\mathcal{S}} \subseteq \mathbb{R}^3$  be the union of the triangles in  $\mathcal{S}$ . A mesh parametrization is a piecewise linear function  $\psi : \Omega_{\mathcal{S}} \rightarrow \mathbb{R}^2$  which maps each vertex, edge and triangle of  $\mathcal{S}$  to a corresponding vertex, edge and triangle in  $\mathbb{R}^2$ . Such a mapping is completely determined by the the points  $\psi(\mathbf{v})$ ,  $\mathbf{v} \in V$ . The procedure is the following. First the boundary vertices and edges of  $\mathcal{S}$  are mapped into a polygon in  $\mathbb{R}^2$  with no self intersections, e.g. a square.

Then, if  $V_I$  denote the interior vertices of  $\mathcal{S}$ , for  $\mathbf{v} \in V_I$ , we define the "1-ring neighbourhood" of  $\mathbf{v}$  as

$$N_{\mathbf{v}} = \{\mathbf{w} \in V : [\mathbf{v}, \mathbf{w}] \in E\},$$

and we choose strictly positive weights  $\{\lambda_{\mathbf{vw}} \in (0, 1) : \mathbf{w} \in N_{\mathbf{v}}\}$ , such that

$$\sum_{\mathbf{w} \in N_{\mathbf{v}}} \lambda_{\mathbf{vw}} = 1.$$

Once these are set, we determine the value of  $\psi(\mathbf{v})$  in  $\mathbb{R}^2$ , for  $\mathbf{v} \in V_I$ , by solving the linear system

$$\psi(\mathbf{v}) = \sum_{\mathbf{w} \in N_{\mathbf{v}}} \lambda_{\mathbf{vw}} \psi(\mathbf{w}) \quad \mathbf{v} \in V_I.$$

It is proved in [12, Proposition 1] that such system has a unique solution for any set of positive convex weights  $\lambda_{\mathbf{vw}}$ , for all  $\mathbf{v} \in V_I$ . The choice of them determines the mesh parametrization. As opposed to [32], in which the  $\lambda_{\mathbf{vw}}$  are uniformly defined as  $1/|N_{\mathbf{v}}|$ , a popular choice is to use weights that have the so called reproduction property: if  $\mathbf{v}$  and its neighbours  $\mathbf{w} \in N_{\mathbf{v}}$  lie in a plane then

$$\mathbf{v} = \sum_{\mathbf{w} \in N_{\mathbf{v}}} \lambda_{\mathbf{vw}} \mathbf{w}.$$

Such a condition guarantees that the mesh parametrization  $\psi$  is locally an isometry whenever possible [13, Section 6.3], and therefore the shape of the triangles in  $\mathcal{T}$  tends to mimic the shape of the triangles in  $\mathcal{S}$ . This eventually leads to a better spline surface approximation.

It is then natural to use generalized barycentric coordinates in this context to determine weights with the reproduction property. In particular, the use of the mean value coordinates for mesh parametrization is widely spread because of their fast and direct computation and the fact that the resulting mesh parametrization will depend smoothly on the vertices of the triangulation.

### 1.3.1 Mean value coordinates

In 1678, Giovanni Ceva [4] proved that for any point  $\mathbf{x}$  inside a planar triangle  $T = [\mathbf{v}_1, \mathbf{v}_2, \mathbf{v}_3]$ , there exist three positive numbers, or masses,  $w_1, w_2, w_3$  such that

$$\mathbf{x} = \sum_{i=1}^3 w_i \mathbf{v}_i / \sum_{i=1}^3 w_i. \tag{1.8}$$

Later, in 1827 August F. Möbius generalized Equation (1.8) to simplices in any dimension and, by considering also negative  $w_i$ , to any  $\mathbf{x}$ , see [27]. The coefficients  $w_i$ , for  $i = 1, 2, 3$ , are often called homogeneous barycentric coordinates of  $\mathbf{x}$  and, by their definition, they are unique up to a common factor. The **barycentric coordinates of  $\mathbf{x}$**  are defined as the normalization of

## 1. Introduction

---

the homogeneous barycentric coordinates by their sum, and therefore they are unique:

$$\lambda_i(\mathbf{x}) = w_i / \sum_{i=1}^3 w_i \quad i = 1, 2, 3, \quad (1.9)$$

By their definition, the barycentric coordinates have the following properties:

- positivity:  $\lambda_i(\mathbf{x}) \geq 0$  for  $i = 1, 2, 3$ , for all  $\mathbf{x} \in T$ ,
- partition of unity:  $\sum_{i=1}^3 \lambda_i(\mathbf{x}) = 1$ , for all  $\mathbf{x} \in \mathbb{R}^2$ ,
- reproduction:  $\sum_{i=1}^3 \lambda_i(\mathbf{x})\mathbf{v}_i = \mathbf{x}$  for all  $\mathbf{x} \in \mathbb{R}^2$ ,
- Lagrange property:  $\lambda_i(\mathbf{v}_j) = \delta_{ij}$  for  $i, j \in \{1, 2, 3\}$ .

There are several ways to generalize the barycentric coordinates to an arbitrary polygon of  $n$  vertices, see e.g. [10, 26, 29, 33, 34]. However, for most choices, the resulting generalized barycentric coordinates either are not well-defined everywhere in  $\mathbb{R}^2$  or do not satisfy the constraints of the Lagrange property. On the other hand, the mean value coordinates [10, 18] fulfill both conditions and have a number of other important properties, such as (infinite) smoothness, linear independence, and refinability.

**Definition 1.3.1.** Let  $\Omega \subseteq \mathbb{R}^2$  be a polygon of  $n \geq 3$  vertices,  $\mathbf{v}_1, \dots, \mathbf{v}_n$ , ordered anticlockwise. Let  $e_i = [\mathbf{v}_i, \mathbf{v}_{i+1}]$ , for  $i = 1, \dots, n-1$ , and  $e_n = [\mathbf{v}_{n-1}, \mathbf{v}_1]$  be the edges of  $\Omega$  and  $\mathbf{n}_{e_i}$  be the outward unit normal to edge  $e_i$ , for  $i = 1, \dots, n$ . For any  $\mathbf{x} \in \mathbb{R}^2$ , let  $r_i = \|\mathbf{v}_i - \mathbf{x}\|$ ,  $\alpha_{e_i}(\mathbf{x})$  be the angle at  $\mathbf{x}$  in the triangle  $[\mathbf{x}, \mathbf{v}_i, \mathbf{v}_{i+1}]$  and let  $h_{e_i}(\mathbf{x})$  be the signed distance of  $\mathbf{x}$  to the straight line through the edge  $e_i$ , so that

$$h_{e_i}(\mathbf{x}) = (\mathbf{y} - \mathbf{x}) \cdot \mathbf{n}_{e_i} \quad \text{for a fixed point } \mathbf{y} \in e_i.$$

Finally, let  $\tau_{e_i}(\mathbf{x}) = \text{sign}(h_{e_i}(\mathbf{x}))$ . Define

$$w_i(\mathbf{x}) = \frac{1}{r_i} (\tau_{e_{i-1}}(\mathbf{x}) \tan(\alpha_{e_{i-1}}(\mathbf{x})/2) + \tau_{e_i}(\mathbf{x}) \tan(\alpha_{e_i}(\mathbf{x})/2)). \quad (1.10)$$

The **mean value coordinates** of  $\Omega$  are the functions  $\lambda_i : \mathbb{R}^2 \rightarrow \mathbb{R}$  for  $i = 1, \dots, n$  with

$$\lambda_i(\mathbf{x}) = \begin{cases} w_i(\mathbf{x}) / \sum_{i=1}^n w_i(\mathbf{x}) & \text{for } \mathbf{x} \notin \partial\Omega \text{ with } w_i(\mathbf{x}) \text{ defined in Eq. (1.10),} \\ (1 - \mu)\delta_{ij} + \mu\delta_{i(j+1)} & \text{for } \mathbf{x} \in e_j, \mathbf{x} = (1 - \mu)\mathbf{v}_j + \mu\mathbf{v}_{j+1} \text{ for } \mu \in [0, 1]. \end{cases}$$

Figure 1.12(a) shows the notation used in Definition 1.3.1 for a particular choice of point and polygon.

Note that if  $\Omega$  is convex and  $\mathbf{x} \in \Omega$  then  $\tau_{e_i}(\mathbf{x}) = 1$  for all  $i = 1, \dots, n$  and we can drop them in the expression of the  $w_i(\mathbf{x})$ . More in general  $\tau_{e_i}(\mathbf{x}) = 1$  for all  $\mathbf{x}$  in the **kernel** of  $\Omega$ , which is the set of points  $\mathbf{x} \in \Omega$  such that the segments  $[\mathbf{x}, \mathbf{v}_i]$  for  $i = 1, \dots, n$  are in  $\Omega$ . If  $\Omega$  has non-empty kernel, then  $\Omega$

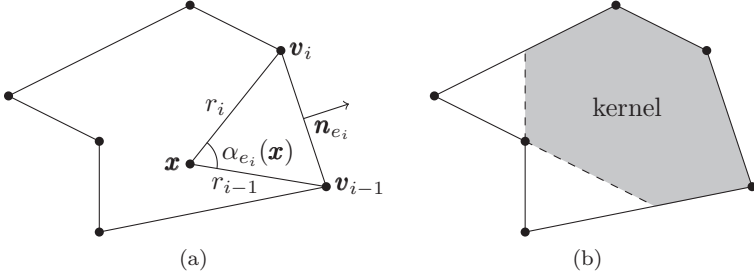


Figure 1.12: The notation used in Definition 1.3.1 (a) and the kernel of the considered polygon (b).

is called **star-shaped**. In particular if  $\Omega$  is convex, then it is star-shaped and coincides with its kernel. An example of a kernel of a non-convex, star-shaped polygon is reported in Figure 1.12(b). In the following proposition we list the main properties of the mean value coordinates.

**Proposition 1.3.2** ([18, Corollary 4.8]). *Given a polygon  $\Omega \subseteq \mathbb{R}^2$  of  $n \geq 3$  vertices,  $\mathbf{v}_1, \dots, \mathbf{v}_n$ , ordered anticlockwise. The mean value coordinates  $\lambda_i$ , for  $i = 1, \dots, n$  have the following properties:*

- *positivity:*  $\lambda_i(\mathbf{x}) \geq 0$  for  $\mathbf{x}$  in the kernel of  $\Omega$ ,
- *partition of unity:*  $\sum_{i=1}^n \lambda_i(\mathbf{x}) = 1$  for all  $\mathbf{x} \in \mathbb{R}^2$ ,
- *reproduction:*  $\mathbf{x} = \sum_{i=1}^n \lambda_i(\mathbf{x})\mathbf{v}_i$  for all  $\mathbf{x} \in \mathbb{R}^2$ ,
- *Lagrange property:*  $\lambda_i(\mathbf{v}_j) = \delta_{ij}$ ,
- *smoothness:*  $\lambda_i$  is  $C^\infty$  everywhere, except at the vertices of  $\Omega$ , where it is  $C^0$ ,
- *linear independence:* if  $\sum_{i=1}^n c_i \lambda_i(\mathbf{x}) = 0$  for all  $\mathbf{x} \in \mathbb{R}^2$ , then all  $c_i = 0$  must be zero,
- *refinability:* if we refine  $\Omega$  to  $\hat{\Omega}$  by splitting edge  $e_j$  at  $\hat{\mathbf{v}} = (1-\mu)\mathbf{v}_j + \mu\mathbf{v}_{j+1}$ , then  $\lambda_j = \hat{\lambda}_j + (1-\mu)\hat{\lambda}$ ,  $\lambda_{j+1} = \hat{\lambda}_{j+1} + \mu\hat{\lambda}$ , and  $\lambda_i = \hat{\lambda}_i$  for  $i \neq j, j+1$ ,
- *similarity invariance:* if  $\psi$  is a similarity and  $\hat{\Omega} = \psi(\Omega)$ , then  $\lambda_i(\mathbf{x}) = \hat{\lambda}_i(\psi(\mathbf{x}))$ .

Note that, in particular, the partition of unity and reproduction properties imply that the mean value coordinates have **affine precision**, that is, for any affine function  $\phi : \mathbb{R}^2 \rightarrow \mathbb{R}^d$ , it holds

$$\sum_{i=1}^n \lambda_i(\mathbf{x})\phi(\mathbf{v}_i) = \phi(\mathbf{x}). \quad (1.11)$$

The mean value coordinates have been also defined for sets of (possibly nested) polygons [18] and in the kernel of polyhedra with triangular facets in 3D [14].

### 1.3.2 Transfinite mean value interpolation

One of the main uses of generalized barycentric coordinates is to interpolate data  $f_i \in \mathbb{R}^d$  prescribed at the vertices of a polygon  $\Omega$  with a smooth function  $g : \Omega \rightarrow \mathbb{R}^d$ ,

$$g(\mathbf{x}) = \sum_{i=1}^n \lambda_i(\mathbf{x}) f_i. \quad (1.12)$$

This kind of barycentric interpolation has been used, for example, in computer graphics, as the basis for image warping [18], and in higher dimension, for mesh deformation [24].

This interpolant construction extends in a natural way to any continuous boundary data  $f : \partial\Omega \rightarrow \mathbb{R}^d$ , prescribed at the boundary of a general domain  $\Omega$ , thus providing a transfinite interpolant [8, 21]. Specifically, suppose that the boundary of  $\Omega$  is represented as a closed parametric curve  $\mathbf{p} : [a, b] \rightarrow \mathbb{R}^2$ , with  $\mathbf{p}(b) = \mathbf{p}(a)$ . Then, any sequence of parameter values  $t_1, \dots, t_n$ , with  $a \leq t_1 < \dots < t_n < b$  defines a polygon  $\Omega_h$ , where  $h = \max(t_{i+1} - t_i)$ , with vertices  $\mathbf{v}_i = \mathbf{p}(t_i)$ . The barycentric interpolant (1.12) with respect to this polygon is then

$$g_h(\mathbf{x}) = \sum_{i=1}^n \lambda_i(\mathbf{x}) f(\mathbf{p}(t_i)).$$

If the limit  $g = \lim_{h \rightarrow 0} g_h$  exists, then it has the form:

$$g(\mathbf{x}) = \int_a^b \lambda(\mathbf{x}, t) f(\mathbf{p}(t)) dt.$$

In the case of the mean value interpolation,  $\lambda(\mathbf{x}, t)$  is well-defined and, analogously to the discrete case, has expression

$$\lambda(\mathbf{x}, t) = w(\mathbf{x}, t) / \int_a^b w(\mathbf{x}, t) dt$$

where  $w(\mathbf{x}, t)$  is

$$w(\mathbf{x}, t) = \frac{(\mathbf{p}(t) - \mathbf{x}) \times \mathbf{p}'(t)}{\|\mathbf{p}(t) - \mathbf{x}\|^3}.$$

Transfinite interpolation could have various applications, one of which is its use as a building block for interpolants of higher order that also match derivative data on the boundary. However, there is currently no mathematical proof of interpolation in the transfinite setting in all cases, only numerical evidence. In fact, interpolation was shown in [8] only under the condition that the distance between the external medial axis of  $\Omega$  and the domain boundary is strictly positive. The external medial axis of  $\Omega$  is the set of points in  $\Omega^C$  having more than one closest point on  $\partial\Omega$ , or, in other words, it is the locus of the centers

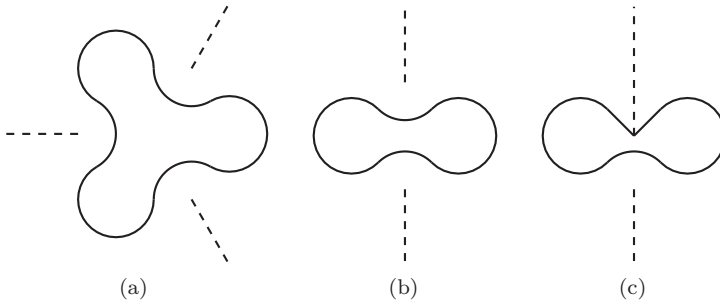


Figure 1.13: External medial axis (dashed lines) for three different domains. In (a)–(b) the distance between the external medial axis and the domain boundary is positive, while in (c) it is zero due to the presence of a non-convex vertex.

of circles in  $\Omega^C$  that are tangent to  $\partial\Omega$  in two or more points. Examples of external medial axes are depicted in Figure 1.13. The condition of [8] to prove interpolation trivially holds for convex domains since there is no external medial axis in this case. However, it still leaves open the question of whether the transfinite mean value interpolant really interpolates any continuous data on the boundary of an arbitrary polygon, with non-convex vertices, and this is what is established in Paper 3.

## 1.4 Summary of Papers

**Paper I** provides geometric necessary conditions to encounter a linear dependence relation in the MS and LR B-spline sets.

**Definition 1.4.1.** We say that functions  $\phi_1, \dots, \phi_n : \mathbb{R}^2 \rightarrow \mathbb{R}$  are **actively linearly dependent** on  $\mathbb{R}^2$  if there exist  $\alpha_i \in \mathbb{R}$ ,  $\alpha_i \neq 0$  for all  $i = 1, \dots, n$ , such that

$$\sum_{i=1}^n \alpha_i \phi_i(\mathbf{x}) = 0, \quad \forall \mathbf{x} \in \mathbb{R}^2.$$

As opposed to the definition of linearly dependent functions, Definition 1.4.1 forbids zero coefficients in the linear dependence relation, paying attention only to the minimal set of linearly dependent functions.

Given an LR-mesh, suppose  $\mathcal{B} \subseteq \mathcal{B}^{\text{MS}}(\mathcal{N})$ , or  $\mathcal{B}^{\text{LR}}(\mathcal{N})$  respectively, is a subcollection of actively linearly dependent functions. Then

- defining  $\mathcal{R} = \cup_{B \in \mathcal{B}} \text{supp } B$  as the region on  $\mathbb{R}^2$  where the linear dependence relation among the B-splines in  $\mathcal{B}$  occurs, there exist  $B_1, B_2 \in \mathcal{B}$  such that  $B_2 \preceq B_1$  at every (convex) corner of  $\mathcal{R}$ ,
- there exist at least 4 T-vertices, one per orientation, inside  $\overset{\circ}{\mathcal{R}}$  corresponding to pairs of knots in B-splines of  $\mathcal{B}$ ,

## 1. Introduction

---

- each such T-vertex is shared by at least two B-splines in  $\mathcal{B}$ .

By using these conditions we also prove that

- the minimal number of MS B-splines necessarily actively involved in a linear dependence relation is 6, while for LR B-splines it is 8, regardless of the bidegree chosen,
- these numbers are sharp for any bidegree  $(p_1, p_2)$  in the MS B-spline set and with  $p_k \geq 2$  for some  $k$ , for the LR B-splines.

Finally, Paper 1 shows how to use the necessary condition on the T-vertices to improve the Peeling algorithm (Algorithm 1.1) in order to sort out more cases.

**Paper II** defines a new and easy to implement local refinement strategy, called  $N_2S$  structured mesh refinement, that guarantees the local linear independence of the final LR B-spline set. This strong property requires a particular displacement of the LR B-spline supports on the underlying locally refined mesh and it has never been achieved before for truly adaptive refinements. The paper contains two application sections to illustrate the qualities of the refinement strategy in quasi-interpolation and simulation contexts.

**Paper III** investigates the transfinite mean value interpolant in a general (non-convex) polygon for continuous function along the boundary of the polygon, and shows that it has the property of transfinite interpolation, that is, it coincides with the data on the boundary. This fact was only known before for convex polygons and, more in general, for domains with positive distance to their external medial axis. In addition to the proof of this property, numerical examples illustrate it.

## References

- [1] Bressan, A. “Some properties of LR-splines”. In: *Computer Aided Geometric Design* vol. 30, no. 8 (2013), pp. 778–794.
- [2] Bressan, A. and Jüttler, B. “A hierarchical construction of LR meshes in 2D”. In: *Computer Aided Geometric Design* vol. 37 (2015), pp. 9–24.
- [3] Buffa, A., Cho, D., and Sangalli, G. “Linear independence of the T-spline blending functions associated with some particular T-meshes”. In: *Computer Methods in Applied Mechanics and Engineering* vol. 199, no. 23–24 (2010), pp. 1437–1445.
- [4] Ceva, G. “De lineis rectis se invicem secantibus, statica constructio”. In: *Ludovici Montiae, Mediolanum* (1678).
- [5] de Boor, C. *A Practical Guide to Splines*. revised. Springer-Verlag New York, 2001.

- 
- [6] Deng, J. et al. “Polynomial splines over hierarchical T-meshes”. In: *Graphical models* vol. 70, no. 4 (2008), pp. 76–86.
- [7] Dokken, T., Lyche, T., and Pettersen, K. F. “Polynomial splines over locally refined box-partitions”. In: *Computer Aided Geometric Design* vol. 30, no. 3 (2013), pp. 331–356.
- [8] Dyken, C. and Floater, M. S. “Transfinite mean value interpolation”. In: *Computer Aided Geometric Design* vol. 26 (2009), pp. 117–134.
- [9] Engleitner, N. and Jüttler, B. “Patchwork B-spline refinement”. In: *Computer-Aided Design* vol. 90 (2017), pp. 168–179.
- [10] Floater, M. S. “Mean value coordinates”. In: *Computer Aided Geometric Design* vol. 20, no. 1 (2003), pp. 19–27.
- [11] Floater, M. S. “Meshless parameterization and B-spline surface approximation”. In: *The Mathematics of Surfaces IX*. Springer, 2000, pp. 1–18.
- [12] Floater, M. S. “Parametrization and smooth approximation of surface triangulations”. In: *Computer Aided Geometric Design* vol. 14, no. 3 (1997), pp. 231–250.
- [13] Floater, M. S. and Hormann, K. “Surface parameterization: a tutorial and survey”. In: *Advances in Multiresolution for Geometric Modelling*. Springer, 2005, pp. 157–186.
- [14] Floater, M. S., Kós, G., and Reimers, M. “Mean value coordinates in 3D”. In: *Computer Aided Geometric Design* vol. 22, no. 7 (2005), pp. 623–631.
- [15] Forsey, D. R. and Bartels, R. H. “Hierarchical B-spline refinement”. In: *ACM Siggraph Computer Graphics* vol. 22, no. 4 (1988), pp. 205–212.
- [16] Giannelli, C., Jüttler, B., and Speleers, H. “THB-splines: The truncated basis for hierarchical splines”. In: *Computer Aided Geometric Design* vol. 29, no. 7 (2012), pp. 485–498.
- [17] Greiner, G. and Hormann, K. “Interpolating and approximating scattered 3D-data with hierarchical tensor product B-splines”. In: *Proceedings of Chamonix*. Vol. 1. 1996.
- [18] Hormann, K. and Floater, M. S. “Mean value coordinates for arbitrary planar polygons”. In: *ACM Transactions on Graphics* vol. 25, no. 4 (2006), pp. 1424–1441.
- [19] Hughes, T. J. R., Cottrell, J. A., and Bazilevs, Y. “Isogeometric analysis: CAD, finite elements, NURBS, exact geometry and mesh refinement”. In: *Computer Methods in Applied Mechanics and Engineering* vol. 194, no. 39–41 (2005), pp. 4135–4195.
- [20] Johannessen, K. A., Kvamsdal, T., and Dokken, T. “Isogeometric analysis using LR B-splines”. In: *Computer Methods in Applied Mechanics and Engineering* vol. 269 (2014), pp. 471–514.

## 1. Introduction

---

- [21] Ju, T., Schaefer, S., and Warren, J. “Mean value coordinates for closed triangular meshes”. In: *ACM Transactions on Graphics* vol. 24 (2005), pp. 561–566.
- [22] Li, X. and Chen, F. “On the instability in the dimension of splines spaces over T-meshes”. In: *Computer Aided Geometric Design* vol. 28, no. 7 (2011), pp. 420–426.
- [23] Li, X. et al. “On linear independence of T-spline blending functions”. In: *Computer Aided Geometric Design* vol. 29, no. 1 (2012), pp. 63–76.
- [24] Lipman, Y. et al. “GPU-assisted positive mean value coordinates for mesh deformations”. In: *Symposium on Geometry Processing*. 2007.
- [25] Ma, W. and Kruth, J. P. “Parameterization of randomly measured points for least squares fitting of B-spline curves and surfaces”. In: *Computer-Aided Design* vol. 27, no. 9 (1995), pp. 663–675.
- [26] Meyer, M. et al. “Generalized barycentric coordinates on irregular polygons”. In: *Journal of Graphics Tools* vol. 7, no. 1 (2002), pp. 13–22.
- [27] Möbius, A. F. “Der Barycentrische Calcul”. In: *Johann Ambrosius Barth, Leipzig* (1827).
- [28] Pettersen, K. F. “On the dimension of multivariate spline spaces”. In: *SINTEF Report A23875* (2013).
- [29] Pinkall, U. and Polthier, K. “Computing discrete minimal surfaces and their conjugates”. In: *Experimental Mathematics* vol. 2, no. 1 (1993), pp. 15–36.
- [30] Schumaker, L. L. *Spline Functions: Basic Theory*. third. Cambridge University Press, 2007.
- [31] Sederberg, T. W. et al. “T-splines and T-NURCCs”. In: *ACM Transactions on Graphics*. Vol. 22. 3. ACM. 2003, pp. 477–484.
- [32] Tutte, W. T. “How to draw a graph”. In: *Proceedings of the London Mathematical Society* vol. 3, no. 1 (1963), pp. 743–767.
- [33] Wachspress, E. L. *A rational finite element basis*. Elsevier, 1975.
- [34] Warren, J. “Barycentric coordinates for convex polytopes”. In: *Advances in Computational Mathematics* vol. 6, no. 1 (1996), pp. 97–108.

# Papers



## Paper I

# Linear dependence of bivariate Minimal Support and Locally Refined B-splines over LR-meshes

**Francesco Patrizi, Tor Dokken**

To appear in *Computer Aided Geometric Design*. arXiv: 1811.04919.

### Abstract

The focus on locally refined spline spaces has grown rapidly in recent years due to the need in Isogeometric Analysis (IgA) of spline spaces with local adaptivity: a property not offered by the strict regular structure of tensor product B-spline spaces. However, this flexibility sometimes results in collections of B-splines spanning the space that are not linearly independent. In this paper we address the minimal number of Minimal Support B-splines (MS B-splines) and of Locally Refined B-splines (LR B-splines) that can form a linear dependence relation. We show that such minimal numbers are six for MS B-splines and eight for LR B-splines. Further results are established to help detecting collections of B-splines that are linearly independent.

### 1.1 Introduction

In 2005 Thomas J.R. Hughes et al. [12] proposed to reconstitute finite element analysis (FEA) within the geometric framework of CAD technologies. This gave rise to Isogeometric Analysis (IgA). It unifies the fields of CAD and FEA by extending the isoparametric concept of the standard finite elements to other shape functions, such as B-splines and non-uniform rational B-splines (NURBS), used in CAD. This does not only allow for an accurate geometrical description, but it also improves smoothness properties. As a consequence, IgA methods often reach a required accuracy using a much smaller number of degrees of freedom [11]. Moreover, in some situations, the increased smoothness also improves the stability of the approximations resulting in fewer nonphysical oscillations [12, 15].

## I. Linear dependence of bivariate Minimal Support and Locally Refined B-splines over LR-meshes

---

However, in numerical simulations, local (adaptive) refinements are frequently used for balancing accuracy and computational costs. Traditional B-splines and NURBS spaces are formulated as tensor products of univariate B-spline spaces. This means that refining in one of the univariate B-spline spaces will cause the insertion of an entire new row or column of knots in the bivariate spline space, resulting in a global refinement. In order to break the tensor product structure of the underlying mesh, new formulations of multivariate B-splines have been introduced addressing local refineability.

### I.1.1 Overview of locally refined spline methods

The first local refinement method introduced were the Hierarchical B-splines, or HB-splines [8], whose properties were further analyzed in [13]. The HB-splines are linearly independent and non-negative. However, partition of unity, which is a necessary for the convex hull property (essential for interpreting the B-spline coefficients as control points), was still missing. To rectify this, Truncated Hierarchical B-splines, or THB-splines, were proposed in [10] and further analyzed in [9]. In [9] they show how the construction of HB-splines can be modified while preserving the properties of HB-splines, gaining the partition of unity and smaller support of the basis functions.

A different approach, for local refinement, was introduced in [18] with the T-splines. These are defined over *T-meshes*, where T-junctions between axis aligned segments are allowed. T-splines have been used efficiently in CAD applications, being able to produce watertight and locally refined models. However, the use of the most general T-spline concept in IgA is limited by the risk of linear dependence of the resulting splines [1]. It is desirable in numerical simulations to use linearly independent basis functions to ensure that the resulting mass and stiffness matrices have full rank and avoid the algorithmic complexity posed by singular matrices. Analysis-Suitable T-splines, or AST-splines, were therefore introduced in [2]. As T-splines, AST-splines provide watertight models, obey the convex hull property, and moreover are linearly independent.

There are many other definitions of B-splines over meshes with local refinements, such as PHT-splines [4], PB-splines [7] and LR B-splines [5]. A discussion of the differences and similarities of HB-splines, THB-splines, T-splines, AST-splines and LR B-splines can be found in [6].

### I.1.2 LR B-splines and MS B-splines

In this paper we look at Locally Refined B-splines, or LR B-splines, introduced in [5]. The idea is to extend the knot insertion refinement of univariate B-splines to insertion of local line segments in tensor meshes. The process starts by considering the tensor product B-spline space over a coarse tensor mesh. Then, when a new inserted local line segment divides the support of one or more LR B-splines in two parts, we perform knot insertion to split such B-splines into two (or more) new ones. The final collection of functions does not sum to one in

general. However, it is possible to scale them by means of positive weights so that they form a partition of unity; see [5, Section 7].

The LR B-splines are a subset of the Minimal Support B-splines, or MS B-splines. As one can guess from their name, MS B-splines are the tensor product B-splines with minimal support, i.e., without superfluous line segments crossing their support, identifiable on the locally refined mesh. The main difference between LR and MS B-splines is that the former ones are defined algorithmically, while the latter are defined by the topology of the mesh.

### 1.1.3 Content of the paper

The freedom in the refinement process can result in undesirable collections of LR B-splines. Namely, the LR B-splines obtained at the end of the refinement process may be linearly dependent. Assumptions on the refinement process have to be established in order to ensure linear independence. We start such analysis by looking at conditions on the mesh necessary for linear dependence. We say that functions  $\phi_1, \dots, \phi_n : \mathbb{R}^d \rightarrow \mathbb{R}$  are **actively linearly dependent** on  $\mathbb{R}^d$  if there exist  $\alpha_i \in \mathbb{R}$ ,  $\alpha_i \neq 0$  for all  $i = 1, \dots, n$ , such that

$$\sum_{i=1}^n \alpha_i \phi_i(\mathbf{x}) = 0, \quad \forall \mathbf{x} \in \mathbb{R}^d.$$

Note that we consequentially look at the minimal set of linearly dependent functions by forbidding zero coefficients in the linear combination.

In this work we show that:

- For any bidegree  $\mathbf{p}$ , the minimal number of active MS B-splines in a linear dependence relation is six, while for LR B-splines it is eight.
- These numbers are sharp for any bidegree  $\mathbf{p} = (p_1, p_2)$  for the MS B-splines and with  $p_k \geq 2$ , for some  $k \in \{1, 2\}$ , for the LR B-splines.

We look at the minimal configurations of linear dependence because we conjecture that any linear dependence relation is a refinement of one of these minimal cases. In other words, they are the roots for the linear dependence. In particular, if this is true, by avoiding the minimal cases, the MS B-splines and LR B-splines are always linearly independent and form a basis. Furthermore, to get such lower bounds, we prove results that can be used to understand if the set of B-splines considered is linearly independent or not. In particular, they can be used to improve the Peeling Algorithm [5, Algorithm 6.3] to verify if the LR B-splines defined on a given mesh are linearly independent.

### 1.1.4 Structure of the paper

In Section I.2 we provide an introduction to the concepts of box-partitions, meshes and LR-meshes. In Section I.3 we define the univariate spline space over a knot vector sequence and the bivariate spline space over a box-partition and

## I. Linear dependence of bivariate Minimal Support and Locally Refined B-splines over LR-meshes

---

we recall the dimension formula presented in [16]. Then we discuss conditions on the mesh for ensuring that the dimension formula depends only on the topology of the mesh. In Section I.4 we recall univariate and bivariate B-splines, their basic properties and the knot insertion procedure. In Section I.5 we define the MS B-splines and the LR B-splines and we show when these two sets are different. In Section I.6 we study the spanning properties of the LR and MS B-splines. In particular we state necessary and sufficient conditions for spanning the full spline space. Knowing the dimension of the spline space, we can check linear dependencies just by counting the elements in the LR, or MS, B-spline set. In Section I.7, we identify necessary features for a linear dependence relation and we derive the minimal number of active MS B-splines needed in a linear dependence relation. In Section I.8, we compute the minimal number of active LR B-splines in a linear dependence relation. In Section I.9 we recall briefly the Peeling Algorithm for checking linear independence and we show how to improve it by using the results of Section I.7. Finally, we summarize the main results and discuss future work in Section I.10.

### I.2 Box-partitions and LR-meshes

The purpose of this section is to describe box-partitions in 2D and define bivariate LR-meshes. For our scope, and sake of simplicity, we decided to restrict general definitions, valid in any dimension, to the 2D case; we refer to [5] for the general theory.

**Definition I.2.1.** Given an axis-aligned rectangle  $\Omega \subseteq \mathbb{R}^2$ , a **box-partition** of  $\Omega$  is a finite collection  $\mathcal{E}$  of axis-aligned rectangles in  $\Omega$ , called **elements**, such that:

1.  $\beta_1 \cap \beta_2 = \emptyset$  for any  $\beta_1, \beta_2 \in \mathcal{E}$ , with  $\beta_1 \neq \beta_2$ .
2.  $\bigcup_{\beta \in \mathcal{E}} \beta = \Omega$ .

**Definition I.2.2.** Given a box-partition  $\mathcal{E}$ , we define the **vertices of  $\mathcal{E}$**  as the vertices of its elements. In particular, a vertex of  $\mathcal{E}$  is called **T-vertex** if it is the intersection of three elements edges. We denote as  $\mathcal{V}$  the set of vertices of  $\mathcal{E}$ .

**Definition I.2.3.** Given a box-partition  $\mathcal{E}$  of a rectangle  $\Omega \in \mathbb{R}^2$ , a **meshline** of  $\mathcal{E}$  is a segment contained in an element edge, connecting two and only two vertices of  $\mathcal{V}$  at its end-points. The collection of all the meshlines of the box-partition is called **mesh**,  $\mathcal{M}$ . Given a mesh  $\mathcal{M}$ , one can define a multiplicity function  $\mu : \mathcal{M} \rightarrow \mathbb{N}^*$  that associates a positive integer to every meshline, called **multiplicity of the meshline**. A mesh that has an assigned multiplicity function  $\mu$  is called  **$\mu$ -extended mesh**.

When the T-vertices of  $\mathcal{E}$  occur only on  $\partial\Omega$  and every collinear meshlines have same multiplicity, the corresponding  $\mu$ -extended mesh is called **tensor mesh**.

Finally, if every meshline of a box-partition  $\mathcal{E}$  has the same multiplicity  $m$  we say that the corresponding  $\mu$ -extended mesh has multiplicity  $m$ .

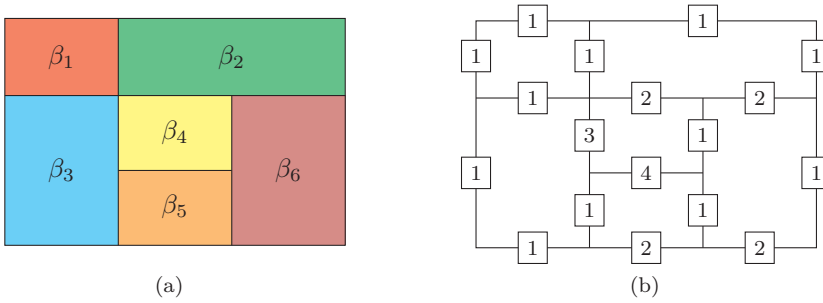


Figure I.1: Example of box-partition and corresponding mesh.

In this work we only consider  $\mu$ -extended meshes. Therefore, we will only write meshes for  $\mu$ -extended meshes to simplify the notation.

Figure I.1 shows an example of box-partition and associated mesh: in (a) the box-partition  $\mathcal{E}$  and in (b) the corresponding mesh  $\mathcal{M}$ . The meshlines are identified by squares reporting the associated multiplicities.

A meshline can be expressed as the Cartesian product of a point in  $\mathbb{R}$  and a finite interval. Let  $\alpha \in \mathbb{R}$  be the value of such a point and let  $k \in \{1, 2\}$  be its position in the Cartesian product. If  $k = 1$  the meshline is vertical and if  $k = 2$  the meshline is horizontal. We sometimes write  $k$ -meshline to specify the direction of the meshline and  $(k, \alpha)$ -meshline to specify exactly on what axis-parallel line in  $\mathbb{R}^2$  the meshline lies.

**Definition I.2.4.** Given a box-partition  $\mathcal{E}$  and an axis-aligned segment  $\gamma$ , we say that  $\gamma$  **traverses**  $\beta \in \mathcal{E}$  if  $\gamma \subseteq \beta$  and the interior of  $\beta$  is divided into two parts by  $\gamma$ , i.e.,  $\beta \setminus \gamma$  is not connected. A split is a finite union of contiguous and collinear axis-aligned segments  $\gamma = \cup_i \gamma_i$  such that every  $\gamma_i$  either is a meshline of the box-partition or  $\gamma_i$  traverses some  $\beta \in \mathcal{E}$ .

As for meshlines, we sometimes write  $k$ -split with  $k \in \{1, 2\}$  to specify the direction of the split or  $(k, \alpha)$ -split to specify on what axis-parallel line in  $\mathbb{R}^2$  the split lies, that is, to specify that it lies on the line  $\{(x_1, x_2) : x_k = \alpha\}$ .

**Definition I.2.5.** A mesh  $\mathcal{M}$  has **constant splits** if any split  $\gamma$  in  $\mathcal{M}$  is made of meshlines of the same multiplicity.

When a split  $\gamma$  is inserted in a box-partition  $\mathcal{E}$ , any traversed  $\beta \in \mathcal{E}$  is replaced by the two subrectangles  $\beta_1, \beta_2$  given by the closures of the connected components of  $\beta \setminus \gamma$ . The resulting new box-partition is indicated as  $\mathcal{E} + \gamma$  and its corresponding mesh as  $\mathcal{M} + \gamma$ . Assigned a positive integer  $\mu_\gamma$  to  $\gamma$ , the multiplicities of the meshlines in  $\mathcal{M} \cap (\mathcal{M} + \gamma)$  not contained in  $\gamma$  are unchanged, while the multiplicities of those that are in  $\gamma$  are increased by  $\mu_\gamma$ . The new meshlines contained in  $(\mathcal{M} + \gamma) \setminus \mathcal{M}$  have multiplicity equal to  $\mu_\gamma$ . If  $\mu$  was the multiplicity function associated to  $\mathcal{M}$ , the multiplicity function on the refined mesh  $\mathcal{M} + \gamma$  is denoted as  $\mu + \mu_\gamma$ . The meshes used in applications are often

## I. Linear dependence of bivariate Minimal Support and Locally Refined B-splines over LR-meshes

---

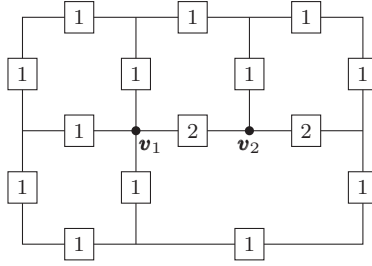


Figure I.2: Example of computation of vertical and horizontal multiplicities.

result of a mesh refinement process, that is, given an initial coarse tensor mesh  $\mathcal{M}_1$  and a sequence of splits  $\gamma_i$  with associated integers  $\mu_{\gamma_i}$  for  $i = 1, \dots, N - 1$ , the meshes considered are the final element of a sequence of meshes of the form  $\mathcal{M}_{i+1} = \mathcal{M}_i + \gamma_i$  where the associated multiplicities are  $\mu_{i+1} = \mu_i + \mu_{\gamma_i}$ . The LR-meshes are a particular subclass of this kind of meshes.

**Definition I.2.6.** An **LR-mesh** is a mesh  $\mathcal{M}$  obtained through a sequence of split insertions:

$\mathcal{M}_1$  is a tensor mesh,

$\mathcal{M}_{i+1} = \mathcal{M}_i + \gamma_i$  has constant splits, for  $i = 1, \dots, N - 1$

and  $\mathcal{M} = \mathcal{M}_N$ , for some  $N$ .

In the remaining of this section we introduce the knot vector on a split and the length of it. These concepts will help us to analyze the spanning properties of the LR B-splines and the increase in the spline space dimension due to a mesh refinement.

**Definition I.2.7.** Given a mesh  $\mathcal{M}$  corresponding to a box-partition  $\mathcal{E}$ , for any vertex  $\mathbf{v}$  in  $\mathcal{V}$  we define

$$\mu_1(\mathbf{v}) = \max\{\mu(\gamma) : \mathbf{v} \in \gamma \text{ and } \gamma \text{ 1-meshline of } \mathcal{M}\}$$

$$\mu_2(\mathbf{v}) = \max\{\mu(\gamma) : \mathbf{v} \in \gamma \text{ and } \gamma \text{ 2-meshline of } \mathcal{M}\}$$

$\mu_1(\mathbf{v})$  is called **vertical multiplicity** and  $\mu_2(\mathbf{v})$  **horizontal multiplicity** of vertex  $\mathbf{v}$ .

In Figure I.2 is reported an example of computation of horizontal and vertical multiplicities for two vertices of a box-partition. The meshlines on the left and right hand-side of  $\mathbf{v}_1$  have multiplicity 1 and 2 respectively. So  $\mu_2(\mathbf{v}_1) = \max\{1, 2\} = 2$ . The meshlines above and below  $\mathbf{v}_1$  have both multiplicity 1, so that  $\mu_1(\mathbf{v}_1) = 1$ . Concerning  $\mathbf{v}_2$ , we have  $\mu_2(\mathbf{v}_2) = 2$ , whereas  $\mu_1(\mathbf{v}_2) = \max\{1\} = 1$  since there is no meshline below  $\mathbf{v}_2$ .

**Definition I.2.8.** Given a  $(k, \alpha)$ -split  $\gamma$  in a mesh  $\mathcal{M}$ , all the vertices where  $\gamma$  intersects the meshlines of  $\mathcal{M}$ , orthogonal to it, have  $k$ th-coordinate equal to

$\alpha$  and different  $(3 - k)$ th-coordinate. We define the **knot vector on**  $\gamma$  as the increasing sequence  $\boldsymbol{\tau} \subseteq \mathbb{R}$  given by such  $(3 - k)$ th-coordinates. The elements of such sequence are called **knots**. We further define the multiplicity function of the knot vector as the  $\mu_{3-k}$  multiplicity function of the corresponding vertices. We say that  $\boldsymbol{\tau}$  has **length**  $d$  if the multiplicities of its knots sum to  $d$ .

### 1.3 Spline spaces

In this section we define the univariate spline space over a knot vector and the bivariate spline space over a box-partition. In particular we provide the dimension formula of such spaces. For the bivariate space, the formula, introduced in [16], presents terms depending on the size of the box-partition elements. This means that the dimension is unstable, i.e., spline spaces on meshes with the same topology might have a different dimension. Therefore, we recall sufficient conditions for avoiding such terms, making the formula dependent only on the mesh topology.

#### 1.3.1 Spline space on a knot vector sequence

**Definition 1.3.1.** Given an increasing sequence  $\boldsymbol{\tau} = (\tau_1, \dots, \tau_n)$  of real numbers, a positive integer  $p$  and a function  $\mu : \boldsymbol{\tau} \rightarrow \mathbb{N}^*$  such that  $0 \leq \mu(\tau_i) \leq p + 1$  for all  $i$ , we define the corresponding **spline knot vector** as the triple  $\boldsymbol{\tau}_p^\mu = (\boldsymbol{\tau}, \mu, p)$ .

Given a spline knot vector  $\boldsymbol{\tau}_p^\mu$ , we say that  $\tau_i \in \boldsymbol{\tau}$  has **full multiplicity** if  $\mu(\tau_i) = p + 1$  and we say that  $\boldsymbol{\tau}_p^\mu$  is **open** if  $\tau_1$  and  $\tau_n$  have full multiplicity.

Sometimes it is more convenient to write a spline knot vector, in the equivalent way, as the couple  $\boldsymbol{t}_p = (\boldsymbol{t}, p)$  where  $\boldsymbol{t}$  is a non-decreasing sequence  $\boldsymbol{t} = (t_1, \dots, t_\ell)$ , i.e, with  $t_i \leq t_{i+1}$ , where  $\ell = \sum_{i=1}^n \mu(\tau_i)$  and

$$\underbrace{t_1 = \dots = t_{\mu(\tau_1)}}_{=\tau_1} < \underbrace{t_{\mu(\tau_1)+1} = \dots = t_{\mu(\tau_1)+\mu(\tau_2)}}_{=\tau_2} < \dots$$

We use bold Greek letters with the multiplicity function in superscript in the first way of expression and bold Latin letters for the second way.

Given a degree  $p$ , we denote as  $\Pi_p \subset \mathbb{R}[t]$  the vector space spanned by the monomials  $t^j$  such that  $0 \leq j \leq p$ .

**Definition 1.3.2.** Given a spline knot vector  $\boldsymbol{\tau}_p^\mu = (\boldsymbol{\tau}, \mu, p)$  with  $\boldsymbol{\tau} = (\tau_1, \dots, \tau_n)$ , we define the univariate **spline space on the spline knot vector**  $\boldsymbol{\tau}_p^\mu$ , denoted  $\mathbb{S}(\boldsymbol{\tau}_p^\mu)$  or equivalently  $\mathbb{S}(\boldsymbol{t}_p)$ , as the set of all functions  $f : \mathbb{R} \rightarrow \mathbb{R}$  such that

1.  $f$  is zero outside  $[\tau_1, \tau_n]$ ,
2. the restrictions of  $f$  to the intervals  $[\tau_i, \tau_{i+1})$  for  $i < n - 1$  and  $[\tau_{n-1}, \tau_n]$  are polynomials in  $\Pi_p$ ,
3.  $f$  is  $C^{p-\mu(\tau_i)}$ -continuous at  $\tau_i$ .

## I. Linear dependence of bivariate Minimal Support and Locally Refined B-splines over LR-meshes

---

The following is the dimension of the spline space over a knot vector. It is a well-known result, proved, e.g., in [17].

**Theorem I.3.3.** *Given a spline knot vector  $\boldsymbol{\tau}_p^\mu = (\boldsymbol{\tau}, \mu, p)$  with  $\boldsymbol{\tau} = (\tau_1, \dots, \tau_n)$ , the corresponding spline space  $\mathbb{S}(\boldsymbol{\tau}_p^\mu)$  has dimension*

$$\dim \mathbb{S}(\boldsymbol{\tau}_p^\mu) = \max \left\{ \sum_{i=1}^n \mu(\tau_i) - (p+1), 0 \right\}. \quad (\text{I.1})$$

Therefore, if  $\mathbf{t}_p$  has cardinality  $p+r+1$  for some  $r \geq 1$ , then  $\dim \mathbb{S}(\mathbf{t}_p) = r$ . There are many possible bases for  $\mathbb{S}(\mathbf{t}_p)$ . One possibility is provided by a classical result in spline theory, called Curry-Schoenberg Theorem [3, Theorem 44]. It ensures that the so called B-spline functions of degree  $p$ , defined on the knot vector  $\mathbf{t}_p$ , can be used as a possible basis:

$$\mathbb{S}(\mathbf{t}_p) = \text{span} \{B[\mathbf{t}_p^i]\}_{i=1}^r \quad \text{with } \mathbf{t}_p^i = (t_i, \dots, t_{i+p+1}) \subseteq \mathbf{t}_p.$$

For a brief introduction to B-splines we refer to Section I.4.

### I.3.2 Spline space on a box-partition

**Definition I.3.4.** A **spline mesh** in  $\mathbb{R}^2$  is a triple  $\mathcal{N} = (\mathcal{M}, \mu, \mathbf{p})$  where  $\mathcal{M}$  is a mesh from a box-partition  $\mathcal{E}$ ,  $\mathbf{p} = (p_1, p_2)$  is a pair of positive integers and  $\mu : \mathcal{M} \rightarrow \mathbb{N}^*$  is a multiplicity function such that  $1 \leq \mu(\gamma) \leq p_k + 1$  for every  $k$ -meshline  $\gamma \in \mathcal{M}$ . In particular, if a  $k$ -meshline  $\gamma$  has multiplicity  $p_k + 1$  we say that  $\gamma$  has **full multiplicity** and a spline mesh  $\mathcal{N}$  is **open** if every boundary meshline has full multiplicity. A spline mesh  $\mathcal{N}$  where  $\mathcal{M}$  is an LR-mesh will be called **spline LR-mesh**.

*Remark I.3.5.* Given a spline mesh  $\mathcal{N} = (\mathcal{M}, \mu, \mathbf{p})$ , one can define a spline knot vector on any  $k$ -split of  $\mathcal{M}$ , for  $k \in \{1, 2\}$ : the sequence  $\boldsymbol{\tau}$  and the multiplicity function  $\mu_{3-k}$  are described in Definition I.2.8 and the degree is  $p_{3-k}$ .

Given a bidegree  $\mathbf{p} = (p_1, p_2)$ , we denote as  $\Pi_{\mathbf{p}} \subset \mathbb{R}[x, y]$  the vector space spanned by the monomials  $x^{i_1}y^{i_2}$  such that  $0 \leq i_k \leq p_k$  for  $k = 1, 2$ .

**Definition I.3.6.** Given a spline mesh  $\mathcal{N} = (\mathcal{M}, \mu, \mathbf{p})$  corresponding to a box-partition  $\mathcal{E}$  of a rectangle  $\Omega = [a_1, b_1] \times [a_2, b_2]$ , for any element  $\beta \in \mathcal{E}$ ,  $\beta = J_1 \times J_2$  with  $J_k = [a_{\beta,k}, b_{\beta,k}]$ , we set

$$\tilde{\beta} = \tilde{J}_1 \times \tilde{J}_2 \quad \text{with } \tilde{J}_k = \begin{cases} [a_{\beta,k}, b_{\beta,k}) & \text{if } b_{\beta,k} < b_k \\ [a_{\beta,k}, b_{\beta,k}] & \text{if } b_{\beta,k} = b_k. \end{cases} \quad (\text{I.2})$$

The **spline space on  $\mathcal{N}$** , denoted by  $\mathbb{S}(\mathcal{N})$ , is the set of all functions  $f : \mathbb{R}^2 \rightarrow \mathbb{R}$  such that

1.  $f$  is zero outside  $\Omega$ ,

2. for each element  $\beta \in \mathcal{E}$ , the restriction of  $f$  to  $\tilde{\beta}$  is a bivariate polynomial function in  $\Pi_{\mathbf{p}}$ ,
3. for each  $k$ -meshline  $\gamma \in \mathcal{M}$ ,  $f$  is  $C^{p_k - \mu(\gamma)}$ -continuous across  $\gamma$ .

The general dimension formula of the spline space over spline meshes is presented in [16] and has terms depending on the size of the box-partition elements. This makes the dimension of the spline space unstable [14], i.e., not only dependent on the mesh topology. However, if we consider the spline space over a spline LR-mesh built so that

- **LR-rule 1:** the starting tensor mesh  $\mathcal{M}_1$  has at least  $p_1 + 2$  vertical splits and  $p_2 + 2$  horizontal splits counting their multiplicities,
- **LR-rule 2:** for  $k \in \{1, 2\}$ , the knot vector on any maximal  $k$ -split has length at least  $p_{3-k} + 2$  at any step in the construction of the LR-mesh,

then, one can prove, by using the results in [16], that, called  $\mathcal{M}^k$  the set of all the  $k$ -meshlines in  $\mathcal{M}$ , for  $k \in \{1, 2\}$ , and  $|\mathcal{E}|$  the cardinality of  $\mathcal{E}$ , we have

$$\begin{aligned} \dim \mathbb{S}(\mathcal{N}) &= \sum_{\mathbf{v} \in \mathcal{V}} [(p_1 - \mu_1(\mathbf{v}) + 1)(p_2 - \mu_2(\mathbf{v}) + 1)] \\ &\quad - (p_2 + 1) \sum_{\beta \in \mathcal{M}^1} [(p_1 - \mu(\beta) + 1)] - (p_1 + 1) \sum_{\beta \in \mathcal{M}^2} [(p_2 - \mu(\beta) + 1)] \\ &\quad + |\mathcal{E}|(p_1 + 1)(p_2 + 1), \end{aligned} \tag{I.3}$$

which depends only on the topology of the mesh. In this paper we will always assume the LR-rules for constructing LR-meshes.

*Remark I.3.7.* In the LR-mesh building process, any extension of an older split is allowed being LR-rule 2 satisfied on the new mesh.

From equation (I.3), it is possible to prove the dimension increasing formula [5, Theorem 5.5]. Knowing  $\dim \mathbb{S}(\mathcal{N})$ , through this formula, one can easily compute the dimension of the spline space on a refined spline mesh  $\mathcal{N} + \gamma := (\mathcal{M} + \gamma, \mu + \mu_\gamma, \mathbf{p})$ . First, we need to introduce the concept of expanded spline knot vector on a split.

**Definition I.3.8.** When a spline mesh  $\mathcal{N} = (\mathcal{M}, \mu, \mathbf{p})$  is refined by inserting a  $k$ -split  $\gamma$ , since it is a split in  $\mathcal{M} + \gamma$ ,  $\gamma$  has a spline knot vector on it,  $\boldsymbol{\tau}_{p_{3-k}}^{\mu_{3-k}}$ , with assigned multiplicity  $\mu_{3-k}$ . The **expanded spline knot vector** on  $\gamma$ ,  $\boldsymbol{\tau}_{p_{3-k}}^{\mu_{3-k}}$ , has same sequence  $\boldsymbol{\tau}$ , same degree  $p_{3-k}$  and same multiplicity function  $\mu_{3-k}$  except that, in case  $\gamma$  is an extension of a split of  $\mathcal{M}$ , it is assigned full multiplicity to the point of  $\boldsymbol{\tau}$  corresponding to the joint vertex of the extension.

In particular, if  $\gamma$  is an extension of two splits  $\gamma_1, \gamma_2$  in  $\mathcal{M}$ , i.e.,  $\gamma$  is the link between  $\gamma_1, \gamma_2$ , then the first and last knots in the expanded spline knot vector on  $\gamma$  have full multiplicity.

We can now give the dimension increasing formula.

## I. Linear dependence of bivariate Minimal Support and Locally Refined B-splines over LR-meshes

---

**Theorem I.3.9.** *Given a spline LR-mesh  $\mathcal{N}$  and a new  $k$ -split  $\gamma$  such that the expanded spline knot vector  $\boldsymbol{\tau}_{p_{3-k}}^{\mu_{3-k}}$  on  $\gamma$  has length  $p_{3-k} + r + 1$  with  $r \geq 1$ , then the spline space on the refined spline mesh  $\mathcal{N} + \gamma := (\mathcal{M} + \gamma, \mu + \mu_\gamma, \mathbf{p})$  has dimension*

$$\dim \mathbb{S}(\mathcal{N} + \gamma) = \dim \mathbb{S}(\mathcal{N}) + \dim \mathbb{S}(\boldsymbol{\tau}_{p_{3-k}}^{\mu_{3-k}}) = \dim \mathbb{S}(\mathcal{N}) + r.$$

### I.4 Univariate B-splines and bivariate B-splines

In this section we recall the definition of B-splines and their main properties. In particular, we state the knot insertion algorithm, which is used for the definition of LR B-splines. For a complete overview on B-splines we refer to [3] and [17].

#### I.4.1 Univariate B-splines

**Definition I.4.1.** For a non-decreasing sequence  $\mathbf{t} = (t_1, t_2, \dots, t_{p+2})$  we define a **B-spline**  $B[\mathbf{t}] : \mathbb{R} \rightarrow \mathbb{R}$  of **degree**  $p \geq 0$  recursively by

$$B[\mathbf{t}](t) = \frac{t - t_1}{t_{p+1} - t_1} B[t_1, \dots, t_{p+1}](t) + \frac{t_{p+2} - t}{t_{p+2} - t_2} B[t_2, \dots, t_{p+2}](t), \quad (\text{I.4})$$

where each time a fraction with zero denominator appears, it is taken as zero. The initial B-splines of degree 0 on  $\mathbf{t}$  are defined as

$$B[t_i, t_{i+1}](t) := \begin{cases} 1 & \text{if } t_i \leq t < t_{i+1}; \\ 0 & \text{otherwise;} \end{cases} \quad \text{for } i = 1, \dots, p+1. \quad (\text{I.5})$$

The sequence  $\mathbf{t}$  is called **knot vector** of  $B[\mathbf{t}]$  and  $t_j$  are its **knots**. A knot  $t_j$  has multiplicity  $\mu(t_j)$  if it appears  $\mu(t_j)$  times in  $\mathbf{t}$ .

**Proposition I.4.2** (Properties). *Given a degree  $p \geq 0$  and a knot vector  $\mathbf{t} = (t_1, \dots, t_{p+2})$ ,*

- $\text{supp } B[\mathbf{t}] = [t_1, t_{p+2}]$ ,
- $B[\mathbf{t}]$  restricted to every nontrivial half-open element  $[t_i, t_{i+1})$  is in  $\Pi_p$ ,
- $B[\mathbf{t}]$  is  $C^{p-\mu(t_j)}$ -continuous at any knot  $t_j$  of multiplicity  $\mu(t_j)$ .

**Theorem I.4.3** (knot insertion). *Given a degree  $p$  and a knot vector  $\mathbf{t} = (t_1, \dots, t_{p+2})$ , suppose we insert a knot  $\hat{t} \in (t_1, t_{p+2})$ . We obtain two knot vectors  $\mathbf{t}_1$  and  $\mathbf{t}_2$ , considering the first and the last  $p+2$  knots respectively in  $(t_1, \dots, \hat{t}, \dots, t_{p+2})$ . Then there exist  $\alpha_1, \alpha_2 \in (0, 1]$  such that*

$$B[\mathbf{t}] = \alpha_1 B[\mathbf{t}_1] + \alpha_2 B[\mathbf{t}_2]. \quad (\text{I.6})$$

## 1.4.2 Bivariate B-splines

**Definition 1.4.4.** Consider a bidegree  $\mathbf{p} = (p_1, p_2)$ . Let  $\mathbf{x} = (x_1, \dots, x_{p_1+2})$  and  $\mathbf{y} = (y_1, \dots, y_{p_2+2})$  be nondecreasing sequences. We define the **tensor product B-spline**  $B[\mathbf{x}, \mathbf{y}] : \mathbb{R}^2 \rightarrow \mathbb{R}$  by

$$B[\mathbf{x}, \mathbf{y}](x, y) := B[\mathbf{x}](x)B[\mathbf{y}](y), \quad (\text{I.7})$$

where  $B[\mathbf{x}]$  and  $B[\mathbf{y}]$  are the univariate B-splines defined on  $\mathbf{x}$  and  $\mathbf{y}$  respectively.

The pair  $\mathbf{x}, \mathbf{y}$  identifies a tensor mesh in  $[x_1, x_{p_1+2}] \times [y_1, y_{p_2+2}]$ ,  $\mathcal{M}[\mathbf{x}, \mathbf{y}]$ . In fact, a knot in the  $x$ -direction  $x_i$  corresponds to the 1-split

$$\gamma = \bigcup_{j=1}^{p_2+1} \gamma_j \quad \text{with } \gamma_j = \{x_i\} \times [y_j, y_{j+1}]$$

and multiplicity  $\mu[\mathbf{x}, \mathbf{y}](\gamma_j)$  equal to the multiplicity of  $x_i$  in  $\mathbf{x}$ , for all  $j$ . In the same way the knots  $y_j$  in  $\mathbf{y}$  identify the 2-splits in  $\mathcal{M}[\mathbf{x}, \mathbf{y}]$  and their assigned multiplicities.

The properties of univariate B-splines are conserved by the tensor product B-splines:

- $\text{supp } B[\mathbf{x}, \mathbf{y}] = [x_1, x_{p_1+2}] \times [y_1, y_{p_2+2}]$ .
- $B[\mathbf{x}, \mathbf{y}]$  is a piecewise bivariate polynomial of bidegree  $\mathbf{p}$ .
- $B[\mathbf{x}, \mathbf{y}]$  is  $C^{p_k - \mu(\gamma)}$ -continuous across each  $k$ -meshline  $\gamma$  of  $\mathcal{M}[\mathbf{x}, \mathbf{y}]$ .

As in the univariate case, after the insertion of a knot  $\hat{x}$  in  $\mathbf{x}$ , we define  $\mathbf{x}_1$  and  $\mathbf{x}_2$  considering in  $(x_1, \dots, \hat{x}, \dots, x_{p_1+2})$  the first and last  $p_1 + 2$  knots respectively and we can write  $B[\mathbf{x}, \mathbf{y}]$  in terms of two B-splines defined on the two new pairs of knot vectors

$$B[\mathbf{x}, \mathbf{y}] = \alpha_1 B[\mathbf{x}_1, \mathbf{y}] + \alpha_2 B[\mathbf{x}_2, \mathbf{y}] \quad \text{with } \alpha_1, \alpha_2 \in (0, 1]. \quad (\text{I.8})$$

The same holds when inserting a knot  $\hat{y}$  in  $\mathbf{y}$ .

Finally, consider a spline mesh  $\mathcal{N} = (\mathcal{M}, \mu, \mathbf{p})$  with  $\mathcal{M}$  a tensor mesh. Then there exist two spline knot vectors  $\mathbf{x}_{p_1}$  and  $\mathbf{y}_{p_2}$  that identify  $\mathcal{M}$ ,  $\mathcal{M} = \mathcal{M}[\mathbf{x}_{p_1}, \mathbf{y}_{p_2}]$ , as explained before for the tensor mesh  $\mathcal{M}[\mathbf{x}, \mathbf{y}]$  in the support of  $B[\mathbf{x}, \mathbf{y}]$ . Assume that  $\mathbf{x}_{p_1}$  and  $\mathbf{y}_{p_2}$  have length  $p_1 + r_1 + 1$  and  $p_2 + r_2 + 1$  respectively, with  $r_1, r_2 \geq 1$ . We can apply the Curry-Schoenberg Theorem on each spline knot vector and state that

$$\mathbb{S}(\mathcal{N}) = \text{span} \{B[\mathbf{x}_{p_1}^i, \mathbf{y}_{p_2}^j]\} \quad \text{with } i = 1, \dots, r_1 \text{ and } j = 1, \dots, r_2,$$

where  $\mathbf{x}_{p_1}^i = (x_i, \dots, x_{i+p_1+1}) \subseteq \mathbf{x}_{p_1}$  and  $\mathbf{y}_{p_2}^j = (y_j, \dots, y_{j+p_2+1}) \subseteq \mathbf{y}_{p_2}$ .

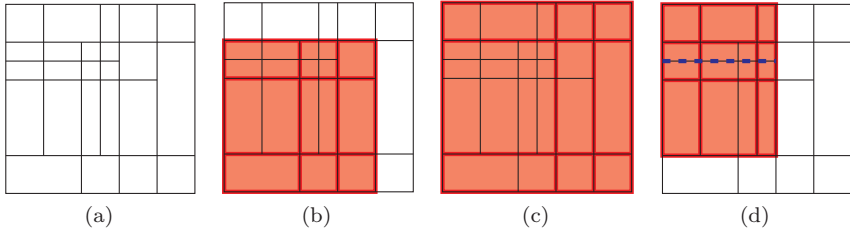


Figure I.3: Support of B-splines of bidegree  $(2, 2)$  on a mesh  $\mathcal{M}$  of multiplicity 1. The mesh is shown in (a). The B-splines whose supports are depicted in (b) and (c) have minimal support on  $\mathcal{M}$ . The tensor meshes defined by their knots in their supports are highlighted with thicker lines. On the other hand, the B-spline in (d) does not have minimal support on  $\mathcal{M}$ : the collection of meshlines contained in the dashed line disconnects the support.

## I.5 Minimal Support B-splines and Locally Refined B-splines

In this section we define first the Minimal Support B-splines, or MS B-splines, and then the Locally Refined B-splines, or LR B-splines. As we will see the LR B-splines are created algorithmically, refining, after the insertion of a split in the mesh, the B-splines whose support is traversed by the split through the knot insertion procedure. The main difference with the MS B-splines is that these latter are not always the result of a knot insertion. For a given bidegree, they depend only on the position and multiplicities of the meshlines on the mesh.

**Definition I.5.1.** Given a bivariate B-spline  $B[\mathbf{x}, \mathbf{y}]$  and a split  $\gamma$ , we say that  $\gamma$  **traverses**  $B[\mathbf{x}, \mathbf{y}]$  if  $\text{supp } B[\mathbf{x}, \mathbf{y}] \setminus \gamma$  is not connected.

**Definition I.5.2.** Given a mesh  $\mathcal{M}$  and a B-spline  $B[\mathbf{x}, \mathbf{y}]$ , we say that  $B[\mathbf{x}, \mathbf{y}]$  has **support** on  $\mathcal{M}$  if the meshlines in  $\mathcal{M}[\mathbf{x}, \mathbf{y}]$  can be obtained as unions of meshlines in  $\mathcal{M}$ , and their multiplicities in  $\mathcal{M}[\mathbf{x}, \mathbf{y}]$  are less than or equal to the multiplicities of the corresponding meshlines in  $\mathcal{M}$ . Furthermore, we say that  $B[\mathbf{x}, \mathbf{y}]$  has **minimal support** on  $\mathcal{M}$  if it has support on  $\mathcal{M}$ , the multiplicities of the interior meshlines in  $\mathcal{M}[\mathbf{x}, \mathbf{y}]$  are equal to the multiplicities of the corresponding meshlines in  $\mathcal{M}$  and there is no split  $\gamma$  in  $\mathcal{M} \setminus \mathcal{M}[\mathbf{x}, \mathbf{y}]$  that traverses  $B[\mathbf{x}, \mathbf{y}]$ . Given a spline mesh  $\mathcal{N} = (\mathcal{M}, \mu, \mathbf{p})$ , the set of the minimal support B-splines, or MS B-splines, on  $\mathcal{N}$  of bidegree  $\mathbf{p}$  is denoted as  $\mathcal{B}^{\text{MS}}(\mathcal{N})$ .

Figure I.3 shows examples of B-splines of bidegree  $(2, 2)$  with support on a mesh of multiplicity 1. In particular, the B-splines considered in Figure I.3(b)–(c) have minimal support, while the support of the B-spline in Figure I.3(d) can be disconnected by the split  $\gamma$ , visualized by dashed lines in the figure.

Given a mesh  $\mathcal{M}$  and a B-spline  $B[\mathbf{x}, \mathbf{y}]$  with support in  $\mathcal{M}$ , assume that there exists a  $(k, \alpha)$ -split  $\gamma$  in  $\mathcal{M} \setminus \mathcal{M}[\mathbf{x}, \mathbf{y}]$  that traverses  $B[\mathbf{x}, \mathbf{y}]$ . Assume also

that the meshlines in  $\gamma$  have all the same multiplicity  $m$ . One could then consider  $\alpha$  as an extra knot of multiplicity  $m$  in the  $k$ th knot vectors of  $B[\mathbf{x}, \mathbf{y}]$  (in  $\mathbf{x}$  if  $k = 1$  and in  $\mathbf{y}$  if  $k = 2$ ) and perform the knot insertion on  $B[\mathbf{x}, \mathbf{y}]$ . The resulting generated B-splines would still have support on  $\mathcal{M}$  and eventually they would also have minimal support on  $\mathcal{M}$ . The LR B-splines are generated throughout the construction of an LR-mesh following this procedure.

**Definition I.5.3.** Given a spline LR-mesh  $\mathcal{N} = (\mathcal{M}, \mu, \mathbf{p})$  with  $\mathcal{M} = \mathcal{M}_N$  final mesh of a mesh sequence as described in Definition I.2.6, the **LR B-spline set**  $\mathcal{B}^{\mathcal{LR}}(\mathcal{N})$  is provided algorithmically as follows. We start by considering the set  $\mathcal{B}_1$  of standard B-splines on the initial coarse tensor mesh  $\mathcal{M}_1$ . Then, for any intermediate step  $\mathcal{M}_{i+1} = \mathcal{M}_i + \gamma_i$  with  $i = 1, \dots, N - 1$  in the construction of the LR-mesh, we produce a new set of B-splines  $\mathcal{B}_{i+1}$  by the following algorithm:

1. initialize  $\mathcal{B}_{i+1} \leftarrow \mathcal{B}_i$ ,
2. as long as there exists  $B[\mathbf{x}^j, \mathbf{y}^j] \in \mathcal{B}_{i+1}$  with no minimal support on  $\mathcal{M}_{i+1}$ ,

a) apply knot insertion:

$$\exists B[\mathbf{x}_1^j, \mathbf{y}_1^j], B[\mathbf{x}_2^j, \mathbf{y}_2^j] : B[\mathbf{x}^j, \mathbf{y}^j] = \alpha_1 B[\mathbf{x}_1^j, \mathbf{y}_1^j] + \alpha_2 B[\mathbf{x}_2^j, \mathbf{y}_2^j],$$

b) update the set:  $\mathcal{B}_{i+1} \leftarrow (\mathcal{B}_{i+1} \setminus \{B[\mathbf{x}^j, \mathbf{y}^j]\}) \cup \{B[\mathbf{x}_1^j, \mathbf{y}_1^j], B[\mathbf{x}_2^j, \mathbf{y}_2^j]\}$ ,

3.  $\mathcal{B}^{\mathcal{LR}}(\mathcal{N}) := \mathcal{B}_N$ .

*Remark I.5.4.* For any spline LR-mesh  $\mathcal{N} = (\mathcal{M}, \mu, \mathbf{p})$ ,  $\text{span } \mathcal{B}^{\mathcal{LR}}(\mathcal{N}) \subseteq \text{span } \mathcal{B}^{\mathcal{MS}}(\mathcal{N}) \subseteq \mathbb{S}(\mathcal{N})$ . If  $\mathcal{M}$  is a tensor mesh then  $\mathcal{B}^{\mathcal{LR}}(\mathcal{N}) = \mathcal{B}^{\mathcal{MS}}(\mathcal{N})$  and they are nothing more than the standard bivariate B-splines. The Curry-Schoenberg Theorem ensures that  $\text{span } \mathcal{B}^{\mathcal{LR}}(\mathcal{N}) = \text{span } \mathcal{B}^{\mathcal{MS}}(\mathcal{N}) = \mathbb{S}(\mathcal{N})$  and the elements of  $\mathcal{B}^{\mathcal{LR}}(\mathcal{M}) = \mathcal{B}^{\mathcal{MS}}(\mathcal{M})$  are linearly independent. However, there are other cases where this equality holds; we will see them in the next section.

After performing the LR B-splines generation algorithm, the functions created will generally not sum to one. For this reason, in [5, Section 7] is provided a procedure for positive scaling weights of the LR B-splines to reinstate the partition of unity.

**Example I.5.5** ( $\mathcal{B}^{\mathcal{LR}}(\mathcal{N}) \neq \mathcal{B}^{\mathcal{MS}}(\mathcal{N})$ ).

In Figure I.4(a) we have an LR-mesh  $\mathcal{M}$  of multiplicity 1. Suppose  $\mathbf{p} = (2, 2)$ . This mesh is obtained by inserting two 2-splits and two 1-splits in a tensor mesh  $\mathcal{M}_1$ . In Figure I.4(b) we see the supports of the LR B-splines on  $\mathcal{M}$ , i.e., the elements of  $\mathcal{B}^{\mathcal{LR}}(\mathcal{N})$ , with  $\mathcal{N} = (\mathcal{M}, 1, (2, 2))$ , obtained by refining the B-splines with no minimal support during the insertion of the splits. However if we look at the final mesh  $\mathcal{M}$  in Figure I.4(a), we see that there is one MS B-spline, whose support is depicted in Figure I.4(c), not in  $\mathcal{B}^{\mathcal{LR}}(\mathcal{N})$ , defined on the mesh.

## I. Linear dependence of bivariate Minimal Support and Locally Refined B-splines over LR-meshes

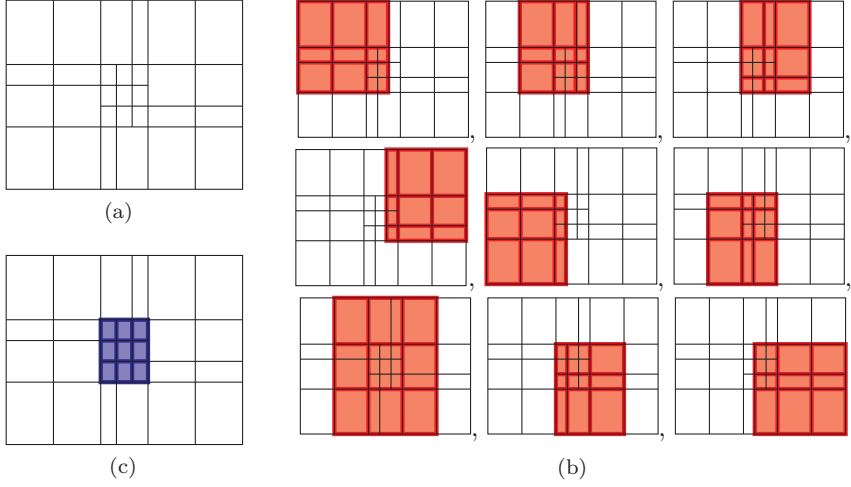


Figure I.4: (a) an LR-mesh  $\mathcal{M}$  of multiplicity 1. (b) Supports of the biquadratic LR B-splines defined on  $\mathcal{M}$ . (c) Support of a minimal support B-spline on the mesh but not in  $\mathcal{B}^{\mathcal{LR}}(\mathcal{N})$ .

### I.6 Hand-in-hand principle

In this section we describe the spanning properties of the sets  $\mathcal{B}^{\mathcal{MS}}(\mathcal{N})$  and  $\mathcal{B}^{\mathcal{LR}}(\mathcal{N})$ . Any LR-mesh  $\mathcal{M} = \mathcal{M}_N$  is defined through a sequence  $\mathcal{M}_{i+1} = \mathcal{M}_i + \gamma_i$  starting from a tensor mesh  $\mathcal{M}_1$ . We know that on  $\mathcal{N}_1 = (\mathcal{M}_1, \mu_1, \mathbf{p})$ ,  $\text{span } \mathcal{B}^{\mathcal{MS}}(\mathcal{N}_1) = \mathbb{S}(\mathcal{N}_1)$  as well as  $\text{span } \mathcal{B}^{\mathcal{LR}}(\mathcal{N}_1) = \mathbb{S}(\mathcal{N}_1)$ . We want to preserve these equalities throughout the construction of  $\mathcal{M}_N$  for two reasons. First, we maximize the approximation power of the considered B-splines because the full spline space is spanned, and second, since we have a dimension formula for the spline space, we can use it to determine if the B-splines are linearly dependent or not. Indeed, since they span the whole spline space, if there are more B-splines than the dimension, they must be linearly dependent.

**Definition I.6.1.** Given a spline LR-mesh  $\mathcal{N} = (\mathcal{M}, \mu, \mathbf{p})$ , assume that  $\text{span } \mathcal{B}^{\mathcal{MS}}(\mathcal{N}) = \mathbb{S}(\mathcal{N})$ , or  $\text{span } \mathcal{B}^{\mathcal{LR}}(\mathcal{N}) = \mathbb{S}(\mathcal{N})$  respectively. Let  $\gamma$  be a new split and let  $\mathcal{N} + \gamma = (\mathcal{M} + \gamma, \mu + \mu_\gamma, \mathbf{p})$  be the refined spline mesh. We say that  $\mathcal{N} + \gamma$  goes **MS-wise**, or **LR-wise** respectively, **hand-in-hand** with  $\mathcal{N}$  if  $\text{span } \mathcal{B}^{\mathcal{MS}}(\mathcal{N} + \gamma) = \mathbb{S}(\mathcal{N} + \gamma)$ , or  $\text{span } \mathcal{B}^{\mathcal{LR}}(\mathcal{N} + \gamma) = \mathbb{S}(\mathcal{N} + \gamma)$  respectively.

In other words, going hand-in-hand means that if the considered B-splines on the spline mesh  $\mathcal{N}$  span the whole spline space  $\mathbb{S}(\mathcal{N})$ , then also the refined B-splines defined on  $\mathcal{N} + \gamma$  will span the refined spline space  $\mathbb{S}(\mathcal{N} + \gamma)$ .

*Remark I.6.2.* If  $\mathcal{N} + \gamma$  goes LR-wise hand-in-hand with  $\mathcal{N}$ , then it also goes MS-wise hand-in-hand with  $\mathcal{N}$ . This is trivial because  $\mathcal{B}^{\mathcal{LR}}(\mathcal{N} + \gamma) \subseteq \mathcal{B}^{\mathcal{MS}}(\mathcal{N} + \gamma)$ . The converse is not true in general.

In order to keep spanning the spline space during the construction of an

LR-mesh, we have to ensure that all the intermediate spline meshes go MS-wise, or LR-wise, hand-in-hand. A condition to achieve this is stated in the following result, which is a reformulation of [5, Theorem 5.10].

**Theorem I.6.3.** *Let  $\mathcal{N} = (\mathcal{M}, \mu, \mathbf{p})$  be a spline LR-mesh. Assume that  $\text{span } \mathcal{B}^{\mathcal{MS}}(\mathcal{N}) = \mathbb{S}(\mathcal{N})$ , or  $\text{span } \mathcal{B}^{\mathcal{LR}}(\mathcal{N}) = \mathbb{S}(\mathcal{N})$  respectively. Let  $\gamma$  be a new  $k$ -split to insert and  $\tau_{p_{3-k}}^{\tilde{\mu}_{3-k}}$  be the expanded spline knot vector on it. Let  $\mathcal{B}^{\mathcal{MS}}(\gamma)$ , or  $\mathcal{B}^{\mathcal{LR}}(\gamma)$  respectively, be the collections of the new B-splines created in the MS, or LR, B-spline set after the insertion of  $\gamma$ . For any  $B \in \mathcal{B}^{\mathcal{MS}}(\gamma)$ , or  $B \in \mathcal{B}^{\mathcal{LR}}(\gamma)$  respectively, let  $B_\gamma$  be the univariate B-spline in the  $y$  variable if  $k = 1$  or in the  $x$  variable if  $k = 2$ , in the expression of  $B$  as in Definition I.4.4. Then  $\mathcal{N} + \gamma$  goes MS-wise, or LR-wise respectively, hand-in-hand with  $\mathcal{N}$  if and only if*

$$\text{span } \{B_\gamma\}_{B \in \mathcal{B}^{\mathcal{MS}}(\gamma) \text{ (or } \mathcal{B}^{\mathcal{LR}}(\gamma) \text{ resp.)}} = \mathbb{S}(\tau_{p_{3-k}}^{\tilde{\mu}_{3-k}}).$$

Theorem I.6.3 allows to check the hand-in-hand of the meshes by looking at the span of univariate B-splines. Note that, since all the  $B_\gamma$  are contained in  $\mathbb{S}(\tau_{p_{3-k}}^{\tilde{\mu}_{3-k}})$ , we always have

$$\dim \text{span} \{B_\gamma\}_{B \in \mathcal{B}^{\mathcal{MS}}(\gamma) \text{ (or } \mathcal{B}^{\mathcal{LR}}(\gamma) \text{ resp.)}} \leq \dim \mathbb{S}(\tau_{p_{3-k}}^{\tilde{\mu}_{3-k}}).$$

We distinguish two cases when this is a strict inequality:

1. The cardinality of  $\mathcal{B}^{\mathcal{MS}}(\gamma)$ , or  $\mathcal{B}^{\mathcal{LR}}(\gamma)$  respectively, is less than  $\dim \mathbb{S}(\tau_{p_{3-k}}^{\tilde{\mu}_{3-k}})$ ,
2. the cardinality of  $\mathcal{B}^{\mathcal{MS}}(\gamma)$ , or  $\mathcal{B}^{\mathcal{LR}}(\gamma)$  respectively, is at least equal to  $\dim \mathbb{S}(\tau_{p_{3-k}}^{\tilde{\mu}_{3-k}})$  but the linearly independent univariate B-splines  $B_\gamma$  are less than such dimension.

The cardinality of  $\mathcal{B}^{\mathcal{MS}}(\gamma)$ , or  $\mathcal{B}^{\mathcal{LR}}(\gamma)$ , depends on the mutual position of the splits in  $\mathcal{M} + \gamma$ . However, by slight modifications of the mesh or by extending  $\gamma$  we can always guarantee that  $\mathcal{B}^{\mathcal{MS}}(\gamma)$  and  $\mathcal{B}^{\mathcal{LR}}(\gamma)$  have at least  $\dim \mathbb{S}(\tau_{p_{3-k}}^{\tilde{\mu}_{3-k}})$  elements, as explained in Figure I.5. There we consider bidegree  $\mathbf{p} = (2, 2)$  and a 1-split  $\gamma$  to insert into the LR-mesh  $\mathcal{M}$  of multiplicity 1 as shown in Figures I.5(a). Since the expanded spline knot vector on  $\gamma$  has length 4,  $\dim \mathbb{S}(\mathcal{N} + \gamma) = \dim \mathbb{S}(\mathcal{N}) + 1$  by Theorem I.3.9. Therefore, a new B-spline of the considered kind must be generated to have  $\mathcal{N} + \gamma$  going MS-wise or LR-wise hand-in-hand with  $\mathcal{N}$ .

Unfortunately, no B-splines are created after the insertion due to the splits mutual position. Thus  $\mathcal{B}^{\mathcal{MS}}(\mathcal{N} + \gamma) = \mathcal{B}^{\mathcal{MS}}(\mathcal{N})$ ,  $\mathcal{B}^{\mathcal{LR}}(\mathcal{N} + \gamma) = \mathcal{B}^{\mathcal{LR}}(\mathcal{N})$  and  $\mathcal{N} + \gamma$  cannot go neither LR-wise nor MS-wise hand-in-hand with  $\mathcal{N}$ . However, if we extend by one meshline a split on  $\mathcal{N}$ , we create a new MS B-spline when inserting  $\gamma$ , whose support is highlighted in Figure I.5(b). In this case,  $\mathcal{N} + \gamma$  goes MS-wise hand-in-hand (but not LR-wise). Instead, if we extend by two meshlines the same split, as in Figure I.5(c), or we extend by one meshlines both the splits, as in Figure I.5(d), there is an LR B-spline on the mesh to refine

## I. Linear dependence of bivariate Minimal Support and Locally Refined B-splines over LR-meshes

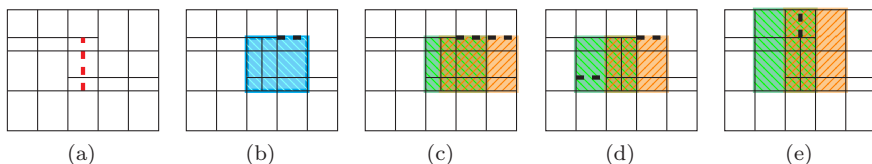


Figure I.5: (a) LR-mesh  $\mathcal{M}$  of multiplicity 1 and a new split (dashed) to insert. (b) modification of  $\mathcal{M}$  (dashed) to go MS-wise hand-in-hand. (c),(d),(e) modification of  $\mathcal{M}$  (dashed) to go LR-wise hand-in-hand.

after the insertion of  $\gamma$  and  $\mathcal{N} + \gamma$  goes LR-wise hand-in-hand with  $\mathcal{N}$ . Another strategy is to extend  $\gamma$ . Indeed, if we decide to insert  $\gamma$  one meshline longer, as in Figure I.5(e), then the spline space increases by 2 for Theorem I.3.9 but  $\mathcal{N} + \gamma$  goes LR-wise, and so MS-wise, hand-in-hand with  $\mathcal{N}$  because the two LR B-splines with supports in the upper left and upper right corner of  $\mathcal{M}$  will be refined.

However, although the cardinality of such sets is sufficiently large, the linearly independent univariate B-splines  $B_\gamma$  can be insufficient for spanning the whole spline space  $\mathbb{S}(\tau_{p_{3-k}}^{\mu_{3-k}})$ . An example is reported in Figure I.6. We again consider bidegree (2, 2), an LR-mesh  $\mathcal{M}$  of multiplicity 1 and a new 2-split  $\gamma$  as shown in Figure I.6(a).

The expanded spline knot vector on  $\gamma$  has length 7 so that  $\dim \mathbb{S}(\mathcal{N} + \gamma) = \dim \mathbb{S}(\mathcal{N}) + 4$  by Theorem I.3.9. Moreover, it is easy to check that  $\mathcal{N}$  can be constructed LR-wise hand-in-hand. Therefore,  $\mathcal{B}^{\mathcal{LR}}(\mathcal{N}) = \mathcal{B}^{\mathcal{MS}}(\mathcal{N})$  and they span the spline space  $\mathbb{S}(\mathcal{N})$ . When  $\gamma$  is inserted, there are 5 LR B-splines,  $B^1, B^2, B^3, B^4, B^5$ , in  $\mathcal{B}^{\mathcal{LR}}(\gamma)$ , whose support is depicted in Figure I.6(b). The cardinalities  $|\mathcal{B}^{\mathcal{LR}}(\gamma)|, |\mathcal{B}^{\mathcal{MS}}(\gamma)|$  are therefore large enough for  $\mathcal{N} + \gamma$  to go hand-in-hand with  $\mathcal{N}$ . However, if we look at the univariate B-splines  $B_\gamma$ , depicted in Figure I.6(c), we can see that the  $B_\gamma^4 = B_\gamma^5$  and  $B_\gamma^3$  can be easily written, via knot insertion, as a linear combination of  $B_\gamma^1, B_\gamma^2$ . Thus, there are only 3 linearly independent B-splines in  $\{B_\gamma\}_{B \in \mathcal{B}^{\mathcal{LR}}(\gamma)}$  and the spline mesh  $\mathcal{N} + \gamma$  cannot go neither LR-wise nor MS-wise hand-in-hand with  $\mathcal{N}$ .

Nevertheless, if the expanded spline knot vector on  $\gamma$  has length  $p_{3-k} + 2$  or  $p_{3-k} + 3$ , this phenomenon cannot happen. Indeed, if it has length  $p_{3-k} + 2$ , the spline space on it has dimension one and there exists at least one  $B_\gamma$ . Similarly, if it has length  $p_{3-k} + 3$ , the spline space on it has dimension 2 and there are at least two different (and so linearly independent) univariate restrictions  $B_\gamma$ .

### I.7 Characterization of linear dependence in $\mathcal{B}^{\mathcal{MS}}(\mathcal{N})$

The purpose of this section is to investigate the minimal number of MS B-splines required for a linear dependence relation on a spline mesh  $\mathcal{N}$  and features needed in such configurations. In particular, the main results of this section are that at least six MS B-splines are necessary for a linear dependence for any bidegree

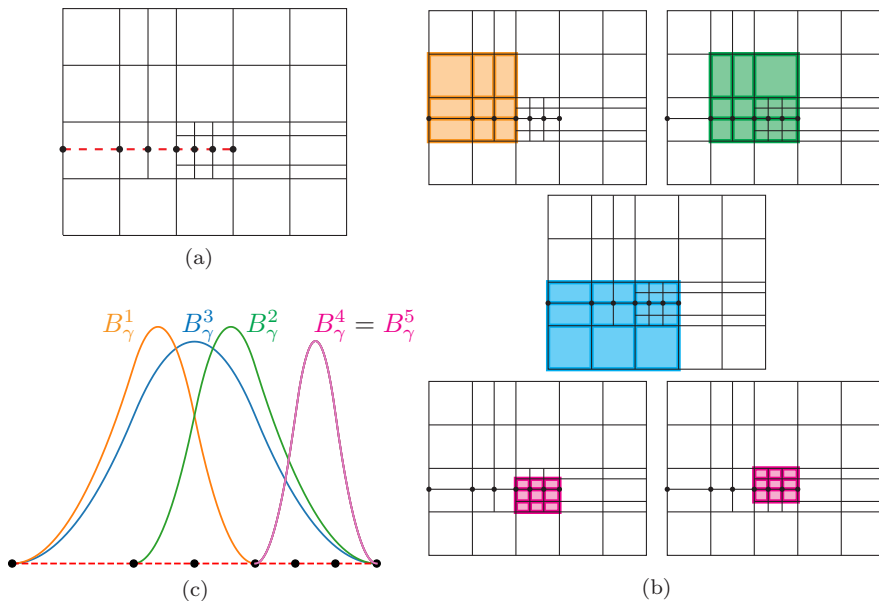


Figure I.6: (a) LR-mesh  $\mathcal{M}$  of multiplicity 1 and a new 2-split  $\gamma$  (dashed) with their intersections (black dots). Consider bidegree  $(2, 2)$ . In (b) the supports of the LR B-splines  $B^1, B^2$  (top),  $B^3$  (center),  $B^4, B^5$  (bottom) in  $\mathcal{B}^{\mathcal{LR}}(\gamma)$ . In (c) their corresponding univariate B-splines.

$\mathbf{p} = (p_1, p_2)$  (Proposition I.7.15) and that in a configuration of linear dependence with exactly six B-splines, one of them is not an LR B-spline (Proposition I.7.16). We achieve these results by looking at the minimal number of B-splines needed to satisfy necessary conditions for having a linear dependence relation. First we introduce the *nestedness condition* (Proposition I.7.3): at any corner of the region of the mesh where we have linear dependence, there is a B-spline in the linear dependence relation whose support is fully contained in the support of another larger B-spline in the linear dependence relation as well. This implies that the number of B-splines involved in the linear dependence relation is at least five (Corollary I.7.4). Then we have to prove that it is impossible to have a linear dependence with only these five. Therefore, first we show the possible arrangements of the supports in case a linear dependence relation has only five B-splines (Lemma I.7.5). Then we introduce another necessary condition for linear dependencies regarding the T-vertices in the region of the mesh where the linear dependence occurs (Corollary I.7.10). This new condition narrows the possible arrangements of the supports found in Lemma I.7.5. Finally, by looking at the position of the five B-splines in this remaining configurations, one can prove Proposition I.7.15 mentioned above.

*Remark I.7.1.* We recall that our meaning of linearly dependent functions is slightly different from the standard definition. We consider only functions

## I. Linear dependence of bivariate Minimal Support and Locally Refined B-splines over LR-meshes

---

that are actively linearly dependent, i.e., that have nonzero coefficient in the dependence relation.

**Definition I.7.2.** Given a mesh  $\mathcal{M}$  and two MS B-splines  $B[\mathbf{x}^1, \mathbf{y}^1]$ ,  $B[\mathbf{x}^2, \mathbf{y}^2]$ , defined on  $\mathcal{M}$ , we say that  $B[\mathbf{x}^1, \mathbf{y}^1]$  is **nested into**  $B[\mathbf{x}^2, \mathbf{y}^2]$  if  $\text{supp } B[\mathbf{x}^1, \mathbf{y}^1] \subset \text{supp } B[\mathbf{x}^2, \mathbf{y}^2]$  and  $\text{supp } B[\mathbf{x}^1, \mathbf{y}^1], \text{supp } B[\mathbf{x}^2, \mathbf{y}^2]$  share one, and only one, vertex.

**Proposition I.7.3** (Nestedness condition). *Let  $\mathcal{B}^{\text{MS}}(\mathcal{N})$  be the set of MS B-splines on a spline mesh  $\mathcal{N} = (\mathcal{M}, \mu, \mathbf{p})$ . Let  $\mathcal{B} \subseteq \mathcal{B}^{\text{MS}}(\mathcal{N})$  be a subset of linearly dependent MS B-splines and  $\mathcal{R}$  be the region in  $\mathbb{R}^2$  given by the union of their supports. Let  $(\bar{x}, \bar{y})$  be any (convex) corner in  $\mathcal{R}$  and define  $\mu_{\bar{x}}$  as the maximal multiplicity that is assigned to  $\bar{x}$  among the knot vectors in the  $x$ -direction of the B-splines in  $\mathcal{B}$ . Consider the set*

$$\mathcal{B}_{\mu_{\bar{x}}} := \{B[\mathbf{x}, \mathbf{y}] \in \mathcal{B} : \bar{x} \in \mathbf{x} \text{ with } \mu(\bar{x}) = \mu_{\bar{x}}\}.$$

Define  $\mu_{\bar{y}}$  as the maximal multiplicity that is assigned to  $\bar{y}$  among the knot vectors in the  $y$ -direction of the B-splines in  $\mathcal{B}_{\mu_{\bar{x}}}$  and consider the set

$$\mathcal{B}' = \{B[\mathbf{x}, \mathbf{y}] \in \mathcal{B}_{\mu_{\bar{x}}} : \bar{y} \in \mathbf{y} \text{ with } \mu(\bar{y}) = \mu_{\bar{y}}\}.$$

Finally, define  $h_x = \min_{B \in \mathcal{B}'} |x_{p_1+2} - x_1|$ ,  $h_y = \min_{B \in \mathcal{B}'} |y_{p_2+2} - y_1|$  and the set of MS B-splines in  $\mathcal{B}'$  with smallest support, in both directions:

$$\mathcal{L} = \{B[\mathbf{x}, \mathbf{y}] \in \mathcal{B}' : |x_{p_1+2} - x_1| = h_x \text{ and } |y_{p_2+2} - y_1| = h_y\}.$$

Then

1.  $\mathcal{L}$  has a unique B-spline  $B[\mathbf{x}^m, \mathbf{y}^m]$ ,
2. There exists another B-spline  $B[\mathbf{x}, \mathbf{y}] \in \mathcal{B}'$  such that  $B[\mathbf{x}^m, \mathbf{y}^m]$  is nested into  $B[\mathbf{x}, \mathbf{y}]$ .

*Proof.*

1. Let us first show that  $\mathcal{L} \neq \emptyset$ . Consider the element of the box-partition in  $\mathcal{R}$  that has  $(\bar{x}, \bar{y})$  as vertex. If  $\mathcal{L} = \emptyset$ , it would mean that such element in the corner of  $\mathcal{R}$  is contained in at least the supports of two B-splines  $B^1 = B[\mathbf{x}^1, \mathbf{y}^1]$ ,  $B^2 = B[\mathbf{x}^2, \mathbf{y}^2] \in \mathcal{B}'$  such that  $B^2$  is taller than  $B^1$  but narrower as reported in Figure I.7.

Thus, there are  $p_2 + 2 - \mu_{\bar{y}}$  horizontal splits of  $B^1$  traversing the interior of  $\text{supp } B^2$ . Only  $p_2 + 1 - \mu_{\bar{y}}$  of them (at most) can be also splits of  $B^2$ . This is a contradiction because an extra split traverses the support of  $B^2$  and so it has not minimal support on the mesh. Hence  $|\mathcal{L}| \geq 1$ . Let us assume there are two MS B-splines in  $\mathcal{L}$ ,  $B^1 = B[\mathbf{x}^1, \mathbf{y}^1]$  and  $B^2 = B[\mathbf{x}^2, \mathbf{y}^2]$ . So

$$\begin{aligned} x_1^1 &= x_1^2 & y_1^1 &= y_1^2 \\ x_{p_1+2}^1 &= x_{p_1+2}^2 & y_{p_2+2}^1 &= y_{p_2+2}^2. \end{aligned}$$

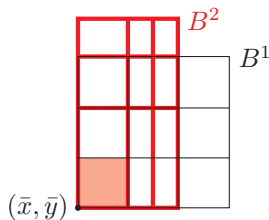


Figure I.7: The support of the two B-splines considered in the proof of Proposition I.7.3.

If also the internal knots of  $B^1$  and  $B^2$  are the same in both directions, it would mean that  $B^2 = B^1$  and there is nothing to prove. Thus, let us assume there is at least one different knot in the  $x$ - or  $y$ -direction. For instance, suppose there is a different internal knot  $x_i^2 \in \mathbf{x}^2$  for some  $i$ , with respect to  $\mathbf{x}^1$ . Then the corresponding vertical split  $\{x_i^2\} \times [y_1^2, y_{p_2+2}^2]$  would traverse the support of  $B^1$ . This is a contradiction because  $B^1$  has minimal support.

2.  $B^m = B[\mathbf{x}^m, \mathbf{y}^m]$  is in a linear dependence relation, so the smoothness of it at  $\bar{x} \times \mathbb{R}$  and  $\mathbb{R} \times \bar{y}$  must be reproduced. Therefore, there must exist at least another B-spline in  $\mathcal{B}'$ .

Such a MS B-spline  $B \in \mathcal{B}'$  cannot be fully contained in the support of  $B^m$  because of the minimality of such support. Hence,  $\text{supp } B$  exceeds on the right, or on the top, or both on the right and on the top, the support of  $B^m$ . By using the same argument adopted to prove that  $|\mathcal{L}| \neq \emptyset$ , one shows that only the last case can happen. ■

Therefore, in every corner of  $\mathcal{R}$  there are at least two MS B-splines of the linear dependence relation, one nested into the other. Note that this nestedness condition cannot be satisfied if the mesh considered is an LR-mesh and the bidegree is  $(0, 0)$ . Indeed, nesting a B-spline into another during the LR-mesh building process would imply to end a split in the middle of an element, which is not allowed. Since Proposition I.7.3 is not verified, we conclude that the set of MS (and LR) B-splines of degree  $(0, 0)$  is linearly independent on any LR-mesh. On the other hand, it is possible to have nested MS B-splines at the corners of  $\mathcal{R}$  in general meshes, even for bidegree  $(0, 0)$ . Figure I.15 (k)–(l), at the end of this section, will illustrate an example of linear dependence for MS B-splines of bidegree  $(0, 0)$ .

**Corollary I.7.4.** *We need at least 5 MS B-splines for a linear dependence relation in  $\mathcal{B}^{\mathcal{MS}}(\mathcal{N})$ .*

*Proof.*  $\mathcal{R}$  has at least four corners and there is a MS B-spline at each of them. The minimal number needed for the nestedness condition is then 5, that is when

## I. Linear dependence of bivariate Minimal Support and Locally Refined B-splines over LR-meshes

---

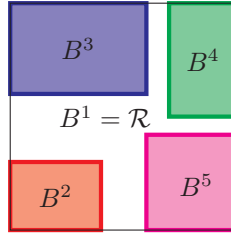


Figure I.8: Configuration with 5 MS B-splines satisfying the nested supports condition for linear dependence.

the 4 MS B-splines at the corners are all nested into the same MS B-spline whose support coincides with  $\mathcal{R}$  (see Figure I.8). ■

The question now is if five MS B-splines are enough for a linear dependence relation. From the previous results, we know that if so, we have four MS B-splines with supports in the four corners of  $\mathcal{R}$  and one larger MS B-spline with support covering the entire region. The rest of this section is devoted to show that five MS B-splines are not enough. For sake of simplicity, we keep the notation used in Figure I.8. So  $B^1$  will be the larger MS B-spline whose support coincides with  $\mathcal{R}$  and  $B^2, B^3, B^4, B^5$  are the MS B-splines at the corners ordered clockwise starting from the lower left corner. The knot vectors of  $B^i$ , for  $i = 1, \dots, 5$ , will be denoted as  $\mathbf{x}^i = (x_1^i, \dots, x_{p_1+2}^i)$  and  $\mathbf{y}^i = (y_1^i, \dots, y_{p_2+2}^i)$ .

In order to have a linear dependence relation, in every point of  $\mathcal{R}$  we must have at least two MS B-splines different from zero. In the following Lemma we present how this fact implies spatial relations of the supports in case the linear dependence relation involves only  $B^1, B^2, B^3, B^4$  and  $B^5$ .

**Lemma I.7.5.** *Suppose only five MS B-splines are in a linear dependence relation on  $\mathcal{R}$ . Then*

1. *the supports of  $B^2$  and  $B^5$  intersect each other as well as the supports of  $B^3$  and  $B^4$ ,*
2. *the supports of  $B^2$  and  $B^3$  intersect each other as well as the supports of  $B^4$  and  $B^5$ ,*
3. *at least one couple among  $\text{supp } B^2, \text{supp } B^4$  and  $\text{supp } B^3, \text{supp } B^5$  intersect each other.*

*Proof.* Every point in  $\text{supp } B^1$  must be inside the support of another B-spline in the linear dependence relation, i.e., the supports of  $B^2, B^3, B^4, B^5$  must be such that there are no white spots left inside  $\mathcal{R}$  in Figure I.8.

1. We notice that  $y_1^2 = y_1^5$  and, by Proposition I.7.3, the  $y$ -widths of the supports of  $B^3$  and  $B^4$  must be smaller than the  $y$ -width of  $\mathcal{R}$ , i.e.,  $y_1^3, y_1^4 > y_1^1$ . Let  $\bar{y} := \min\{y_1^3, y_1^4\}$ . There exists an horizontal band,

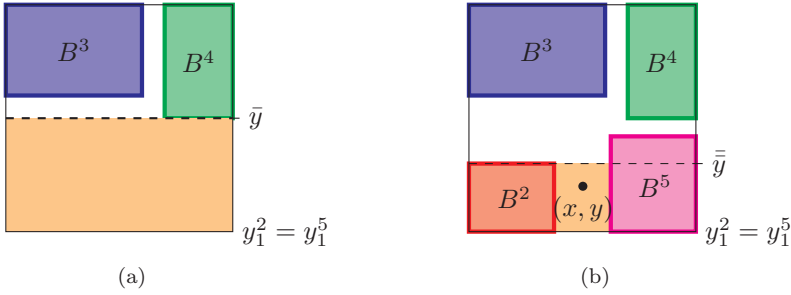


Figure I.9: In (a) the horizontal band of  $\mathcal{R}$  not intersected by  $\text{supp } B^3$  and  $\text{supp } B^4$  is highlighted. In (b), the colored subregion of  $\mathcal{R}$  contains a point  $(x, y)$  for the proof of the first item of Lemma I.7.5.

$[x_1^2, x_{p_1+2}^5] \times (y_1^2, \bar{y}) \subset \mathcal{R}$  that cannot be intersected by  $\text{supp } B^3$  and  $\text{supp } B^4$  (see the lower band in Figure I.9(a)). We want to prove that  $\text{supp } B^2 \cap \text{supp } B^5 \neq \emptyset$ . If  $\text{supp } B^2 \cap \text{supp } B^5 = \emptyset$  then, defined  $\bar{y} := \min\{\bar{y}, y_{p_2+2}^2, y_{p_2+2}^5\}$ , there would exist a point  $(x, y) \in (x_{p_1+2}^2, x_1^5) \times (y_1^2, \bar{y})$  where none of the four B-splines with supports at the corners of  $\mathcal{R}$  would be different from zero (see Figure I.9(b)).  $(x, y)$  would only be in the support of  $B^1$ . This is a contradiction. An analogous argument yields that  $\text{supp } B^3 \cap \text{supp } B^4 \neq \emptyset$ .

2. By exchanging the axes, we can use the same argument adopted in the previous item.
3. Assume the B-splines in the two couples  $B^2, B^4$  and  $B^3, B^5$  do not intersect. Then, since the previous statements are proved, we must have

$$\begin{cases} x_{p_1+2}^3 < x_1^5 \\ y_{p_2+2}^2 < y_1^4 \end{cases} \quad \text{or} \quad \begin{cases} x_{p_1+2}^2 < x_1^4 \\ y_{p_2+2}^5 < y_1^3 \end{cases}$$

These two cases, depicted in Figure I.10(a)–(b), can be treated in the same way, so we focus only on the first.

Consider a point  $(x, y) \in (x_{p_1+2}^3, x_1^5) \times (y_{p_2+2}^2, y_1^4)$ . Since  $x \in (x_{p_1+2}^3, x_1^5)$  we have  $(x, y) \notin \text{supp } B_3, \text{supp } B_5$ . While, since  $y \in (y_{p_2+2}^2, y_1^4)$ , we have  $(x, y) \notin \text{supp } B^2, \text{supp } B^4$ . Therefore  $(x, y)$  is only in  $\text{supp } B^1$ , which is a contradiction. ■

Figure I.11 shows possible arrangements of the supports of  $B^1, B^2, B^3, B^4, B^5$  to satisfy Proposition I.7.3 and Lemma I.7.5. In Figure I.11(a) the supports of  $B^3$  and  $B^5$  intersect each other while the supports of  $B^2$  and  $B^4$  do not intersect. In Figure I.11(b)–(c) both the pairs at opposing corners of  $\mathcal{R}$  intersect each other. In particular, in Figure I.11(c)  $B^2$  is as tall as  $B^5$ ,  $B^3$  is tall as  $B^4$ ,  $B^2$  is as wide as  $B^3$  and  $B^4$  is as wide as  $B^5$ .

# I. Linear dependence of bivariate Minimal Support and Locally Refined B-splines over LR-meshes

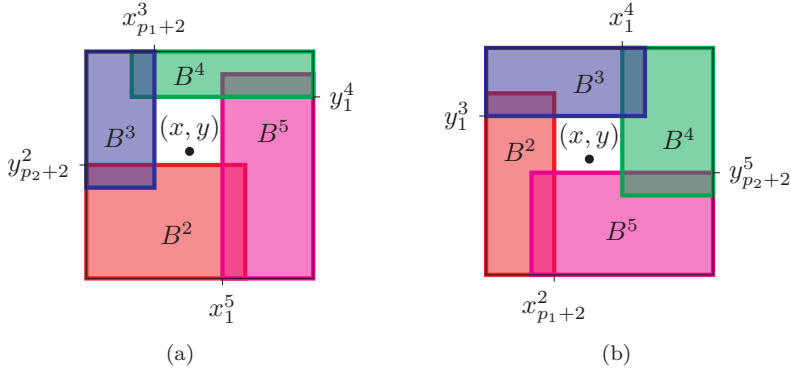


Figure I.10: (a) and (b) are the two possible arrangements of the supports of  $B^2, B^3, B^4, B^5$  inside the support of  $B^1$  when the first two items of Lemma I.7.5 hold but not the last.

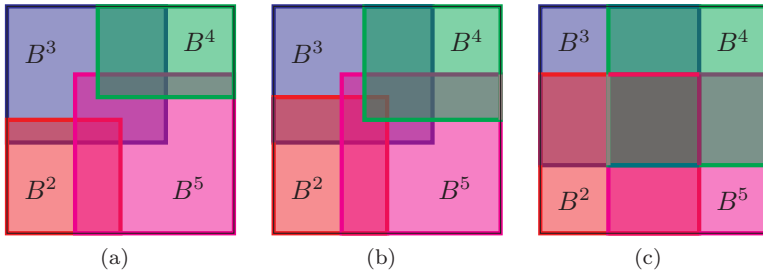


Figure I.11: Arrangements of the four B-splines at corners of  $\text{supp} B^1$  satisfying Lemma I.7.5.

The value of a bivariate B-splines  $B[\mathbf{x}, \mathbf{y}]$  at the lower and left edges of its support can be different from zero if the multiplicity of the knots  $y_1$  and  $x_1$  in  $\mathbf{y}$  and  $\mathbf{x}$  is  $p_2 + 1$  and  $p_1 + 1$  respectively. If one of  $B_2, B_3, B_4, B_5$  is different from zero on an edge of its support then some of the support intersections described in Lemma I.7.5 can be just a part of an edge. In particular, this is what happens when  $(p_1, p_2) = (0, 0)$ . In this case, the intersections described in Lemma I.7.5 1.–2. must be edge intersections in order for the nested B-splines to have minimal support. However, these edge intersections will be aligned, at least in one direction, i.e., there would exist at least one split traversing  $\mathcal{R}$  entirely, that is,  $B^1$  would not have minimal support, which is a contradiction. We conclude that 5 MS B-splines are not enough for a linear dependence relation if  $(p_1, p_2) = (0, 0)$ .

In the rest of this section, for sake of simplicity and brevity, we do not treat the cases with edge intersections. However, the arguments used to get our

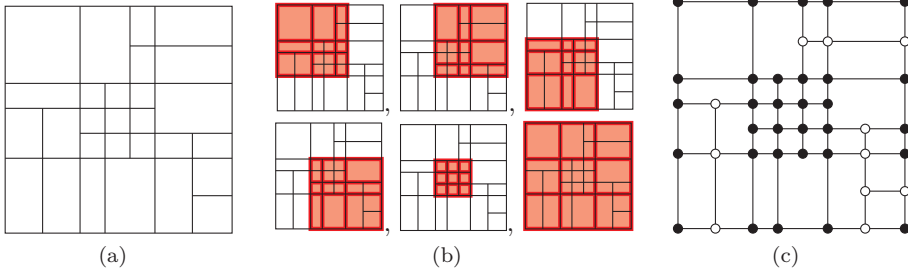


Figure I.12: Consider the mesh on the region  $\mathcal{R}$  depicted in (a). Every meshline has multiplicity 1 and consider bidegree (2,2). In (b) we see the supports of the MS B-splines on  $\mathcal{R}$ . We will prove they are linearly dependent in Example I.7.17. In (c) we see the relevant vertices in black and the non-relevant vertices in white.

results can be adapted for these cases by collapsing the regions we consider in our proofs in splits of meshlines of higher multiplicities.

We now investigate more the B-spline support arrangements in the presence of a linear dependence by looking at the T-vertices inside the region  $\mathcal{R}$ .

**Definition I.7.6.** Let  $B[\mathbf{x}, \mathbf{y}]$  be a MS B-splines on a mesh  $\mathcal{M}$ . Then its knots define a tensor mesh  $\mathcal{M}[\mathbf{x}, \mathbf{y}]$ , as described in Section 4. We define the **meshlines of  $B[\mathbf{x}, \mathbf{y}]$**  as the meshlines in  $\mathcal{M}$  forming the tensor mesh  $\mathcal{M}[\mathbf{x}, \mathbf{y}]$  and the **splits of  $B[\mathbf{x}, \mathbf{y}]$**  as the splits in  $\mathcal{M}$  made of such meshlines.

**Definition I.7.7.** A vertex  $(\bar{x}, \bar{y})$  in  $\mathcal{R}$  is called **relevant** if it corresponds to a pair of knots in at least one MS B-spline in the linear dependence relation (see Figure I.12). A meshline  $\gamma$  is called **relevant** if it is a meshline of a MS B-spline in the linear dependence relation.

An example of relevant vertices and meshlines in a mesh is reported in Figure I.12.

**Lemma I.7.8.** *Any relevant vertex in  $\mathcal{R}$  is the intersection of orthogonal relevant meshlines.*

*Proof.* Let  $(\bar{x}, \bar{y})$  be a relevant vertex in  $\mathcal{R}$ . Then it corresponds to a pair of knots of  $B[\mathbf{x}, \mathbf{y}]$  for some B-spline  $B$  involved in the linear dependence. In particular,  $(\bar{x}, \bar{y})$  is in the orthogonal splits  $[x_1^j, x_{p_1+2}^j] \times \{\bar{y}\}$  and  $\{\bar{x}\} \times [y_1^j, y_{p_2+2}^j]$ . Therefore there must exist at least 2 orthogonal relevant meshlines contained in such splits intersecting in  $(\bar{x}, \bar{y})$ . ■

**Proposition I.7.9.** *Any relevant meshline is a meshline of at least two MS B-splines in the linear dependence relation.*

*Proof.* Let  $\mathcal{B} = \{B[\mathbf{x}^j, \mathbf{y}^j]\}_{j=1}^n$  be the set of linearly dependent MS B-splines. Let  $\gamma$  be any  $k$ -meshline of  $B[\mathbf{x}^1, \mathbf{y}^1]$ . Assume that  $\gamma$  is not a meshline of any

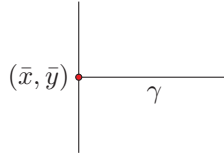


Figure I.13: The T-vertex used in the proof of Corollary I.7.10.

other MS B-spline in  $\mathcal{B}$ . We know that  $B[\mathbf{x}^1, \mathbf{y}^1]$  is  $C^{p_k - \mu(\gamma)}$ -continuous on  $\gamma$ . The linear dependence relation in  $\mathcal{B}$ ,

$$\alpha_1 B[\mathbf{x}^1, \mathbf{y}^1](x, y) + \sum_{j=2}^n \alpha_j B[\mathbf{x}^j, \mathbf{y}^j](x, y) = 0 \quad \forall (x, y) \in \mathcal{R},$$

can be rewritten expressing  $B[\mathbf{x}^1, \mathbf{y}^1]$  in terms of the others

$$B[\mathbf{x}^1, \mathbf{y}^1](x, y) = -\frac{1}{\alpha_1} \cdot \sum_{j=2}^n \alpha_j B[\mathbf{x}^j, \mathbf{y}^j](x, y) \quad \forall (x, y) \in \mathcal{R} \quad (\text{I.9})$$

because  $\alpha_j \neq 0$  for every  $j = 1, \dots, n$ . Consider now  $(x, y) \in \gamma \subset \mathcal{R}$ . Since  $\gamma$  is not a meshline of any MS B-spline  $B[\mathbf{x}^j, \mathbf{y}^j]$  in  $\mathcal{B}$  with  $j \geq 2$ , the right-hand side is a  $C^\infty$ -continuous function on  $\gamma$  while the left-hand side is only  $C^{p_k - \mu(\gamma)}$ -continuous on  $\gamma$ , which is a contradiction. ■

**Corollary I.7.10.** *Any relevant T-vertex corresponds to a pair of knots shared by at least two MS B-splines in the linear dependence relation.*

*Proof.* Let  $(\bar{x}, \bar{y})$  be a relevant T-vertex as in Figure I.13. The other three possible cases of T-vertex can be treated similarly.

Since  $(\bar{x}, \bar{y})$  is relevant,  $\gamma$  must be relevant from Lemma I.7.8. By Proposition I.7.9,  $\gamma$  is shared by at least two MS B-splines in the linear dependence relation,  $B[\mathbf{x}^1, \mathbf{y}^1], B[\mathbf{x}^2, \mathbf{y}^2]$ . This means there are two knots  $y_r^1 \in \mathbf{y}^1$  and  $y_s^2 \in \mathbf{y}^2$  such that  $y_r^1 = \bar{y} = y_s^2$  and  $[x_1^1, x_{p_1+2}^1] \times \{\bar{y}\}, [x_1^2, x_{p_1+2}^2] \times \{\bar{y}\}$  are splits in the mesh containing  $\gamma$ . Since  $(\bar{x}, \bar{y})$  is a T-vertex, it ends such splits, that is,  $(x_1^1, y_r^1) = (\bar{x}, \bar{y}) = (x_1^2, y_s^2)$ , i.e.,  $(\bar{x}, \bar{y})$  is a pair of knots shared by  $B[\mathbf{x}^1, \mathbf{y}^1]$  and  $B_2[\mathbf{x}^2, \mathbf{y}^2]$ . ■

In Section I.9 we will see that one can use the previous result to improve the Peeling Algorithm [5, Algorithm 6.3], a tool to check if the LR B-splines considered are linearly independent.

**Definition I.7.11.** Any T-vertex  $\mathbf{v}$  in a box-partition is composed of two collinear meshlines and another meshline  $\gamma$  orthogonal to them. We assign an orientation to these vertices in the following way. We say that the T-vertex  $\mathbf{v}$  is **downward** if  $\gamma$  is below  $\mathbf{v}$ , **upward** if  $\gamma$  is above  $\mathbf{v}$ , **rightward** if  $\gamma$  is on the right of  $\mathbf{v}$  and **leftward** if  $\gamma$  is on the left of  $\mathbf{v}$ .

It might happen that a relevant vertex  $\mathbf{v}$  in  $\mathring{\mathcal{R}}$  is a cross-vertex, i.e., the intersection of four meshlines, but one meshline ending in  $\mathbf{v}$  is not relevant. It means that  $\mathbf{v}$  behaves as a T-vertex for the B-splines in the linear dependence relation. Therefore, we extend the definition of relevant T-vertex and of its orientation also to these vertices in  $\mathring{\mathcal{R}}$ .

**Theorem I.7.12.** *Assume five MS B-splines are linearly dependent inside the region  $\mathcal{R}$ . Then there are at least 4 relevant T-vertices in  $\mathring{\mathcal{R}}$ , one per orientation.*

*Proof.* For the sake of simplicity and without loss of generality, we can assume there are only relevant meshlines in  $\mathcal{R}$ . Referring to any of the examples in Figure I.11, let us consider the vertical splits of  $B^2$  and  $B^5$  in the interior of the support of  $B^1$ , i.e., in  $\mathring{\mathcal{R}}$ . In order to find the minimal number of relevant T-vertices in  $\mathring{\mathcal{R}}$ , we assume that the parameter values of such vertical splits are the same for  $B^2$  and  $B^5$ . We assume the same for  $B^3$  and  $B^4$ : the vertical splits of  $B^4$  are included into the vertical splits of  $B^3$ .

Suppose first that the multiplicities of the knots in the  $x$ -direction corresponding to the vertical edges of  $\mathcal{R}$ , i.e.,  $x_1^i$ , for  $i = 1, 2, 3$  and  $x_{p_1+2}^i$  for  $i = 1, 4, 5$ , are equal to 1. Then, in  $\mathring{\mathcal{R}}$  there are  $p_1 + 1$  vertical splits of  $B^5$  and  $p_1 + 1$  for  $B^3$ , counting the multiplicities. If an end vertex of a vertical split of  $B^3$  or  $B^5$  corresponds to a relevant cross-vertex, it is contained in a split traversing the entire region  $\mathcal{R}$ , that is, it is contained in a vertical split of  $B^1$ . There are  $p_1$  vertical splits of  $B^1$  in  $\mathring{\mathcal{R}}$ , counting the multiplicities. Therefore, at most  $p_1$  vertical splits in  $\mathring{\mathcal{R}}$  of  $B^3$  and  $B^5$  can end with a relevant cross-vertex. Thus there exists at least one relevant vertex of  $B^5$  left on the upper edge of  $\text{supp } B^5$  inside  $\mathcal{R}$  that cannot be a cross-vertex. The same holds for the relevant vertices in  $B^3$ . This proves the existence of two relevant T-vertices in  $\mathring{\mathcal{R}}$ , one downward and one upward. If the knots in the  $x$ -direction corresponding to the vertical edges of  $\mathcal{R}$  have higher multiplicities, one can apply the same argument, by subtracting such multiplicities from the count of the vertical splits. Still the difference between the vertical splits in  $B^3, B^5$  and  $B^1$  will be greater than or equal to one and there will be at least one vertical T-vertex per direction necessarily. Applying the same argument to the horizontal splits of  $B^3$  and  $B^5$  we complete the proof. ■

Theorem I.7.12 holds also if the number of B-splines involved in the linear dependence relation is larger than 5 because of the necessary presence of nested B-splines at the corners.

In order to carry out the proof of the next Proposition I.7.15, we need the following definition.

**Definition I.7.13.** Given a spline mesh  $\mathcal{N} = (\mathcal{M}, \mu, \mathbf{p})$ , let  $\gamma$  be a  $(k, \alpha)$ -split in  $\mathcal{M}$  for some  $k \in \{1, 2\}$ . For instance, assume  $k = 1$ . Let  $F : \mathbb{R}^2 \rightarrow \mathbb{R}$  be a spline function in  $\mathbb{S}(\mathcal{N})$ .  $F$  is a piecewise polynomial and therefore, for sufficiently small  $\varepsilon > 0$ , the functions  $F^+ = F|_{(\alpha, \alpha+\varepsilon) \times \mathbb{R}}$  and  $F^- = F|_{(\alpha-\varepsilon, \alpha) \times \mathbb{R}}$  are polynomials

## I. Linear dependence of bivariate Minimal Support and Locally Refined B-splines over LR-meshes

---

in  $x$  (but splines in  $y$ ), i.e.,

$$F^+ = \sum_{i=0}^{p_1} f_i^+(y) \cdot (x - \alpha)^i, \quad F^- = \sum_{i=0}^{p_1} f_i^-(y) \cdot (x - \alpha)^i$$

for  $f_i^+, f_i^-$  univariate spline functions. Then we can extend the expression of  $F^+$  and  $F^-$  to  $\mathbb{R}^2$ . We define the **jump function** of  $F$  with respect to  $\gamma$  as  $J(F)(x, y) = F^+ - F^-$ .

*Remark I.7.14.*

- If  $\gamma$  is not in a split traversing the support of  $F$  and is not on its boundary, then  $F$  is  $C^\infty(\gamma)$  and in particular  $F^+ = F^-$  so that  $J(F)(x, y) = 0$ .
- When  $F$  is a bivariate B-spline,  $F = B[\mathbf{x}, \mathbf{y}]$  and  $\gamma$  corresponds to a knot in  $\mathbf{x}$ , that is  $x_j = \alpha$  for some  $j$  and  $\gamma = \{x_j\} \times [y_1, y_{p_2+2}]$ , then

$$J(B)(x, y) = J'(B[\mathbf{x}])(x) \cdot B[\mathbf{y}](y)$$

where  $J'(B[\mathbf{x}])(x)$  is a polynomial of the form:

$$J'(B[\mathbf{x}])(x) = \sum_{i=p_1-\mu(\gamma)+1}^{p_1} a_i(x - \alpha)^i.$$

- Let  $c_1, c_2$  be real numbers and  $F_1, F_2$  be spline functions. Then  $J(c_1F_1 + c_2F_2)(x, y) = c_1J(F_1)(x, y) + c_2J(F_2)(x, y)$ .

**Proposition I.7.15.** *We need at least 6 minimal support B-splines for a linear dependence relation in  $\mathcal{R}$  for any bidegree.*

*Proof.* Referring to any configuration in Figure I.11, consider a relevant T-vertex  $\mathbf{v}$  in  $B^5$ . By Corollary I.7.10, it has to be shared with at least another MS B-spline. It cannot be shared with  $B^2$  if  $B^2$  is shorter than  $B^5$ , and of course it cannot be shared with  $B^3$  or  $B^4$  because it would not be a T-vertex. Then we have two cases:

- There exists a new MS B-spline in the linear dependence relation with support in the  $y$ -direction covering the space between the supports of  $B^5$  and  $B^2$  and having  $\mathbf{v}$  as pair of knots, or
- $B^2$  is as tall as  $B^5$ .

In the first case we have finished the proof. Let us assume then that  $B^2$  is as tall as  $B^5$ . Applying the same procedure to the other relevant T-vertices, we either have at least a new MS B-spline in the linear dependence relation, or it must be that  $B^4$  is as tall as  $B^3$ ,  $B^2$  is as wide as  $B^3$  and  $B^4$  is as wide as  $B^5$ . In the

first case we have completed the proof. In the second, if no other B-splines are involved, we can write  $B^1$  in terms of  $B^2, B^3, B^4, B^5$ :

$$B^1(x, y) = \alpha_2 B^2(x, y) + \alpha_3 B^3(x, y) + \alpha_4 B^4(x, y) + \alpha_5 B^5(x, y) \quad \text{with } \alpha_j \neq 0. \quad (\text{I.10})$$

Now, consider any T-vertex downward, corresponding to a 1-split  $\gamma$  in  $B^2$  and  $B^5$ . The jump functions of  $B^2 = B[\mathbf{x}^2, \mathbf{y}^2]$  and  $B^5[\mathbf{x}^5, \mathbf{y}^5]$  corresponding to  $\gamma$ , in order to represent  $B^1$  as in equation (I.10), must satisfy

$$\alpha_2 J'(B[\mathbf{x}^2])(x) \cdot B[\mathbf{y}^2](y) = -\alpha_5 J'(B[\mathbf{x}^5])(x) \cdot B[\mathbf{y}^5](y) \quad (\text{I.11})$$

because  $B^1$  is smooth on  $\gamma$  and there are no other MS B-splines in the linear dependence relation with less regularity in the  $x$ -direction on  $\gamma$ . However, the knots of  $\mathbf{y}^2$  and  $\mathbf{y}^5$  are different because of the presence of T-vertices leftward and rightward, and equation (I.11) is impossible to achieve because  $B[\mathbf{y}^2]$  and  $B[\mathbf{y}^5]$  are defined on different knots and cannot be proportional everywhere. ■

**Proposition I.7.16.** *In a linear dependence relation with six MS B-splines on an LR-mesh, the sixth MS B-spline,  $B^6$ , is not an LR B-spline.*

*Proof.* If  $B^6$  is an LR B-spline it has been obtained through knot insertion from an LR B-spline in a coarser mesh. When the knot insertion is applied the size of the refined B-splines is smaller only in the direction where the knot has been inserted. Therefore, for  $B^6$ , in order to be an LR B-spline and be in the linear dependence relation there would exist another B-spline among  $B^2, B^3, B^4$  and  $B^5$  whose support is either as tall or as wide as the support of  $B^6$  and intersects with the support of  $B^6$ . Assume we are in the first case of the proof of Proposition I.7.15 and there are exactly six MS B-splines in linear dependence. Then there are 4 relevant T-vertices in  $\tilde{\mathcal{R}}$  shared with  $B^6$  and identifying the edges of  $\text{supp } B^6$ . Therefore,  $\text{supp } B^6 \subseteq \tilde{\mathcal{R}}$  and cannot be the same as the size of any of  $B^2, B^3, B^4, B^5$  in any direction.

In the second case of the proof of Proposition I.7.15, if  $B^6$  is an LR B-spline, we can assume that  $B^6$  is as tall as  $B^2$  and  $B^5$  (the other cases can be treated similarly). Then there would exist a vertical split of  $B^6$  that traverses the support of  $B^2$ , or  $B^5$ , without being a split of it. This is impossible for the minimality of their supports. ■

**Example I.7.17.** In this example we prove that 6 MS B-splines are enough for a linear dependence relation for any bidegree  $\mathbf{p} = (p_1, p_2)$ . We start with  $\mathbf{p} = (2, 2)$ . Consider the LR-mesh  $\mathcal{M}$  of multiplicity one depicted in Figure I.4(a). The supports of the 10 MS B-splines defined on it are represented in Figure I.4(b)–(c). By using the dimension increasing formula in Theorem I.3.9, since

- the dimension of the underlying tensor mesh is 3,
- by inserting first the horizontal splits, the expanded spline knot vectors on them have length 4, which results in a dimension increase of 1 per insertion, and

## I. Linear dependence of bivariate Minimal Support and Locally Refined B-splines over LR-meshes

---

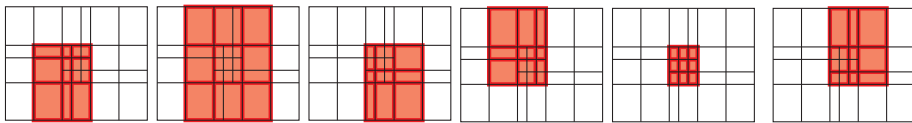


Figure I.14: The supports of the six MS B-splines of degree  $(2,2)$  in linear a dependence relation on the LR-mesh depicted in Figure I.4(a).

- then, by inserting the two vertical splits, the dimension increases by 2 each time,

we easily compute the dimension of the spline space on  $\mathcal{N} = (\mathcal{M}, 1, (2, 2))$ ,

$$\dim \mathbb{S}(\mathcal{N}) = 3 + 1 + 1 + 2 + 2 = 9.$$

Moreover, the construction of  $\mathcal{N}$  went LR-wise, and so MS-wise, hand-in-hand. Therefore, we can conclude that there is a linear dependence relation in  $\mathcal{B}^{\mathcal{MS}}(\mathcal{N})$ . The necessary conditions to be in linear dependence, given in this section, are satisfied by the six MS B-splines whose support is depicted in Figure I.14. Finally, we notice that the 9 LR B-splines on  $\mathcal{M}$ , reported in Figure I.4(b), are still linearly independent and span the spline space on  $\mathcal{N}$ .

For any other bidegree  $(p_1, p_2) \neq (0,0)$ , one can build an LR-mesh preserving the same structure of Figure I.4(a). Figure I.15(a)-(j) shows the cases for  $(p_1, p_2) = (3,3), (4,4), (1,1), (1,0), (3,1)$ . The insertions are the same as for bidegree  $(2,2)$  if  $p_k \geq 2$  for some  $k \in \{1, 2\}$ , while if  $(p_1, p_2) = (1,0), (0,1), (1,1)$ , then it is necessary to use some extensions to get an equivalent arrangement (see the dashed meshlines in the mesh (e) and (g) of Figure I.15). Again the dimension of the spline space is 9 while there are 10 MS B-splines in all the cases. Figure I.15(k)-(l) shows an equivalent arrangement for bidegree  $(0,0)$ . However, the mesh in (k) is not an LR-mesh. As we already pointed out, it is not possible to satisfy the necessary nestedness condition for a linear dependence when considering LR-meshes. However, it can be verified on general meshes. For this example,  $\dim \mathbb{S}(\mathcal{N}) = 5$  and it is spanned by the characteristic functions of the elements of the box-partition. Therefore, the MS B-splines on the mesh span the spline space but are more than its dimension.

### I.8 Minimal number of LR B-splines for a linear dependence relation

In this section we show that at least eight B-splines must be involved for a linear dependence relation in  $\mathcal{B}^{\mathcal{LR}}(\mathcal{N})$ . Then we provide examples for any bidegree  $\mathbf{p} = (p_1, p_2)$  with  $p_k \geq 2$  for some  $k \in \{1, 2\}$  where the LR B-splines in linear dependence are exactly eight. In such examples the meshes will be refinements of the meshes presented in Example I.7.17. As we pointed out in Proposition I.7.16, the sixth MS B-spline  $B^6$  in Example I.7.17 is not an LR B-spline on the

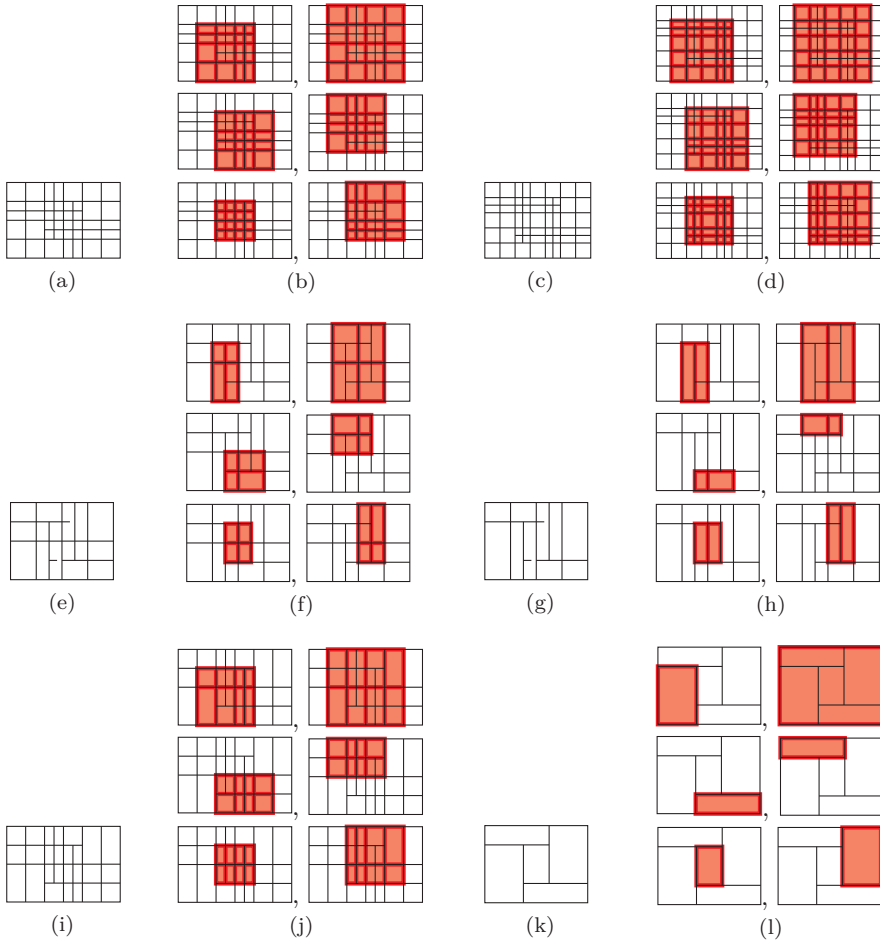


Figure I.15: In (a) an LR-mesh providing MS B-splines of bidegree  $(3,3)$  in an equivalent arrangement of the MS B-splines of bidegree  $(2,2)$  on the mesh in Figure I.4(a). In (b) are shown the supports of the six B-splines in the linear dependence relation. In (c)-(d) the same for bidegree  $(4,4)$ . In (e)-(f) we have the same for bidegree  $(1,1)$ . Note that we have used two extensions (dashed meshlines) to obtain an equivalent arrangement as for the other bidegrees. In (g)-(h) and (i)-(j) we show the equivalent configuration for bidegrees  $(1,0)$  and  $(3,1)$ . Finally, in (k)-(l) we have a comparable arrangement for bidegree  $(0,0)$ . However, the mesh in (k) is not an LR-mesh.

## I. Linear dependence of bivariate Minimal Support and Locally Refined B-splines over LR-meshes

---

mesh  $\mathcal{M}$ . In these new examples we show how to refine  $\mathcal{M}$  in order to refine  $B^6$  into two B-splines that can be now obtained through the knot insertion algorithm from LR B-splines on coarser meshes. This will move the number of MS B-splines involved in the linear dependence from six to eight but all of them will now be LR B-splines.

**Lemma I.8.1.** *Given a spline LR-mesh  $\mathcal{N} = (\mathcal{M}, \mu, \mathbf{p})$ , assume the elements in  $\mathcal{B}^{\mathcal{LR}}(\mathcal{N})$  are linearly independent. If the insertion of a  $k$ -split  $\gamma$  causes a linear dependence relation in  $\mathcal{B}^{\mathcal{LR}}(\mathcal{N} + \gamma)$ , then the expanded spline knot vector on  $\gamma$ ,  $\tau_{p_{3-k}}^{\mu_{3-k}}$ , has length at least  $p_{3-k} + 3$  and the growth of cardinality is  $|\mathcal{B}^{\mathcal{LR}}(\mathcal{N} + \gamma)| - |\mathcal{B}^{\mathcal{LR}}(\mathcal{N})| > 2$ .*

*Proof.* Theorem 5.2 of [5] ensures that if  $\tau_{p_{3-k}}^{\mu_{3-k}}$  has length  $p_{3-k} + 2$  then the elements in  $\mathcal{B}^{\mathcal{LR}}(\mathcal{N} + \gamma)$  are linearly independent. Assume that  $\tau_{p_{3-k}}^{\mu_{3-k}}$  has length  $p_{3-k} + 3$ . From the end of Section I.6, the refinement goes hand-in-hand only if  $|\mathcal{B}^{\mathcal{LR}}(\mathcal{N} + \gamma)| - |\mathcal{B}^{\mathcal{LR}}(\mathcal{N})| \geq 2$  and there is a linear dependence relation if it is a strict inequality. If the refinement does not go hand-in-hand then it must be  $|\mathcal{B}^{\mathcal{LR}}(\mathcal{N} + \gamma)| - |\mathcal{B}^{\mathcal{LR}}(\mathcal{N})| \leq 1$  and the new B-spline (if existing) is linearly independent of the B-splines in  $\mathcal{B}^{\mathcal{LR}}(\mathcal{N})$  as it has a split that intersects  $\gamma$ , which either is not in  $\mathcal{M}$  or it has an higher multiplicity in  $\mathcal{M} + \gamma$ . ■

**Proposition I.8.2.** *Given a spline LR-mesh  $\mathcal{N} = (\mathcal{M}, \mu, \mathbf{p})$ , we need at least 8 LR B-splines for a linear dependence relation in  $\mathcal{B}^{\mathcal{LR}}(\mathcal{N})$ .*

*Proof.* By Proposition I.7.3, we must have four nested B-splines at the four corners of  $\mathcal{R}$ . In order to keep the number of B-splines needed as low as possible we assume as in the proof of Corollary I.7.4 that we only need, for the nestedness condition, five B-splines:  $B^2, B^3, B^4, B^5$  contained in  $B^1$ . By Theorem I.7.12, this implies that there are at least 4 relevant T-vertices. Either

1. the nested B-splines share all these relevant T-vertices between them, or
2. a relevant T-vertex is not shared.

In case 1, we have a configuration as the one reported in Figure I.11(c) and as we have seen in the proof of Proposition I.7.16, if there are no more relevant meshlines apart from those of  $B^2, B^3, B^4, B^5$ , the other MS B-splines that can be generated in  $\mathcal{R}$  using relevant meshlines are not LR B-splines. Therefore, in order to make a linear dependence relation in  $\mathcal{R}$ , there must exist at least another split that has provided, by Lemma I.8.1, a growth in the LR B-spline set of at least three, bringing the number of LR B-splines involved to at least eight. Note that such a split necessarily has refined some of the LR B-splines at the four corners and the LR B-splines generated must all have nonzero coefficients in the linear dependence relation because created via knot insertion from them.

In case 2, there are T-vertices not shared by two B-splines nested at the corners. There must exist other LR B-splines sharing these T-vertices and bringing linear dependence. Hence, there must exist at least another split, aside from those needed for the construction of the nested LR B-splines, that has

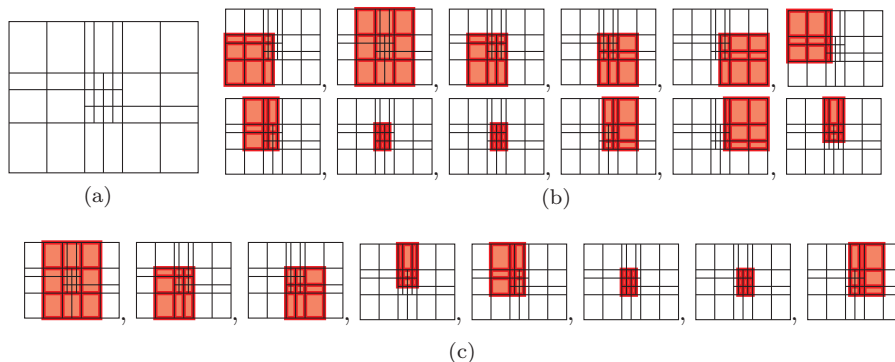


Figure I.16: (a) an LR-mesh of multiplicity 1, (b) the LR B-splines of degree (2,2) on it, (c) the LR B-splines in the linear dependence relation.

provided, by Lemma I.8.1, a growth of at least three in the LR B-spline set, moving the total number to at least eight. Also in this case, we note that all of these three LR B-splines must have nonzero coefficient in the linear dependence relation for the following reason. One of the three B-spline,  $B$ , has necessarily a nonzero coefficient because it is used to share a relevant T-vertices. The other two B-splines have been created together with  $B$  and are related to it through knot insertion relations. Therefore they also must have nonzero coefficients in the linear dependence relation. ■

In the following example we show meshes where there are exactly eight LR B-splines in a linear dependence relation for any bidegree  $\mathbf{p} = (p_1, p_2)$  with  $p_k \geq 2$  for some  $k \in \{1, 2\}$ . Such meshes are refinements of the meshes presented in Example I.7.17.

**Example I.8.3.** Consider the spline mesh  $\mathcal{N} = (\mathcal{M}, 1, (2, 2))$  with  $\mathcal{M}$  as in Figure I.4(a). We have shown in Example I.7.17 that  $\dim \mathbb{S}(\mathcal{N}) = 9$  and the construction of  $\mathcal{M}$  went LR-wise hand-in-hand. Let us now insert a new split  $\gamma$ , whose expanded spline knot vector has length  $p_2 + 3 = 5$ , to get the mesh  $\mathcal{M} + \gamma$  as shown in Figure I.16(a). Then, by Theorem I.3.9,  $\dim \mathbb{S}(\mathcal{N} + \gamma) = \dim \mathbb{S}(\mathcal{N}) + 2 = 11$  and  $\mathcal{N} + \gamma$  went LR-wise hand-in-hand with  $\mathcal{N}$ . Furthermore, the LR B-spline set grows by three,  $|\mathcal{B}^{\mathcal{LR}}(\mathcal{N} + \gamma)| = |\mathcal{B}^{\mathcal{LR}}(\mathcal{N})| + 3 = 12$  as shown in Figure I.16(b). Therefore, there is a linear dependence relation. The only eight LR B-splines satisfying Proposition I.7.3 and Corollary I.7.10 are depicted in Figure I.16(c).

For what concerns the general bidegree  $(p_1, p_2)$ , if  $p_k \geq 2$  for some  $k \in \{1, 2\}$  it is always possible to arrange the LR B-splines in the same way as for bidegree (2,2). For instance, in Figure I.17 are reported the cases for  $(p_1, p_2) = (3, 3), (4, 4), (3, 1), (2, 0)$ . Also here  $\dim \mathbb{S}(\mathcal{N}) = 11$  while  $|\mathcal{B}^{\mathcal{LR}}(\mathcal{N})| = 12$ . For  $(p_1, p_2) = (0, 1), (1, 0)$  and (1,1) we are unable to find an LR B-spline refinement process so that one can insert, via knot insertion, an LR B-spline inside  $\overset{\circ}{\mathcal{R}}$ , to share the relevant T-vertices of the four nested B-splines, without traversing the larger B-spline

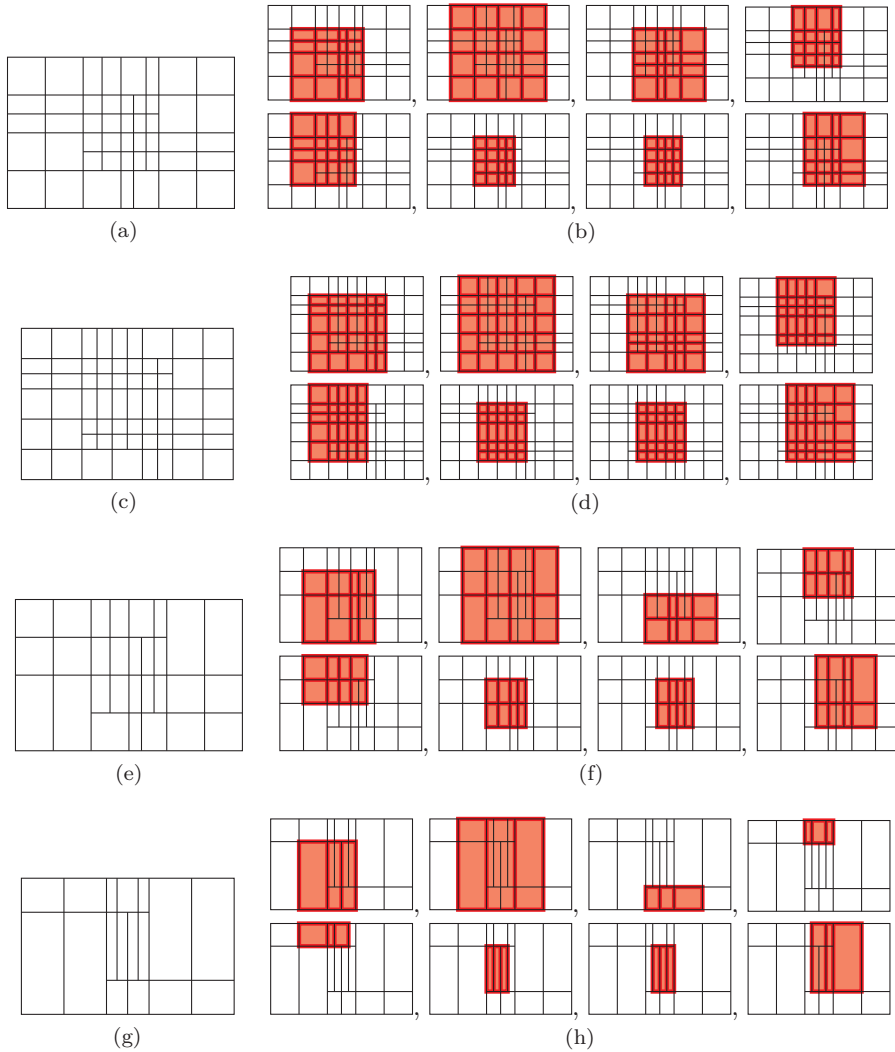


Figure I.17: In (a) is shown an LR-mesh providing LR B-splines of degree (3,3) in an equivalent arrangement of the LR B-splines of bidegree (2,2) on the mesh in Figure I.16 (a). In (b) are shown the supports of the eight B-splines in the linear dependence relation. In (c)-(d) are shown the same for bidegree (4,4), in (e)-(f) for bidegree (3,1) and (g)-(h) for bidegree (2,0).

$B^1$  with an extra split. This split destroys the linear dependence relation by triggering a refinement of  $B^1$ . We conjecture that it is impossible to have a linear dependence relation in  $\mathcal{B}^{\mathcal{LR}}(\mathcal{N})$  for such low bidegrees.

We stress that  $\mathcal{M} + \gamma$  in Figure I.16(a) is obtained by refining the mesh  $\mathcal{M}$  in Figure I.4(a) considered in Example I.7.17. What happens is that with the insertion of a new split, the MS B-spline in the center of mesh  $\mathcal{M}$ ,  $B^6$ , is refined into two MS B-splines that can now be obtained through the knot insertion procedure.

## I.9 Improvement of the Peeling Algorithm

The Peeling Algorithm introduced in [5] is a tool to check if the LR B-splines on a given LR-mesh are linearly independent. However it does not handle every possible configuration, that is, it might end without answering whether the LR B-splines' collection is linearly independent or not. In this section, we briefly recall it and we show how it can be improved, by using Corollary I.7.10, to sort out more cases.

**Definition I.9.1.** An element of the box-partition  $\mathcal{E}$  is **overloaded** if it is in the support of more B-splines than necessary for spanning the corresponding polynomial space  $\Pi_{\mathbf{p}}$ , that is, it is in more than  $(p_1 + 1)(p_2 + 1)$  supports. We call a B-spline overloaded if all the elements in its support are overloaded.

An extra B-spline, in a linear dependence, can be removed without changing spanning properties over the elements of  $\mathcal{E}$  in its support. So, only overloaded B-splines occur in linear dependencies. A linear dependence relation has to involve at least two overloaded B-splines on every element. Therefore, if on an element there is the support of only one overloaded B-spline, such B-spline cannot be active in a linear dependence. This simple observation is the basis of the Peeling Algorithm (Algorithm I.1). The implementation of it is described in [5] in terms of matrices.

However, it might happen that every element of  $\mathcal{E}^{\mathcal{O}}$  is shared but yet the overloaded LR B-splines are linearly independent. An example is reported in Figure I.18. We consider bidegree (2,2) and an LR-mesh of multiplicity one. In the highlighted region in Figure I.18(a) there are the supports of five LR B-splines, reported in Figure I.18(b), that form the collection  $\mathcal{B}^{\mathcal{O}}$  of the algorithm. Then, for each element of the box-partition in such region we count how many of these supports are on it. If an element is only in one support, the corresponding B-spline is placed in the subcollection  $\mathcal{B}_1^{\mathcal{O}}$  of the algorithm. From Figure I.18(c), we see that  $\mathcal{B}_1^{\mathcal{O}} = \emptyset$ . Therefore, the algorithm stops without answering whether the LR B-splines on the mesh are linearly independent or not. However, if we now look at the T-vertices in the region, highlighted in Figure I.18(c), we see that none of them is shared, as pair of knots, in two or more B-splines of  $\mathcal{B}^{\mathcal{O}}$ . Since the necessary condition for linear dependency Corollary I.7.10 is not satisfied, we can conclude that the LR B-splines on the mesh are linearly independent.

## I. Linear dependence of bivariate Minimal Support and Locally Refined B-splines over LR-meshes

### Algorithm I.1: Peeling Algorithm

- 1 From the set of LR splines  $\mathcal{B}^{\mathcal{LR}}(\mathcal{N})$  create the set  $\mathcal{B}^O$  of overloaded LR B-splines;
- 2 Let  $\mathcal{E}^O$  be the elements of  $\mathcal{E}$  in the supports of the LR B-splines in  $\mathcal{B}^O$ ;
- 3 Initialization of a subset  $\mathcal{B}_1^O$  of  $\mathcal{B}^O$  we are going to define,  $\mathcal{B}_1^O = \emptyset$ ;
- 4 **for** every element  $\beta$  in  $\mathcal{E}^O$  **do**
- 5     **if** only one LR B-spline  $B$  of  $\mathcal{B}^O$  has  $\beta$  in its support **then**
- 6          $\mathcal{B}_1^O = \mathcal{B}_1^O \cup \{B\}$
- 7 **if**  $\mathcal{B}^O \setminus \mathcal{B}_1^O = \emptyset$  **then**
- 8     linear independence.
- 9 **else**
- 10     **if**  $\mathcal{B}_1^O = \emptyset$  **then**
- 11         break, but might have linear dependence.
- 12      $\mathcal{B}^O = \mathcal{B}^O \setminus \mathcal{B}_1^O$ ;
- 13     Go to 2;

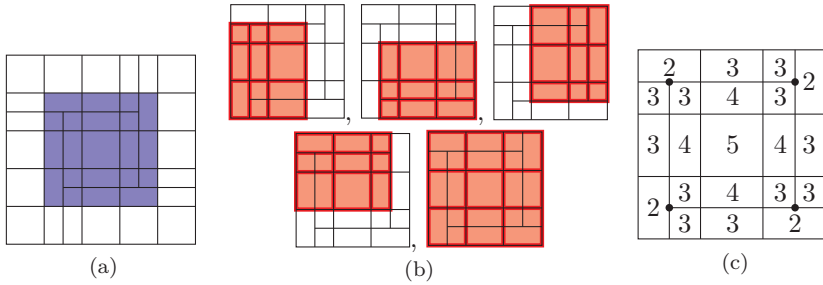


Figure I.18: Consider bidegree (2,2). In the highlighted region in (a) there are the supports of five overloaded LR B-splines, depicted in (b). The numbers in the elements of the region, reported in (c), indicate how many supports of these B-splines are on them. The highlighted vertices are the T-vertices corresponding to pair of knots of the overloaded LR B-splines.

The Peeling Algorithm can therefore be improved by inserting in  $\mathcal{B}_1^O$  also the B-splines of  $\mathcal{B}^O$  that have an exclusive T-vertex as pair of knots. Furthermore, if the cardinality of  $\mathcal{B}^O$  becomes less than 8 at any iteration of the algorithm, we can conclude that the LR B-spline collection is linearly independent thanks to Proposition I.16.

## I.10 Conclusions, conjectures and future work

In this work we have identified necessary features of the mesh to have a linear dependence relation in the MS and LR B-spline sets for any bidegree  $\mathbf{p}$ . Namely,

if the union of the supports of the B-splines involved in the linear dependence relation is denoted as  $\mathcal{R}$ ,

- there are nested B-splines at the corners of  $\mathcal{R}$ , and
- every relevant T-vertex is shared.

Moreover, we have proved that the minimal number of MS B-splines needed for a linear dependence relation is six while for the LR B-splines is eight. These numbers are sharp for any bidegree  $\mathbf{p} = (p_1, p_2)$  for the MS B-splines and for the LR B-splines with  $p_k \geq 2$  for some  $k \in \{1, 2\}$ . When  $(p_1, p_2) = (0, 1)$ ,  $(1, 0)$  or  $(1, 1)$ , we conjecture it is not possible to have a linear dependence relation in the LR B-spline set.

In our future work, we would like to classify the meshes with a linear dependence relation involving this minimal number of MS B-splines. The number of possible cases would then be dependent on the bidegree chosen. Our conjecture is that every possible configuration of linear dependency is a refinement of one of such cases. Note that this is what happens in the meshes of Example I.8.3.

## References

- [1] Buffa, A., Cho, D., and Sangalli, G. “Linear independence of the T-spline blending functions associated with some particular T-meshes”. In: *Computer Methods in Applied Mechanics and Engineering* vol. 199, no. 23-24 (2010), pp. 1437–1445.
- [2] Buffa, A., Cho, D., and Sangalli, G. “Linear independence of the T-spline blending functions associated with some particular T-meshes”. In: *Computer Methods in Applied Mechanics and Engineering* vol. 199, no. 23-24 (2010), pp. 1437–1445.
- [3] de Boor, C. *A Practical Guide to Splines*. revised. Springer-Verlag New York, 2001.
- [4] Deng, J. et al. “Polynomial splines over hierarchical T-meshes”. In: *Graphical models* vol. 70, no. 4 (2008), pp. 76–86.
- [5] Dokken, T., Lyche, T., and Pettersen, K. F. “Polynomial splines over locally refined box-partitions”. In: *Computer Aided Geometric Design* vol. 30, no. 3 (2013), pp. 331–356.
- [6] Dokken, T., Skytt, V., and Barrowclough, O. “Trivariate spline representations for computer aided design and additive manufacturing”. In: *Computers & Mathematics with Applications* vol. 78, no. 7 (2019), pp. 2168–2182.
- [7] Engleitner, N. and Jüttler, B. “Patchwork B-spline refinement”. In: *Computer-Aided Design* vol. 90 (2017), pp. 168–179.
- [8] Forsey, D. R. and Bartels, R. H. “Hierarchical B-spline refinement”. In: *ACM Siggraph Computer Graphics* vol. 22, no. 4 (1988), pp. 205–212.

## I. Linear dependence of bivariate Minimal Support and Locally Refined B-splines over LR-meshes

---

- [9] Giannelli, C., Jüttler, B., and Speleers, H. “Strongly stable bases for adaptively refined multilevel spline spaces”. In: *Advances in Computational Mathematics* vol. 40, no. 2 (2014), pp. 459–490.
- [10] Giannelli, C., Jüttler, B., and Speleers, H. “THB-splines: The truncated basis for hierarchical splines”. In: *Computer Aided Geometric Design* vol. 29, no. 7 (2012), pp. 485–498.
- [11] Großmann, D. et al. “Isogeometric simulation of turbine blades for aircraft engines”. In: *Computer Aided Geometric Design* vol. 29, no. 7 (2012), pp. 519–531.
- [12] Hughes, T. J. R., Cottrell, J. A., and Bazilevs, Y. “Isogeometric analysis: CAD, finite elements, NURBS, exact geometry and mesh refinement”. In: *Computer Methods in Applied Mechanics and Engineering* vol. 194, no. 39–41 (2005), pp. 4135–4195.
- [13] Kraft, R. *Adaptive and linearly independent multilevel B-splines*. SFB 404, Geschäftsstelle, 1997.
- [14] Li, X. and Chen, F. “On the instability in the dimension of splines spaces over T-meshes”. In: *Computer Aided Geometric Design* vol. 28, no. 7 (2011), pp. 420–426.
- [15] Manni, C., Pelosi, F., and Sampoli, M. L. “Isogeometric analysis in advection–diffusion problems: Tension splines approximation”. In: *Journal of Computational and Applied Mathematics* vol. 236, no. 4 (2011), pp. 511–528.
- [16] Pettersen, K. F. “On the dimension of multivariate spline spaces”. In: *SINTEF Report A23875* (2013).
- [17] Schumaker, L. L. *Spline Functions: Basic Theory*. third. Cambridge University Press, 2007.
- [18] Sederberg, T. W. et al. “T-splines and T-NURCCs”. In: *ACM Transactions on Graphics*. Vol. 22. 3. ACM. 2003, pp. 477–484.

# Adaptive refinement with locally linearly independent LR B-splines: Theory and applications

Francesco Patrizi, Carla Manni, Francesca Pelosi, Hendrik Speleers

Submitted.

## Abstract

In this paper we describe an adaptive refinement strategy for LR B-splines. The presented strategy ensures, at each level, local linear independence of the obtained set of LR B-splines. This property is then exploited in two applications: the construction of efficient quasi-interpolation schemes and the numerical solution of elliptic problems using the isogeometric Galerkin method.

## II.1 Introduction

Since the '70s, curves and surfaces in engineering are usually expressed by means of computer aided design (CAD) technologies, such as B-splines and non-uniform rational B-splines (NURBS). Thanks to properties like nonnegativity, local support and partition of unity, they allow for an easy control and modification of the geometries they describe, and this motivates their undisputed success as main modeling tools for objects with complex shapes in engineering; see, e.g., [6, 18, 21] and references therein. On the other hand, B-splines also provide a very efficient representation of smooth piecewise polynomial spaces, and so are a popular ingredient in the construction of approximation schemes; see, e.g., [8, 17, 22] and references therein.

More recently, the advent of isogeometric analysis (IgA) has integrated spline and CAD technologies into finite element analysis (FEA); see, e.g., [1, 7]. IgA aims to unify the geometric description of the domain of the differential problem with its numerical resolution, in order to expedite the simulation process and gaining in accuracy. In addition to the properties listed above, B-splines and NURBS feature other qualities appreciated in this context, such as (local) linear independence and high global smoothness.

## II. Adaptive refinement with locally linearly independent LR B-splines: Theory and applications

---

Tensor structures admit a simple but powerful multivariate extension of univariate splines and B-splines. On the other hand, they lack adequate local refinement. The constantly increasing demand for higher precision in simulations and reverse engineering processes requires the possibility to apply adaptive local refinement strategies, in order to reduce the approximation error while keeping the computational costs low. This request for adaptivity, triggered the interest in new formulations of B-splines and NURBS, still based on local tensor structures [4, 9–13, 23]. All these new classes of functions are defined on locally refined meshes, in which T-vertices in the interior of the domain are allowed, the so-called T-meshes.

Locally refined B-splines, or in short LR B-splines [10], are one of these new formulations, and their definition is inspired by the knot insertion refinement process of tensor B-splines. These latter are defined on global knot vectors, one per direction. The insertion of a new knot in a knot vector corresponds to a line segment in the mesh crossing the entire domain. This refines all the B-splines whose supports are crossed. Instead, LR B-splines are defined on local knot vectors and the insertion of a new knot is always performed with respect to a particular LR B-spline. As a consequence, the LR B-spline definition is consistent with the tensor B-spline definition when the underlying mesh at the end of the process is a tensor mesh, and the formulation of LR B-splines remains broadly similar to classical tensor B-splines even though they allow local refinements. This makes them one of the most elegant extensions of univariate B-splines on local tensor structures.

LR B-splines possess almost all the properties of classical tensor B-splines. Unfortunately, they are not always linearly independent. To this day, it is not yet known what are the precise conditions on the locally refined mesh to ensure a linearly independent set of LR B-splines, but some progress has been made in this direction. In [10] an efficient algorithm to seek and destroy linear dependence relations has been introduced, but it does not handle every possible locally refined mesh. In [20] a first analysis on the necessary conditions for encountering a linear dependence relation has been presented. There, it has also been proved that, for any bidegree, a linear dependence relation in the LR B-spline set involves at least 8 functions. In [3] a characterization of the local linear independence of LR B-splines has been provided. Such a strong property is guaranteed only on locally refined meshes with strong constraints on the lengths and positions of the line segments that yield particular arrangements of the LR B-spline supports. On the other hand, a practical adaptive refinement strategy to produce meshes with the local linear independence property is still missing in the literature. To the best of our knowledge, the only mesh construction that leads to a locally linearly independent set of LR B-splines can be found in [3]. Such a construction, however, cannot be considered as a practical strategy because the regions to be refined and the maximal resolution, i.e., the sizes of the smallest cells in the domain induced by the mesh, must be chosen a priori.

In this paper, we describe a practical refinement strategy ensuring the local linear independence of the corresponding LR B-splines. Such a property is appealing as it admits, e.g., the construction of efficient quasi-interpolation

schemes and the unisolvency of linear systems obtained by isogeometric discretization of differential problems based on such LR-splines. The remainder of the paper is divided into 5 sections. Section II.2 contains the definition of LR B-splines and a summary of their main properties, whereas Section II.3 describes the mesh refinement strategy and is the core of the paper. Sections II.4 and II.5 present applications of the refinement strategy in the context of quasi-interpolation and isogeometric Galerkin discretizations of elliptic problems. We end in Section II.6 with some concluding remarks.

Throughout the paper, we assume the reader to be familiar with the definition and main properties of (univariate) B-splines, in particular with the knot insertion procedure. An introduction to this topic can be found, e.g., in the review papers [17, 18] or in the classical books [8] and [22].

## II.2 Locally refined B-splines

In this section, we introduce locally refined B-splines, or in short LR B-splines, and discuss several of their properties, following the terminology from [20]. We denote by  $\Pi_p$  the space of univariate polynomials of degree less than or equal to  $p$ , and by  $\Pi_{\mathbf{p}}$  the space of bivariate polynomials of degrees less than or equal to  $\mathbf{p} = (p_1, p_2)$  component-wise. Furthermore, we denote by  $B[\mathbf{x}, \mathbf{y}]$  the bivariate B-spline defined on the (local) knot vectors  $\mathbf{x} = (x_1, \dots, x_{p_1+2})$  and  $\mathbf{y} = (y_1, \dots, y_{p_2+2})$ . The bidegree of  $B[\mathbf{x}, \mathbf{y}]$  is  $\mathbf{p} = (p_1, p_2)$  and is implicitly expressed by the length of  $\mathbf{x}$  and  $\mathbf{y}$ .

In order to define LR B-splines, we first introduce the concept of box-partition.

**Definition II.2.1.** Given an axis-aligned rectangle  $\Omega \subseteq \mathbb{R}^2$ , a **box-partition** of  $\Omega$  is a finite collection  $\mathcal{E}$  of axis-aligned rectangles in  $\Omega$  such that:

1.  $\beta_1 \cap \beta_2 = \emptyset$  for any  $\beta_1, \beta_2 \in \mathcal{E}$ , with  $\beta_1 \neq \beta_2$ .
2.  $\bigcup_{\beta \in \mathcal{E}} \beta = \Omega$ .

Given a box-partition  $\mathcal{E}$ , we define the **vertices** of  $\mathcal{E}$  as the vertices of its elements. In particular, a vertex of  $\mathcal{E}$  is called **T-vertex** if it is the intersection of three element edges. A **meshline** is an axis-aligned segment contained in an edge of an element of  $\mathcal{E}$ , connecting two and only two vertices of  $\mathcal{E}$  located at its end-points. The collection of all the meshlines of the box-partition is called **mesh**, and denoted by  $\mathcal{M}$ .

A meshline can be expressed as the Cartesian product of a point in  $\mathbb{R}$  and a finite interval. Let  $\alpha \in \mathbb{R}$  be the value of such a point and let  $k \in \{1, 2\}$  be its position in the Cartesian product. If  $k = 1$  the meshline is vertical and if  $k = 2$  the meshline is horizontal. We sometimes write  $k$ -meshline to specify the direction of the meshline, and  $(k, \alpha)$ -meshline to specify exactly on which axis-parallel line in  $\mathbb{R}^2$  the meshline lies.

For defining splines of a certain bidegree  $\mathbf{p} = (p_1, p_2)$  and smoothness across the meshlines, we also need the notion of **multiplicity** of a meshline. This

## II. Adaptive refinement with locally linearly independent LR B-splines: Theory and applications

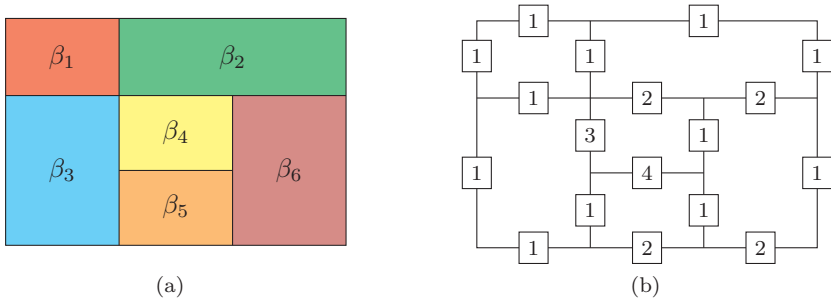


Figure II.1: Example of a box-partition  $\mathcal{E}$  of a rectangle  $\Omega$  in (a), and the mesh corresponding to  $\mathcal{E}$  in (b). The meshlines are identified by squares showing the associated multiplicities.

is a positive integer associated with every meshline in  $\mathcal{M}$ . For a  $k$ -meshline this number is assumed to be maximally  $p_k + 1$ . A meshline in  $\mathcal{M}$  has **full multiplicity** if its multiplicity is maximal, and we say that  $\mathcal{M}$  is **open** if every boundary meshline has full multiplicity. If all the meshlines of the box-partition have the same multiplicity  $m$  we say that  $\mathcal{M}$  has multiplicity  $m$ . When the T-vertices of  $\mathcal{E}$  occur only on  $\partial\Omega$  and all collinear meshlines have the same multiplicity, the corresponding mesh is called **tensor mesh**. Figure II.1 shows an example of a box-partition and its associated mesh.

Given a bivariate B-spline  $B[\mathbf{x}, \mathbf{y}]$ , let  $x_{i_1}, \dots, x_{i_r}$  and  $y_{j_1}, \dots, y_{j_s}$  be the distinct knots in  $\mathbf{x}$  and  $\mathbf{y}$ , respectively. The mesh

$$\begin{aligned} \mathcal{M}(\mathbf{x}, \mathbf{y}) := & \{ \{x_{i_\ell}\} \times [y_{j_n}, y_{j_{n+1}}] : \ell = 1, \dots, r; n = 1, \dots, s - 1 \} \\ & \cup \{ [x_{i_n}, x_{i_{n+1}}] \times \{y_{j_\ell}\} : \ell = 1, \dots, s; n = 1, \dots, r - 1 \} \end{aligned} \quad (\text{II.1})$$

is a tensor mesh in  $\text{supp } B[\mathbf{x}, \mathbf{y}]$ . The multiplicities of the meshlines in  $\mathcal{M}(\mathbf{x}, \mathbf{y})$  are given by the multiplicities of the knots of  $B[\mathbf{x}, \mathbf{y}]$ . For instance, the  $(1, x_{i_\ell})$ -meshlines  $\{x_{i_\ell}\} \times [y_{j_n}, y_{j_{n+1}}]$  for  $n = 1, \dots, s - 1$  have all the same multiplicity equal to the multiplicity of  $x_{i_\ell}$  in  $\mathbf{x}$ .

**Definition II.2.2.** Given a mesh  $\mathcal{M}$  and a B-spline  $B[\mathbf{x}, \mathbf{y}]$ , we say that  $B[\mathbf{x}, \mathbf{y}]$  has **support** on  $\mathcal{M}$  if:

- the meshlines in  $\mathcal{M}(\mathbf{x}, \mathbf{y})$  can be obtained as unions of meshlines in  $\mathcal{M}$ , and
- their multiplicities are less than or equal to the multiplicities of the corresponding meshlines in  $\mathcal{M}$ .

Furthermore, we say that  $B[\mathbf{x}, \mathbf{y}]$  has **minimal support** on  $\mathcal{M}$  if:

- it has support on  $\mathcal{M}$ ,

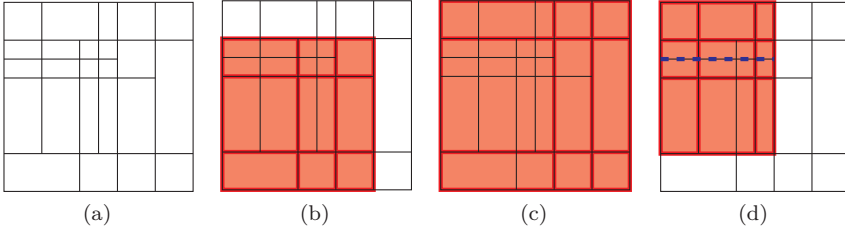


Figure II.2: Support of B-splines of bidegree  $(2, 2)$  on a mesh  $\mathcal{M}$  of multiplicity 1. The mesh is shown in (a). The B-splines whose supports are depicted in (b) and (c) have minimal support on  $\mathcal{M}$ . The tensor meshes defined by the B-spline's knots are highlighted with thicker lines. On the other hand, the B-spline in (d) does not have minimal support on  $\mathcal{M}$ : the collection of meshlines contained in the dashed line disconnects its support.

- the multiplicities of the interior meshlines in  $\mathcal{M}(\mathbf{x}, \mathbf{y})$  are equal to the multiplicities of the corresponding meshlines in  $\mathcal{M}$ , and
- there is no collection  $\gamma$  of collinear meshlines in  $\mathcal{M} \setminus \mathcal{M}(\mathbf{x}, \mathbf{y})$  such that  $\text{supp } B[\mathbf{x}, \mathbf{y}] \setminus \gamma$  is not connected.

Figure II.2 shows examples of B-splines of bidegree  $(2, 2)$  with support on a mesh of multiplicity 1. In particular, the B-splines in (b)–(c) have minimal support, whereas the support of the B-spline in (d) can be disconnected by the collection of meshlines  $\gamma$ , visualized by dashed lines in the figure.

Given a mesh  $\mathcal{M}$  and a B-spline  $B[\mathbf{x}, \mathbf{y}]$  with support in  $\mathcal{M}$ , assume that it does not have minimal support on  $\mathcal{M}$ . Then, there exists a collection of  $(k, \alpha)$ -meshlines  $\gamma$  such that  $\text{supp } B[\mathbf{x}, \mathbf{y}] \setminus \gamma$  is not connected and either  $\gamma$  is in  $\mathcal{M} \setminus \mathcal{M}(\mathbf{x}, \mathbf{y})$  or  $\gamma \subseteq \mathcal{M}(\mathbf{x}, \mathbf{y})$ , i.e.,  $\alpha$  is an internal knot of  $\mathbf{x}$  for  $k = 1$  or  $\mathbf{y}$  for  $k = 2$ , but its meshlines have lower multiplicities in  $\mathcal{M}(\mathbf{x}, \mathbf{y})$  than in  $\mathcal{M}$ . Assume that the meshlines in  $\gamma$  have all the same multiplicity  $m$  in  $\mathcal{M}$ . Denoting by  $\mu(\alpha) \geq 0$  the number of times  $\alpha$  appears in the knot vector of  $B[\mathbf{x}, \mathbf{y}]$  in the  $k$ -th direction, then  $m - \mu(\alpha)$  is strictly positive as  $B[\mathbf{x}, \mathbf{y}]$  has support, but not minimal support, on  $\mathcal{M}$ . One could consider such  $\alpha$  as an extra knot, of multiplicity  $m - \mu(\alpha)$ , with respect to the knot vector of  $B[\mathbf{x}, \mathbf{y}]$  in the  $k$ -th direction (in  $\mathbf{x}$  if  $k = 1$  and in  $\mathbf{y}$  if  $k = 2$ ), and perform knot insertion on  $B[\mathbf{x}, \mathbf{y}]$ . If  $\alpha$  was already a knot of  $B[\mathbf{x}, \mathbf{y}]$ , so  $\mu(\alpha) \geq 1$ , this means rising its multiplicity by  $m - \mu(\alpha)$ . The resulting generated B-splines will still have support on  $\mathcal{M}$  and eventually they will also have minimal support on  $\mathcal{M}$ . As an example, the collection  $\gamma$  highlighted with dashed lines in Figure II.2(d) is made of  $(2, \alpha)$ -meshlines, for some  $\alpha$ , of multiplicity 1. Such  $\alpha$  can be inserted as new knot of multiplicity 1 in the knot vector in the  $y$ -direction of the considered B-spline to refine it in two B-splines via knot insertion.

The LR B-splines are generated by means of the above procedure. We start by considering a coarse tensor mesh and we refine it by inserting collections of

## II. Adaptive refinement with locally linearly independent LR B-splines: Theory and applications

---

collinear meshlines, one at time, of the same multiplicity. On the initial mesh we consider the standard tensor B-splines and whenever a B-spline in our collection has no longer minimal support during the mesh refinement process, we refine it by using the knot insertion procedure. The LR B-splines will be the final set of B-splines produced by this algorithm. In the next definitions we formalize this by describing the mesh refinement process in our framework.

**Definition II.2.3.** Given a box-partition  $\mathcal{E}$  and an axis-aligned segment  $\gamma$ , we say that  $\gamma$  **traverses**  $\beta \in \mathcal{E}$  if  $\gamma \subseteq \beta$  and the interior of  $\beta$  is divided into two parts by  $\gamma$ , i.e.,  $\beta \setminus \gamma$  is not connected. A **split** is a finite union of contiguous and collinear axis-aligned segments  $\gamma = \cup_i \gamma_i$  such that every  $\gamma_i$  either is a meshline of the box-partition or traverses some  $\beta \in \mathcal{E}$ . A mesh  $\mathcal{M}$  has constant splits if each split in it is made of meshlines of the same multiplicity.

The LR B-splines are defined on a class of meshes with constant splits, called **LR-meshes**. Thus, from now on, we restrict our attention to meshes that have constant splits.

When a split  $\gamma$  is inserted in a box-partition  $\mathcal{E}$ , any traversed  $\beta \in \mathcal{E}$  is replaced by the two subrectangles  $\beta_1, \beta_2$  given by the closures of the connected components of  $\beta \setminus \gamma$ . The resulting new box-partition will be denoted by  $\mathcal{E} + \gamma$  and its corresponding mesh by  $\mathcal{M} + \gamma$ . We also assume that a positive integer  $\mu_\gamma$  has been assigned to any split  $\gamma$ . The multiplicities of the meshlines in  $\mathcal{M} \cap (\mathcal{M} + \gamma)$  and not contained in  $\gamma$  are unchanged. Then, if  $\gamma$  is made of new meshlines with respect to  $\mathcal{M}$ , we assign a multiplicity equal to  $\mu_\gamma$  to them, whereas if  $\gamma$  is made of meshlines that were already contained in  $\mathcal{M}$ , we increase their multiplicity by  $\mu_\gamma$ .

**Definition II.2.4.** Given a mesh  $\mathcal{M}$  with constant splits, a B-spline  $B[\mathbf{x}, \mathbf{y}]$  with support on  $\mathcal{M}$  and a split  $\gamma$ , we say that  $\gamma$  **traverses**  $B[\mathbf{x}, \mathbf{y}]$  if the interior of  $\text{supp } B[\mathbf{x}, \mathbf{y}]$  is divided into two parts by  $\gamma$ , i.e.,  $\text{supp } B[\mathbf{x}, \mathbf{y}] \setminus \gamma$  is not connected and either  $\gamma$  is in  $\mathcal{M} \setminus \mathcal{M}(\mathbf{x}, \mathbf{y})$  or  $\gamma \subseteq \mathcal{M}(\mathbf{x}, \mathbf{y})$  but the multiplicity of its meshlines is lower in  $\mathcal{M}(\mathbf{x}, \mathbf{y})$  than in  $\mathcal{M}$ .

We are now ready to define the mesh refinement process and the LR B-splines. The meshes produced by this procedure will be called LR-meshes.

**Definition II.2.5.** Given a bidegree  $\mathbf{p} = (p_1, p_2)$ , let  $\mathcal{M}_1$  be a tensor mesh such that the set of standard tensor B-splines of bidegree  $\mathbf{p}$  on  $\mathcal{M}_1$  is nonempty, and denote it by  $\mathcal{B}_1$ . We then define a sequence of meshes  $\mathcal{M}_2, \mathcal{M}_3, \dots$  and corresponding function sets  $\mathcal{B}_2, \mathcal{B}_3, \dots$  as follows. For  $i = 1, 2, \dots$ , let  $\gamma_i$  be a split such that  $\mathcal{M}_{i+1} := \mathcal{M}_i + \gamma_i$  has constant splits and such that the support of at least one B-spline in  $\mathcal{B}_i$  is traversed by a split in  $\mathcal{M}_{i+1}$ . On this refined mesh  $\mathcal{M}_{i+1}$ , the new set of B-splines  $\mathcal{B}_{i+1}$  is constructed by the following algorithm:

1. Initialize the set by  $\mathcal{B}_{i+1} \leftarrow \mathcal{B}_i$ .
2. As long as there exists  $B[\mathbf{x}^j, \mathbf{y}^j] \in \mathcal{B}_{i+1}$  with no minimal support on  $\mathcal{M}_{i+1}$ :

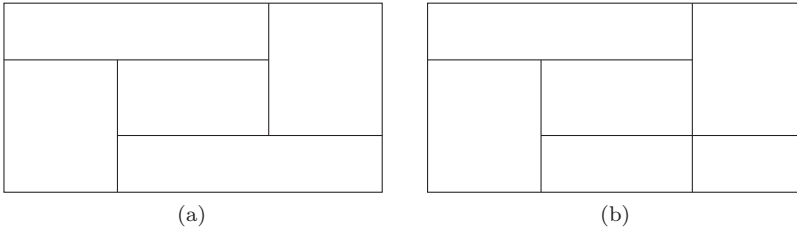


Figure II.3: Two meshes. Assume that the boundary has a multiplicity large enough so that it is possible to define a B-spline of bidegree  $\mathbf{p}$  on it. Then, the mesh in (a) is not an LR-mesh because it cannot be built as a sequence of split insertions. The mesh in (b) is an LR-mesh similar to the one in (a).

- a) Apply knot insertion:  $\exists B[\mathbf{x}_1^j, \mathbf{y}_1^j], B[\mathbf{x}_2^j, \mathbf{y}_2^j] : B[\mathbf{x}^j, \mathbf{y}^j] = \alpha_1 B[\mathbf{x}_1^j, \mathbf{y}_1^j] + \alpha_2 B[\mathbf{x}_2^j, \mathbf{y}_2^j]$ .
- b) Update the set:  $\mathcal{B}_{i+1} \leftarrow (\mathcal{B}_{i+1} \setminus \{B[\mathbf{x}^j, \mathbf{y}^j]\}) \cup \{B[\mathbf{x}_1^j, \mathbf{y}_1^j], B[\mathbf{x}_2^j, \mathbf{y}_2^j]\}$ .

The mesh produced at each step is called **LR-mesh** and the corresponding function set is called **LR B-spline set**.

Obviously not every mesh is an LR-mesh. One could consider meshes that do not have constant splits or meshes that cannot be built through a sequence of split insertions as the mesh depicted in Figure II.3(a). In general, the mesh refinement process producing a given LR-mesh  $\mathcal{M} = \mathcal{M}_N$  is not unique. Indeed, the split insertion ordering can often be changed. Nevertheless, the LR B-spline set on  $\mathcal{M}$  is well defined because it is independent of such insertion ordering, as proved in [10, Theorem 3.4].

Given an LR-mesh, the corresponding LR B-splines have several desirable properties for applications. By their definition, it is clear that

- they are nonnegative,
- they have minimal support, and
- they can be expressed by the LR B-splines on finer LR-meshes using nonnegative coefficients (provided by the knot insertion procedure).

Furthermore, it is possible to scale them by means of positive weights so that they also form a partition of unity; see [10, Section 7].

Unfortunately, they are not always linearly independent. Figure II.4 shows an example of linear dependence among the LR B-splines of bidegree (2, 2) defined on an LR-mesh of multiplicity 1. To this day, it is not yet known what are the precise conditions on the LR-mesh to ensure a linearly independent set of LR B-splines.

In [3] a characterization of the local linear independence of LR B-splines has been provided. Such a strong property is guaranteed only on LR-meshes

## II. Adaptive refinement with locally linearly independent LR B-splines: Theory and applications

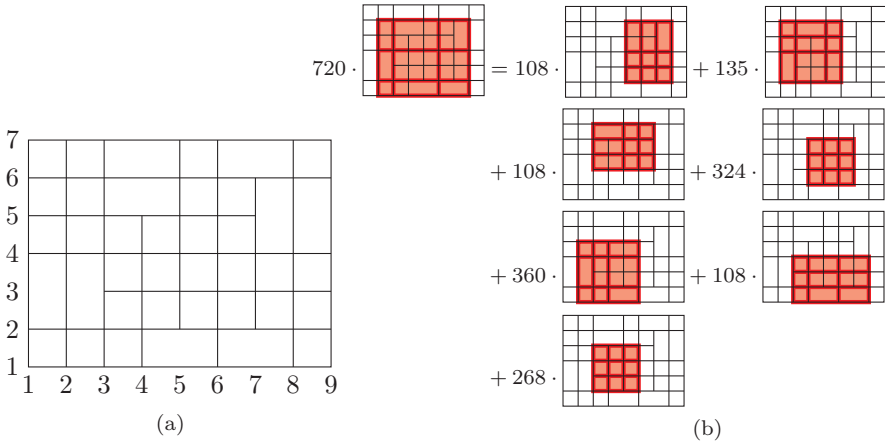


Figure II.4: Example of linear dependence in the LR B-spline set. The parameterization of an LR-mesh  $\mathcal{M}$  of multiplicity 1 is considered in (a), and the linear dependence relation among some of the LR B-splines of bidegree  $(2, 2)$  defined on  $\mathcal{M}$  is illustrated in (b). The LR B-splines are represented by means of their supports on the mesh and the tensor meshes induced by their knots are highlighted with thicker meshlines.

with strong constraints on the split lengths and positions that yield particular arrangements of the LR B-spline supports. This last statement is formalized in the following.

**Definition II.2.6.** Given a mesh  $\mathcal{M}$ , let  $B[\mathbf{x}^1, \mathbf{y}^1], B[\mathbf{x}^2, \mathbf{y}^2]$  be two different LR B-splines defined on  $\mathcal{M}$ . We say that  $B[\mathbf{x}^2, \mathbf{y}^2]$  is **nested** in  $B[\mathbf{x}^1, \mathbf{y}^1]$ , and we write  $B[\mathbf{x}^2, \mathbf{y}^2] \preceq B[\mathbf{x}^1, \mathbf{y}^1]$ , if:

- $\text{supp } B[\mathbf{x}^2, \mathbf{y}^2] \subseteq \text{supp } B[\mathbf{x}^1, \mathbf{y}^1]$ , and
- any meshline  $\gamma$  of  $\mathcal{M}$  in  $\partial\text{supp } B[\mathbf{x}^1, \mathbf{y}^1] \cap \partial\text{supp } B[\mathbf{x}^2, \mathbf{y}^2]$  has a higher (or equal) multiplicity when considered in  $\mathcal{M}(\mathbf{x}^1, \mathbf{y}^1)$  than in  $\mathcal{M}(\mathbf{x}^2, \mathbf{y}^2)$ .

An open mesh where no LR B-spline is nested is said to have the non-nested support property, or in short the  **$\mathbf{N}_2\mathbf{S}$  property**.

The definition of nested LR B-splines was formulated for the first time in [2]. Definition II.2.6 is different but equivalent to it. Figure II.5 shows an example of an LR B-spline nested into another. Note that for meshes of constant multiplicity, e.g., of multiplicity 1,  $B[\mathbf{x}^2, \mathbf{y}^2] \preceq B[\mathbf{x}^1, \mathbf{y}^1]$  if and only if  $\text{supp } B[\mathbf{x}^2, \mathbf{y}^2] \subseteq \text{supp } B[\mathbf{x}^1, \mathbf{y}^1]$ .

The next result, presented in [3], relates the local linear independence of the LR B-splines to the  $\mathbf{N}_2\mathbf{S}$  property of the mesh.

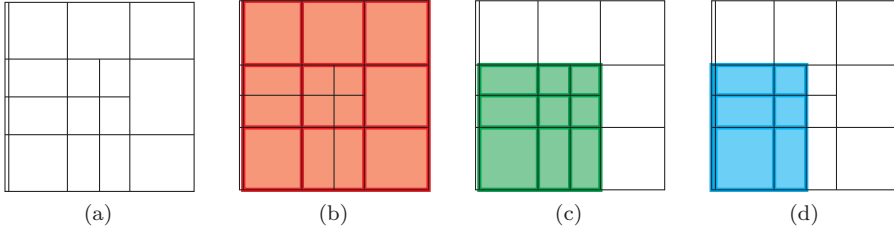


Figure II.5: Example of nested LR B-splines on the mesh  $\mathcal{M}$  shown in (a). All the meshlines have multiplicity 1 except those in the left edge of  $\mathcal{M}$ , highlighted with a double line, which have multiplicity 2. In (b)–(d) three LR B-splines,  $B[\mathbf{x}^1, \mathbf{y}^1]$ ,  $B[\mathbf{x}^2, \mathbf{y}^2]$ ,  $B[\mathbf{x}^3, \mathbf{y}^3]$  respectively, of bidegree  $(2, 2)$  with minimal support on  $\mathcal{M}$  are represented by means of their supports and the tensor meshes induced by their knots. All the knots of these LR B-splines have multiplicity 1 except  $x_1^3$  which has multiplicity 2. Therefore,  $B[\mathbf{x}^2, \mathbf{y}^2] \preceq B[\mathbf{x}^1, \mathbf{y}^1]$  but  $B[\mathbf{x}^3, \mathbf{y}^3] \not\preceq B[\mathbf{x}^2, \mathbf{y}^2]$  and  $B[\mathbf{x}^3, \mathbf{y}^3] \not\preceq B[\mathbf{x}^1, \mathbf{y}^1]$ , despite that  $\text{supp } B[\mathbf{x}^3, \mathbf{y}^3] \subseteq \text{supp } B[\mathbf{x}^2, \mathbf{y}^2]$  and  $\text{supp } B[\mathbf{x}^3, \mathbf{y}^3] \subseteq \text{supp } B[\mathbf{x}^1, \mathbf{y}^1]$ , because the shared meshlines in the left edge of  $\text{supp } B[\mathbf{x}^3, \mathbf{y}^3]$ ,  $\text{supp } B[\mathbf{x}^2, \mathbf{y}^2]$  and  $\text{supp } B[\mathbf{x}^1, \mathbf{y}^1]$  have multiplicity 2 in  $\mathcal{M}(\mathbf{x}^3, \mathbf{y}^3)$  and multiplicity 1 in  $\mathcal{M}(\mathbf{x}^2, \mathbf{y}^2)$  and  $\mathcal{M}(\mathbf{x}^1, \mathbf{y}^1)$ .

**Theorem II.2.7.** *Given a bidegree  $\mathbf{p} = (p_1, p_2)$ , let  $\mathcal{M}$  be an open LR-mesh corresponding to a box-partition  $\mathcal{E}$  and let  $\mathcal{B}^{\mathcal{LR}}(\mathcal{M})$  be the set of LR B-splines of bidegree  $\mathbf{p}$  on  $\mathcal{M}$ . The following statements are equivalent:*

1. *The elements of  $\mathcal{B}^{\mathcal{LR}}(\mathcal{M})$  are locally linearly independent.*
2.  *$\mathcal{M}$  has the  $N_2S$  property.*
3. *For any element  $\beta \in \mathcal{E}$ , the number of nonzero LR B-splines over  $\beta$  satisfies*

$$\#\{B \in \mathcal{B}^{\mathcal{LR}}(\mathcal{M}) : \text{supp } B \supseteq \beta\} = (p_1 + 1)(p_2 + 1).$$
4. *The LR B-splines form a partition of unity, without the use of scaling weights.*

An element of  $\mathcal{E}$  for which statement 3 holds is said to be **non-overloaded**. Note that  $(p_1 + 1)(p_2 + 1)$  is the dimension of the polynomial space over the element.

In [3] one can also find an algorithm to construct LR-meshes so that the  $N_2S$  property is fulfilled. This approach, however, has a relevant drawback for practical purposes: the regions to be refined and the maximal resolution have to be chosen a priori. Moreover, the algorithm cannot be stopped prematurely, before having inserted all the splits determined initially. In practice, one rarely knows in advance where the error will be large and how fine the mesh has to be chosen to reduce it under a certain tolerance.

In the next section, we present an alternative way to generate LR-meshes so that the  $N_2S$  property is guaranteed.

### II.3 $N_2S$ structured mesh refinement strategy

In this section, we define a local refinement strategy that ensures the  $N_2S$  property for the obtained meshes. It consists of two steps. First, we apply the so-called structured mesh refinement, defined in [15], to the LR B-splines whose contribution to the approximation error is larger than a given tolerance. Then, we slightly modify the obtained mesh by prolonging some splits, to recover the  $N_2S$  property. The meshes produced by this refinement are open meshes with internal meshlines of multiplicity one.

As opposed to the classical finite element method, in which the refinement is applied to the box-partition elements, the **structured mesh refinement** is a refinement applied to the function space, i.e., we select for refinement the LR B-splines contributing more to the approximation error rather than the box-partition elements where a larger error occurs. This approach is justified by the fact that on an LR-mesh, any new split inserted must traverse at least the support of one LR B-spline. If we choose to select the elements where the error is larger, then the refinement has to be extended anyway to traverse the support of at least one LR B-spline containing the elements, resulting in a refinement of the LR B-spline basis. Moreover, since several LR B-splines contain such elements, those chosen for the refinement extension could be not those contributing more to the error, resulting in a suboptimal refinement, or we could refine more LR B-splines than necessary, wasting degrees of freedom.

Once the LR B-splines are selected, we refine them by halving the interval steps in their knot vectors. This corresponds to the insertion of a net of meshlines in the B-spline supports on the mesh. We therefore perform the LR B-spline generation algorithm described in Definition II.2.5. Every selected LR B-spline is fragmented into LR B-splines with smaller support and replaced by them. The LR-mesh obtained in this way will be called a **structured LR-mesh**.

In summary, the structured mesh refinement consists of two steps:

1. LR B-splines are selected to be refined and not box-partition elements;
2. the interval steps of their knot vectors are halved to obtain the new LR-mesh.

Figure II.6 shows two iterations of such refinement. In general, the structured mesh refinement does not produce LR-meshes with the  $N_2S$  property. The LR-mesh in Figure II.6(f) is an example as explained in Figure II.7. Furthermore, the structured mesh refinement may produce linearly dependent sets of LR B-splines. Figure II.8 shows an example for bidegree  $(4, 4)$ .

On the other hand, the standard B-splines defined on a plain tensor mesh are locally linearly independent, and the meshes provided by the structured mesh refinement are locally tensor meshes far from the boundary of the region where the structured mesh refinement is applied. The LR B-splines defined in these zones of the mesh behave like the standard B-splines, and therefore are locally linearly independent. On the boundary of the region where the refinement has been applied, LR B-splines with smaller support can be nested in LR B-splines

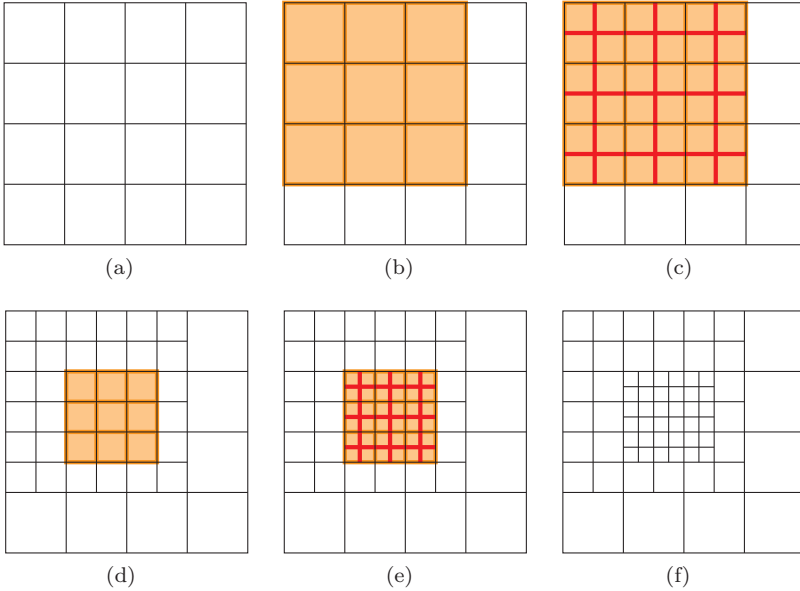


Figure II.6: Two iterations of the structured mesh refinement of bidegree  $(2, 2)$ . We consider the initial open tensor mesh with internal meshlines of multiplicity 1 in (a). Figure (b) shows the support of an LR B-spline selected for refinement. We refine it by halving the interval steps in its knot vectors. This results in the insertion of a net of meshlines in the LR-mesh as shown in (c). In (d) we select another LR B-spline in the new set of LR B-splines and we refine it as illustrated in (e). Figure (f) depicts the final mesh obtained.

with larger support. Hence, in such case the resulting LR-mesh does not have the  $N_2S$  property.

The idea for our refinement strategy, which will be called  **$N_2S$  structured mesh refinement**, is therefore to recover the  $N_2S$  property in the mesh by slightly modifying it in these transition regions. When an LR B-spline  $B[\mathbf{x}^2, \mathbf{y}^2]$  is nested into another LR B-spline  $B[\mathbf{x}^1, \mathbf{y}^1]$ , one could prolong the splits in  $\mathcal{M}(\mathbf{x}^2, \mathbf{y}^2)$  in some direction to traverse entirely  $\text{supp } B[\mathbf{x}^1, \mathbf{y}^1]$ . This, by Definition II.2.5, would refine  $B[\mathbf{x}^1, \mathbf{y}^1]$  in LR B-splines that turn out not to have nested LR B-splines in their supports anymore. This last statement is formalized in Corollary II.3.4. To this end, we first need to introduce the orientation of T-vertices in a box-partition and prove the  $N_2S$  property for LR-meshes with a particular structure.

**Definition II.3.1.** Any T-vertex in a box-partition is the intersection of two collinear meshlines and another meshline, say  $\gamma$ , orthogonal to them. We call the T-vertex **vertical** if  $\gamma$  is vertical, and **horizontal** otherwise.

**Definition II.3.2.** An LR-mesh  $\mathcal{M}$  on the domain  $\Omega$  is said to be **tensorized**

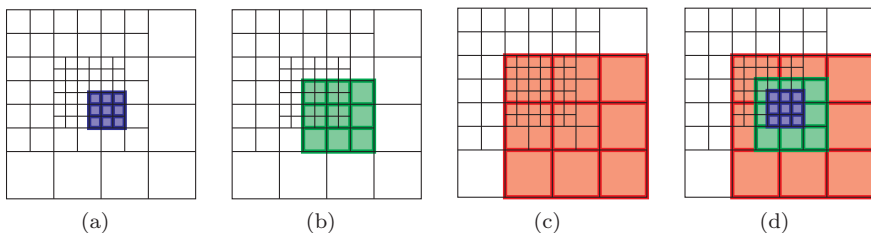


Figure II.7: An LR B-spline nested in another LR B-spline, which in turn is nested in another LR B-spline on a structured LR-mesh for bidegree  $(2, 2)$ . Consider again the mesh in Figure II.6(f). In (a)–(c) we depict the supports of three LR B-splines on this mesh. The support in (a) is contained in the interior of the support in (b) and (c), and the support in (b) is contained in the interior of the support in (c). Therefore, the LR B-spline considered in (a) is nested both in the LR B-splines in (b) and (c), and the LR B-spline in (b) is nested in the LR B-spline in (c). Hence, the considered mesh does not have the  $N_2S$  property.

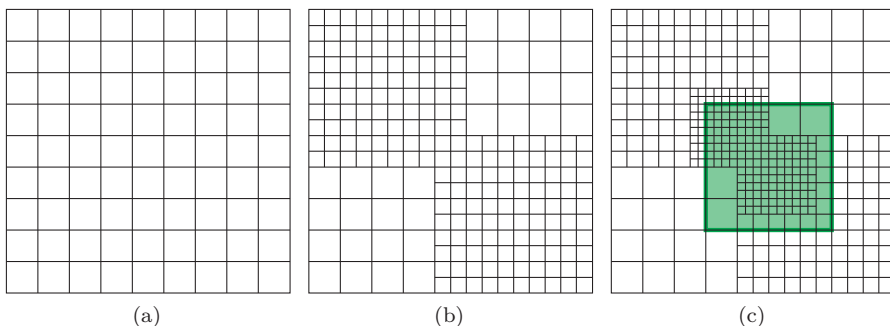


Figure II.8: A structured mesh with a linear dependence relation among the LR B-splines of bidegree  $(4,4)$  defined in the highlighted region in (c). We start by considering an open tensor mesh with interior meshlines of multiplicity 1 as in (a). Then, we apply two iterations of structured mesh as shown in (b)–(c). The LR B-splines with support in the region highlighted in (c) are in a linear dependence relation. In particular, the region corresponds to the support of an LR B-splines that has many nested LR B-splines in it. One can prove the existence of the linear dependence relation by computing the spline space dimension and the number of LR B-splines defined on the mesh as explained in the examples of [20]. This configuration can be reproduced for any bidegree  $(p_1, p_2)$  with  $p_k \geq 4$  for  $k = 1, 2$ .

**in the  $k$ -th direction**, for  $k \in \{1, 2\}$ , if all the internal  $k$ -meshlines in  $\mathcal{M}$  are contained in  $k$ -splits crossing  $\Omega$  entirely, i.e., there are no vertical, if  $k = 1$ , or horizontal, if  $k = 2$ , T-vertices in the interior of  $\Omega$ .

**Proposition II.3.3.** *Let  $\mathcal{M}$  be an LR-mesh tensorized in the  $k$ -th direction for some  $k \in \{1, 2\}$ . Then, the LR B-splines defined on  $\mathcal{M}$  are all non-nested.*

*Proof.* Without loss of generality, we can assume that  $\mathcal{M}$  is tensorized in the first direction, i.e., the vertical meshlines are all contained in vertical splits crossing the domain entirely. This means that in  $\mathcal{M}$  no vertical meshline ends in the interior of the domain and therefore in the interior of the support of any LR B-splines defined on  $\mathcal{M}$ . We now proceed by contradiction and assume that there exists an LR B-spline in  $\mathcal{M}$ , say  $B^2 = B[\mathbf{x}^2, \mathbf{y}^2]$ , nested in another, say  $B^1 = B[\mathbf{x}^1, \mathbf{y}^1]$ ; see Definition II.2.6. This can happen only if they share the same knot vector in the  $x$ -direction,  $\mathbf{x}^1 = \mathbf{x}^2$ . In particular, their supports have the same extreme values in the  $x$ -direction. This implies that all the horizontal splits, counting the multiplicities, of  $\mathcal{M}$  traversing  $\text{supp } B^2$  must traverse  $\text{supp } B^1$  as well. Since  $B^2 \preceq B^1$  and  $B^1$  has minimal support (as it is an LR B-spline), this means  $\mathbf{y}^1 = \mathbf{y}^2$ , and as a consequence we have  $B^1 = B^2$ . This is a contradiction and concludes the proof. ■

**Corollary II.3.4.** *Given an LR-mesh  $\mathcal{M}$ , let  $B = B[\mathbf{x}, \mathbf{y}]$  and  $B^1 = B[\mathbf{x}^1, \mathbf{y}^1], \dots, B^n = B[\mathbf{x}^n, \mathbf{y}^n]$  be LR B-splines defined on  $\mathcal{M}$  such that  $B^1, \dots, B^n \preceq B$ . Let  $\mathcal{N}$  be the mesh defined by the restriction of  $\mathcal{M}$  to the meshlines of  $\mathcal{M}(\mathbf{x}, \mathbf{y}), \mathcal{M}(\mathbf{x}^1, \mathbf{y}^1), \dots, \mathcal{M}(\mathbf{x}^n, \mathbf{y}^n)$ . Then,*

1. *there are at least one horizontal T-vertex and one vertical T-vertex of  $\mathcal{N}$  in the interior of  $\text{supp } B$ ;*
2. *by extending all the splits of  $\mathcal{N}$  in some direction to cross  $\text{supp } B$  entirely,  $B$  is refined, by Definition II.2.5, in LR B-splines that do not have any nested LR B-splines anymore.*

*Proof.*

1. Assume that there are no vertical T-vertices of  $\mathcal{N}$  in the interior of  $\text{supp } B$ . Then,  $\mathcal{N}$  would be tensorized in the first direction. By Proposition II.3.3, it would imply that all the LR B-splines defined on  $\mathcal{N}$  are non-nested, which is a contradiction. Analogously, one can prove that at least one horizontal T-vertex of  $\mathcal{N}$  must be in the interior of  $\text{supp } B$ .
2. Since  $B$  contains the support of other B-splines,  $\mathcal{N} \neq \mathcal{M}(\mathbf{x}, \mathbf{y})$  and in particular there exist at least one horizontal T-vertex and one vertical T-vertex by the previous item. We now focus on the vertical T-vertices, but of course the same argument can also be carried out for the horizontal T-vertices. We extend all the vertical splits in  $\mathcal{N}$  to cross  $\text{supp } B$  entirely, and denote this new mesh as  $\tilde{\mathcal{N}}$ . By Definition II.2.5, the extensions trigger a refinement of  $B$  via knot insertions.  $\tilde{\mathcal{N}}$  is tensorized in the first direction and, by Proposition II.3.3, no LR B-spline defined on  $\tilde{\mathcal{N}}$  is nested into another. ■

## II. Adaptive refinement with locally linearly independent LR B-splines: Theory and applications

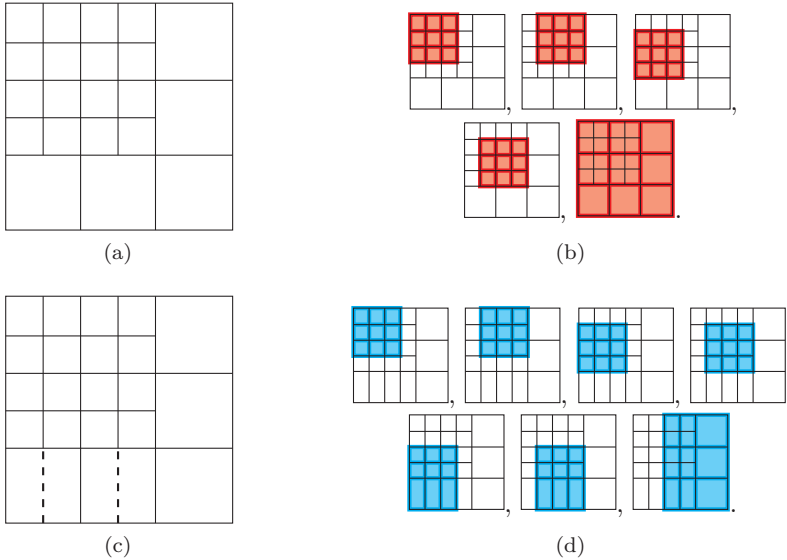


Figure II.9: Example of a vertical tensor expansion. We consider five LR B-splines of bidegree  $(2, 2)$ , namely  $B$  and  $B^1, \dots, B^4$ , with  $\text{supp } B^1, \dots, \text{supp } B^4$  contained in the upper left corner of  $\text{supp } B$ . The mesh  $\mathcal{N}$ , of multiplicity 1, generated by the meshlines of  $B, B^1, \dots, B^4$  is depicted in (a) and the supports of the LR B-splines are shown in (b). In (c) we perform a vertical tensor expansion of  $B^1, \dots, B^4$  in  $B$ . In (d) the supports of the new set of LR B-splines are shown: none of them has a nested LR B-spline anymore.

The extension of the splits considered in item 2 of Corollary II.3.4 will be called a **one-directional tensor expansion** of  $B^1, \dots, B^n$  in  $B$ . An example is illustrated in Figure II.9.

The  $N_2S$  structured mesh refinement is defined algorithmically as follows. We start from a structured mesh refinement to obtain a new set of LR B-splines. We then collect in a set  $\mathcal{B}$  all those LR B-splines that have nested LR B-splines in their supports. If  $\mathcal{B}$  is non-empty, we select an LR B-spline  $B$  in  $\mathcal{B}$  and we apply a one-directional tensor expansion to it. This triggers a refinement of the LR B-spline set, and therefore it changes also the set  $\mathcal{B}$ . We repeat this procedure till  $\mathcal{B}$  becomes empty. In Theorem II.3.5 we shall prove that this always happens in a finite number of steps. This procedure is sketched in Algorithm II.1. The one-directional tensor expansions are performed by alternating the direction for  $i$  even and odd, respectively, in order to bound the thinning of the box-partition elements in a specific direction and preserve the uniformity of the mesh as much as possible. The LR-mesh obtained in this way will be called an  **$N_2S$  structured LR-mesh**, or in short  $N_2S_2$ -mesh.

**Theorem II.3.5.** *Given an axis-aligned rectangular domain  $\Omega \subseteq \mathbb{R}^2$ , let  $\mathcal{B}_1$  be*

**Algorithm II.1:** N<sub>2</sub>S structured mesh refinement.

```

1  $\mathcal{B}_1$  is the B-spline set on the open tensor mesh equal to the domain's
   boundary;
2 for  $i = 1, 2, \dots$  do
3   perform a structured mesh refinement of  $\mathcal{B}_i$ ;
4   initialize  $\mathcal{B}_{i+1}$  as the LR B-spline set defined on the new LR-mesh;
5   define  $\mathcal{B} = \{B \in \mathcal{B}_{i+1} : \exists B' \in \mathcal{B}_{i+1} \text{ with } B' \preceq B\}$ ;
6   while  $\mathcal{B} \neq \emptyset$  do
7     select  $B \in \mathcal{B}$ ;
8     perform a one-directional tensor expansion of the LR B-splines
       nested in  $B$ ;
9     update  $\mathcal{B}_{i+1}$  as the LR B-spline set defined on the new LR-mesh;
10    update  $\mathcal{B} = \{B \in \mathcal{B}_{i+1} : \exists B' \in \mathcal{B}_{i+1} \text{ with } B' \preceq B\}$ ;

```

the set of standard bivariate B-splines defined on the open tensor mesh whose meshlines are the edges of  $\partial\Omega$ . Then,

1. the LR B-spline sets  $\mathcal{B}_i$  provided by Algorithm II.1 are well defined, i.e., the set  $\mathcal{B}$  of the algorithm becomes empty in a finite number of iterations, for every index  $i \geq 2$ ,
2. all the LR B-splines in  $\mathcal{B}_i$  are non-nested, for every  $i \geq 1$ .

*Proof.* Without loss of generality, we can assume that  $\Omega = [0, 1] \times [0, 1]$ . We proceed by induction on the index of the B-spline set. For  $i = 1$ ,  $\mathcal{B}_1$  is the set of standard B-splines on the open tensor mesh equal to the domain's boundary and we know they are locally linearly independent. By Theorem II.2.7 this is equivalent to be all non-nested. Assume now that  $\mathcal{B}_i$  is well defined and that the functions in it are all non-nested. Let us then prove that also  $\mathcal{B}_{i+1}$  is well defined and there is no LR B-spline nested into another LR B-spline of it. At every loop iteration in the algorithm, the LR B-splines that have a nested LR B-spline in their support are collected in the set  $\mathcal{B}$ . Therefore, whenever we can show that  $\mathcal{B}$  becomes empty after a certain iteration of the loop, we can immediately conclude both statements in the theorem.

By Corollary II.3.4, all the one-directional tensor expansions performed to define the set  $\mathcal{B}_{i+1}$  can be done in the same direction  $k \in \{1, 2\}$ , which is therefore fixed once and for all by the index  $i + 1$ . The length of the LR B-spline supports in the  $(3 - k)$ -th direction at any iteration of the loop cannot become shorter than  $2^{-(i+1)}$  regardless of the number of one-directional tensor expansions applied until then. This is because the  $(3 - k)$ -splits on the LR-meshes defined in the loop are fixed by the structured mesh refinement performed on  $\mathcal{B}_i$  at the beginning of the process and the minimal length of the box-partition elements in the  $(3 - k)$ -th direction is  $2^{-(i+1)}$ . Therefore, the split extensions applied when performing a one-directional tensor expansion in the  $k$ -th direction have lengths bounded

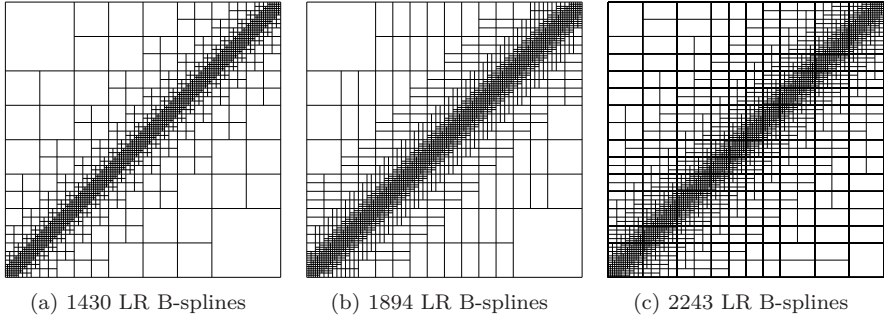


Figure II.10: Visual comparison of the meshes obtained on a diagonal refinement in  $[0, 1]^2$  and for bidegree  $(2, 2)$  when using the structured mesh (a), the  $N_2S$  structured mesh (b) and the mesh refinement proposed in [3] (c).

from below by  $2^{-(i+1)}$  in all the steps of the loop. This means that in a finite number of one-directional tensor expansions a  $k$ -split could be extended up to the domain's boundary, if needed, to remove nestedness issues, as these extensions cannot become arbitrarily small. In the worst case scenario, we must extend all the  $k$ -splits to cross entirely the domain. However, in this case, the resulting LR-mesh would be tensorized in the  $k$ -th direction. By Proposition II.3.3, there are only non-nested LR B-splines on this LR-mesh and thus  $\mathcal{B}$  becomes empty in a finite number of loop iterations. ■

In practice, the loop on  $\mathcal{B}$  stops quickly and the  $N_2S_2$ -meshes are far from being fully tensorized in one direction. In Figure II.10 we compare the structured LR-mesh (a), the corresponding  $N_2S_2$ -mesh (b) and the LR-mesh proposed in [3] (c) on a diagonal refinement in  $[0, 1]^2$ , when using 7 levels of mesh resolution and bidegree  $(2, 2)$ . We also indicate the number of LR B-splines defined on each of these meshes. We recall that the LR B-splines are not locally linearly independent on the structured LR-mesh, whereas they are on the  $N_2S_2$ -mesh and the LR-mesh proposed in [3].

In Figure II.10(b) and Figure II.11 one can see how the refinement in the  $N_2S_2$ -meshes propagates from the region where the structured mesh refinement has been applied. In all the considered cases, the refinement does not heavily spread out. It is important to highlight, however, that the prolongation of the splits needed to recover the  $N_2S$  property is not unique. Indeed, when refining an LR B-spline to remove nestedness issues, the inserted split prolongations refine not only the considered LR B-spline but in general also other LR B-splines in the neighborhood. Then, some of the newly introduced neighboring LR B-splines might not need a one-directional tensor expansion anymore and the ordering used for removing nestedness has thus an effect on the resulting mesh. One might consider to treat all the LR B-splines “in parallel”, i.e., first collect all the split extensions needed to remove nestedness in all the LR B-splines requiring a

treatment and then insert all of them at the same time to refine the function basis. This might result in a more uniform propagation of the refinement out of the region where the structured mesh has been applied. On the other hand, by doing this, some split extensions could be unnecessary for recovering the  $N_2S$  property. Therefore, in general, also the number of LR B-splines on these meshes would be higher than the number obtained when treating one LR B-spline at a time. In the examples presented in this paper we do not remove nestedness “in parallel”. Hence, the resulting  $N_2S_2$ -meshes depend on the order used when the one-directional tensor expansions are applied. On the other hand, the number of LR B-splines will be closer to the number of LR B-splines obtained when performing only the structured mesh refinement, i.e., closer to the “optimal” number of LR B-splines needed to reduce the error while preserving the local linear independence.

We finally remark that one could also opt for full tensor expansions in the supports, instead of one-directional tensor expansions, to solve nestedness issues. The proof of Theorem II.3.5 could be easily rephrased for the case of full tensor expansions. The key is that we only prolong splits provided by the structured mesh refinement performed at the beginning of the process. Therefore, if we do full tensor expansions, in the worst case scenario we would end up with a standard tensor mesh of size  $h = 2^{-(i+1)}$  to define the set  $\mathcal{B}_{i+1}$ , instead of an LR-mesh tensorized in one direction. In such case,  $\mathcal{B}$  would still become empty in a finite number of loop iterations. However, we decided to do the expansion of the splits only in one direction at a time because it reduces the propagation more.

## II.4 Application I: Quasi-interpolation

A quasi-interpolation method is a procedure to compute the coefficients assigned to the basis elements of a prescribed function space, in order to approximate arbitrary functions or data sets in it. The resulting approximant is called a quasi-interpolant (QI). The computation of any of such coefficients may depend only on the data/function restricted to the corresponding basis element’s support (local method), and perhaps some neighboring other basis elements’ supports, or it can depend on the data/function in the entire domain (global method), as in the least-squares method. Given a function  $f$  and an approximation space, whose basis is denoted by  $\mathcal{B}$ , we write a related QI in the form

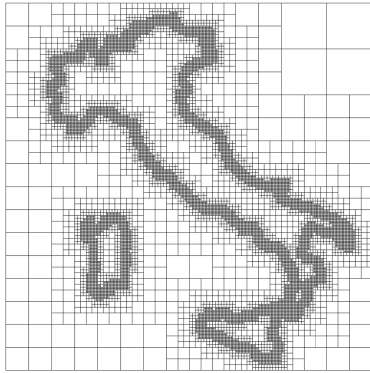
$$\mathcal{Q}f := \sum_{B \in \mathcal{B}} \lambda_B(f)B,$$

where  $\lambda_B(f)$  is the coefficient of the basis element  $B \in \mathcal{B}$  computed by the selected method.

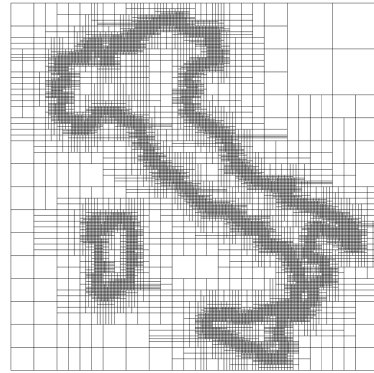
**Definition II.4.1.** A quasi-interpolation method such that  $\mathcal{Q}f = f$  for all  $f$  in a space  $V$  is said to reproduce space  $V$ .

## II. Adaptive refinement with locally linearly independent LR B-splines: Theory and applications

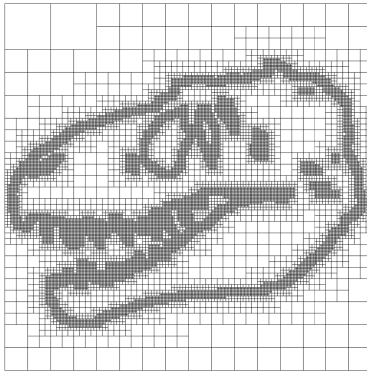
---



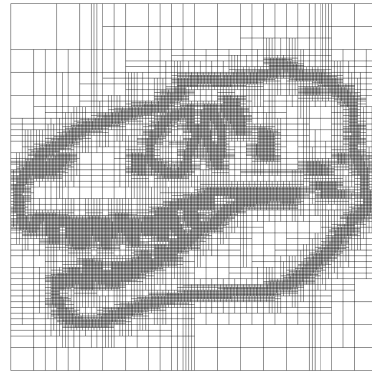
(a) 10281 LR B-splines



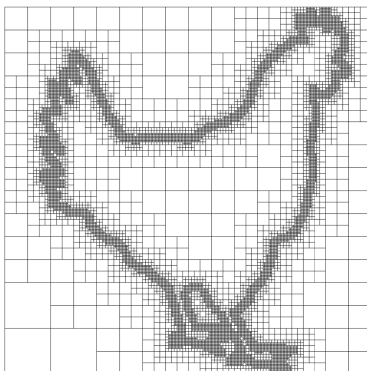
(b) 12438 LR B-splines



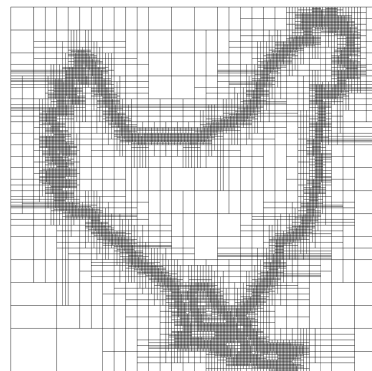
(c) 13459 LR B-splines



(d) 15993 LR B-splines



(e) 8608 LR B-splines



(f) 10841 LR B-splines

Figure II.11: Meshes obtained in  $[0, 1]^2$  with bidegree  $(2, 2)$  for 3 different regions of refinement by performing 8 levels of structured mesh (left column) and corresponding  $N_2S$  structured mesh (right column).

When using spline spaces of bidegree  $\mathbf{p}$  as approximation spaces, a common requirement is that the polynomial space  $\Pi_{\mathbf{p}}$  is reproduced by the quasi-interpolation method, in order to ensure good approximation properties. A general recipe for constructing local quasi-interpolation methods for tensor spline spaces, with the polynomial reproduction property, can be found in [16].

**Recipe II.4.2.** Let  $f$  be a given function defined on the rectangle  $\Omega$ . Given a bidegree  $\mathbf{p}$ , let  $\widetilde{\mathcal{M}}$  be an open tensor mesh on  $\Omega$ , and let  $\mathcal{B}(\widetilde{\mathcal{M}})$  be the set of tensor B-splines of bidegree  $\mathbf{p}$  on  $\widetilde{\mathcal{M}}$ . We compute the coefficient  $\lambda_B(f)$ , for every  $B = B[\mathbf{x}, \mathbf{y}] \in \mathcal{B}(\widetilde{\mathcal{M}})$ , as follows:

1. let  $U \subseteq \mathbb{R}^2$  be an open set that intersects the interior of  $\text{supp } B$  (for instance,  $U$  can be a box-partition element of  $\mathcal{M}(\mathbf{x}, \mathbf{y})$ ) and let  $\mathcal{B}(U)$  be the subset of  $\mathcal{B}(\widetilde{\mathcal{M}})$  consisting of all the tensor B-splines not identically zero on  $U$ ;
2. choose a local approximation method  $\mathfrak{P}_U$  such that  $\mathfrak{P}_U q = q$  for all  $q \in \Pi_{\mathbf{p}}$  defined on  $U$  (typical choices are least-squares or interpolation methods);
3. let  $g|_U$  be the restriction of  $g$  to  $U$ , then

$$(\mathfrak{P}_U f)|_U = \sum_{\widetilde{B} \in \mathcal{B}(U)} b_{\widetilde{B}}(f) \widetilde{B}|_U,$$

for some coefficients  $b_{\widetilde{B}}(f)$  provided by the chosen local approximation method;

4. since  $B \in \mathcal{B}(U)$ , set  $\lambda_B(f) := b_{\widetilde{B}}(f)$ .

Then, define

$$\Omega f := \sum_{B \in \mathcal{B}(\widetilde{\mathcal{M}})} \lambda_B(f) B.$$

Inspired by the above recipe for tensor splines and similar to the local quasi-interpolation strategy developed for THB-splines in [24, 25], we can formulate a general recipe for constructing QIs in the space spanned by  $\mathcal{B}^{\mathcal{LR}}(\mathcal{M})$  on a given open LR-mesh  $\mathcal{M}$  as follows: select for each LR B-spline  $B$  in  $\mathcal{B}^{\mathcal{LR}}(\mathcal{M})$  a local tensor space containing  $B$ , and pick the coefficient corresponding to  $B$  in the expression of any QI in such a tensor space. In particular, when the smallest local tensor space containing each basis function  $B$  is considered, we arrive at the following recipe.

**Recipe II.4.3.** Let  $f$  be a given function defined on the rectangle  $\Omega$ . Given a bidegree  $\mathbf{p}$ , let  $\mathcal{M}$  be an open LR-mesh on  $\Omega$ , and let  $\mathcal{B}^{\mathcal{LR}}(\mathcal{M})$  be the set of LR B-splines of bidegree  $\mathbf{p}$  on  $\mathcal{M}$ . We compute the coefficient  $\lambda_B(f)$ , for every  $B = B[\mathbf{x}, \mathbf{y}] \in \mathcal{B}^{\mathcal{LR}}(\mathcal{M})$ , as follows:

1. let  $\widetilde{\mathcal{M}}_B$  be the open (tensor) mesh obtained by rising the boundary meshline multiplicities of  $\mathcal{M}_B = \mathcal{M}(\mathbf{x}, \mathbf{y})$  to full multiplicity;

## II. Adaptive refinement with locally linearly independent LR B-splines: Theory and applications

---

2. let  $\mathcal{B}(\widetilde{\mathcal{M}}_B)$  be the set of tensor B-splines defined on  $\widetilde{\mathcal{M}}_B$ ;
3. consider a quasi-interpolation method in the space spanned by  $\mathcal{B}(\widetilde{\mathcal{M}}_B)$ ,

$$\mathfrak{Q}_B f = \sum_{\widetilde{B} \in \mathcal{B}(\widetilde{\mathcal{M}}_B)} \lambda_{\widetilde{B}}(f) \widetilde{B},$$

reproducing all  $g \in \Pi_{\mathbf{p}}$  (for instance, use Recipe II.4.2);

Then, define

$$\mathfrak{Q}f := \sum_{B \in \mathcal{B}^{\mathcal{LR}}(\mathcal{M})} \lambda_B(f) B.$$

Since  $B \in \mathcal{B}(\widetilde{\mathcal{M}}_B)$  for any  $B \in \mathcal{B}^{\mathcal{LR}}(\mathcal{M})$ , the function  $\mathfrak{Q}f$  in Recipe II.4.3 is well defined. Moreover, it will reproduce polynomials on the entire domain if the LR-mesh has the  $N_2S$  property as stated in the following proposition.

**Proposition II.4.4.** *Given a bidegree  $\mathbf{p}$ , let  $\mathcal{M}$  be an open LR-mesh and let  $\mathcal{B}^{\mathcal{LR}}(\mathcal{M})$  be the set of LR B-splines of bidegree  $\mathbf{p}$  on  $\mathcal{M}$ . Assume that  $\mathcal{M}$  has the  $N_2S$  property, then:*

$$\mathfrak{Q}g = g, \quad \forall g \in \Pi_{\mathbf{p}},$$

where the quasi-interpolation operator  $\mathfrak{Q}$  is defined in Recipe II.4.3.

*Proof.* From [2, Theorem 4.6], if  $\mathcal{M}$  has the  $N_2S$  property, then for all  $g \in \Pi_{\mathbf{p}}$  we have

$$g = \sum_{B \in \mathcal{B}^{\mathcal{LR}}(\mathcal{M})} g_B B, \quad g_B \in \mathbb{R},$$

where for all  $B \in \mathcal{B}^{\mathcal{LR}}(\mathcal{M})$ , the coefficient  $g_B$  only depends on  $g$  and on the knots defining the LR B-spline  $B$ . Therefore,  $g_B$  remains the same if we represent  $g$  in any set of tensor B-splines containing  $B$ . Since, according to Recipe II.4.3, any  $\mathfrak{Q}_B$  reproduces all polynomials in  $\Pi_{\mathbf{p}}$  we have

$$g_B = \lambda_B(g), \quad \forall B \in \mathcal{B}^{\mathcal{LR}}(\mathcal{M}), \quad g \in \Pi_{\mathbf{p}},$$

which completes the proof. ■

We have tested the quasi-interpolation strategy described in Recipe II.4.3 on  $N_2S_2$ -meshes to approximate polynomials and transcendent functions. Given an  $N_2S_2$ -mesh  $\mathcal{M}$ , we first have computed a QI based on  $\mathcal{B}(\widetilde{\mathcal{M}}_B)$ , for all the LR B-splines  $B \in \mathcal{B}^{\mathcal{LR}}(\mathcal{M})$  of bidegree  $\mathbf{p} = (p_1, p_2)$ . As local approximation in the computation of these QIs we have used interpolation, i.e., we have selected  $(p_1 + 1)(p_2 + 1)$  points in a box-partition element of  $\widetilde{\mathcal{M}}_B$  and then we have set a linear system by evaluating  $f$  and the tensor B-splines in  $\mathcal{B}(\widetilde{\mathcal{M}}_B)$  at these points. By sampling such a number of points in the same box-partition element, this guarantees polynomial reproduction of the quasi-interpolation method in the spaces  $\mathcal{B}(\widetilde{\mathcal{M}}_B)$ , for  $B$  varying in  $\mathcal{B}^{\mathcal{LR}}(\mathcal{M})$ . Therefore, also the resulting quasi-interpolation method on  $\mathcal{B}^{\mathcal{LR}}(\mathcal{M})$  has the polynomial reproduction property

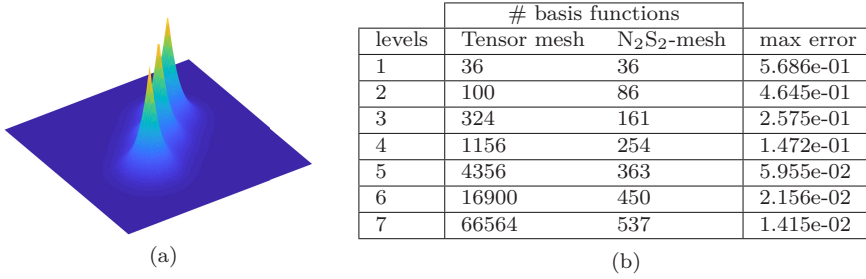


Figure II.12: (a) Transcendent function in  $[-1, 1]^2$ , (b) B-spline set cardinalities of bidegree  $(2, 2)$  for different levels of maximal resolution.

by Proposition II.4.4. Indeed, in all the tests with polynomial functions of bidegree at most  $\mathbf{p}$ , the maximum error was in the order of the machine precision, regardless of the number of iterations performed to construct the  $N_2S_2$ -mesh. The maximum error was computed on a uniform  $150 \times 150$  grid.

As test with a transcendent function, we have considered

$$f(x, y) = \frac{2}{3}e^{-\sqrt{(10x-3)^2+(10y-3)^2}} + \frac{2}{3}e^{-\sqrt{(10x+3)^2+(10y+3)^2}} + \frac{2}{3}e^{-\sqrt{(10x)^2+(10y)^2}},$$

which is characterized by three steep peaks on the square  $[-1, 1]^2$  located at  $(-0.3, -0.3)$ ,  $(0, 0)$  and  $(0.3, 0.3)$ ; see Figure II.12(a). This function has also been used in [25] to investigate the approximation power of a similar quasi-interpolation method developed for THB-splines. In table of Figure II.12(b), we compare the number of basis functions of bidegree  $(2, 2)$  when considering global tensor meshes and local  $N_2S_2$ -meshes for different levels of maximal resolution (for level  $\ell$ , the smallest box-partition elements on the mesh have length  $2^{-\ell}$ ). The  $N_2S_2$ -mesh is produced by refining the LR B-splines whose supports contain one of the three points where a peak occurs via structured mesh and then by recovering the  $N_2S$  property via one-directional tensor expansions. For a given maximal resolution level, the optimal maximum error, i.e., the maximum error when using the global tensor mesh, is preserved by the  $N_2S_2$ -mesh. However, the number of B-splines is significantly different and the discrepancy exponentially grows with the maximal resolution level.

## II.5 Application II: Isogeometric analysis

Isogeometric analysis (IgA), introduced in [14], is a technique to perform numerical simulations on complex geometries. The numerical solution is represented by means of the same functions used for the domain modeling. Nowadays, complex geometries are expressed in terms of computed aided design (CAD) technologies, such as B-splines, non-uniform rational B-splines (NURBS) and their generalizations to address adaptive refinements.

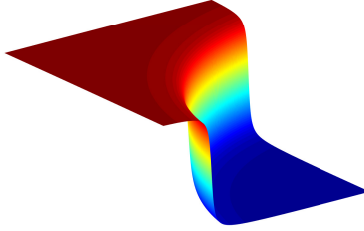


Figure II.13: Exact solution of the Poisson problem.

In this section, we adopt the IgA approach, using our LR refinement strategy, to approximate the solution of the Poisson problem on  $\Omega = [0, 1]^2$ ,

$$\begin{cases} -\Delta u = f & \text{in } \mathring{\Omega} \\ u = u_D, & \text{on } \partial\Omega, \end{cases} \quad (\text{II.2})$$

whose exact solution is

$$u(x, y) = \arctan \left( 100 \left( \sqrt{(x - 1.25)^2 + (y + 0.25)^2} - \frac{\pi}{3} \right) \right);$$

see Figure II.13. This example is a good benchmark for numerical schemes, as the sharp interior layer of the exact solution highlights the approximation quality, and it has been used extensively in the literature; see, e.g., [5, 15, 19].

In the context of Galerkin discretizations, two properties are desirable:

- (local) linear independence of the space generators,
- refinement adaptivity.

The linear independence of the functions used as building blocks of the numerical solution avoids the numerical complexity posed by the singularity of the matrices associated to the problem discretization. The refinement adaptivity is desired for balancing accuracy and computational cost as it allows for a higher precision, only there where it is needed to reproduce fast variations of the exact solution. LR B-splines on  $N_2S_2$ -meshes are suitable candidates as both the (local) linear independence of the space generators and the adaptivity of the refinement are guaranteed.

In Figure II.14 we compare the  $L^\infty$ -norm and the  $L^2$ -norm of the error (Figures II.14(a) and II.14(b) respectively), using bidegree (2, 2) with global tensor meshes and local  $N_2S_2$ -meshes for different levels of maximal resolution to approximate the solution of the Poisson problem (II.2). The  $N_2S_2$ -mesh is computed by first applying the structured mesh to the LR B-splines whose supports intersect the curve where the sharp interior layer in the exact solution occurs, and then by performing one-directional tensor expansions to recover the  $N_2S$  property. The error norms, which are computed discretely on a uniform grid of  $1000 \times 1000$  points, are plotted in log-log scale with respect to the number of LR B-splines on the mesh. The solid line with circular markers shows the decay

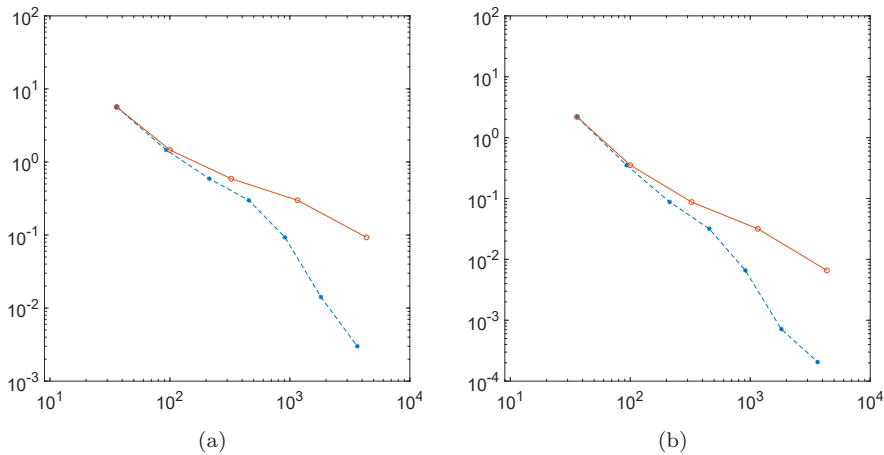


Figure II.14: Decay of the  $L^\infty$ -norm (a) and  $L^2$ -norm (b) of the error when approximating the solution of problem (II.2) with B-splines of bidegree  $(2, 2)$  on tensor meshes (solid line) and  $N_2S_2$ -meshes (dashed line) for different levels of maximal resolution.

when using global tensor meshes, whereas the dashed line with star markers the decay for the  $N_2S_2$ -meshes. In the figures, the first marker corresponds to the  $4 \times 4$  tensor mesh, for maximal resolution level  $\ell = 2$ , and it is the maximal level for which the LR B-spline and standard tensor B-spline sets coincide. When considering a comparable number of functions, the  $N_2S_2$ -mesh leads to a significant reduction of both the  $L^\infty$ -norm and the  $L^2$ -norm of the error with respect to the tensor mesh, thanks to the adaptivity of the refinement.

## II.6 Conclusion

LR B-splines are one of the most elegant extensions of univariate B-splines on local tensor structures that allow local refinement. They possess almost all the properties of classical B-splines, but they are not always linearly independent. Recently, a characterization of LR-meshes ensuring local linear independence of the corresponding LR B-splines has been presented in the literature. However, a practical adaptive refinement strategy for LR-meshes that maintain such a property was missing. In this paper, we have filled this gap by describing an adaptive refinement strategy that produces LR-meshes where the corresponding LR B-splines are locally linearly independent. Subsequently, we have exploited the local linear independence of the LR B-splines to construct efficient quasi-interpolation schemes and to solve elliptic problems using the isogeometric Galerkin method.

## Acknowledgements

We are very grateful to Tor Dokken (SINTEF, Oslo) and K.A. Johannessen (SINTEF, Trondheim) for sharing with us the example in Figure II.8 that shows that the standard structured mesh refinement may produce linearly dependent sets of LR B-splines.

## References

- [1] Beirão da Veiga, L. et al. “Mathematical analysis of variational isogeometric methods”. In: *Acta Numerica* vol. 23 (2014), pp. 157–287.
- [2] Bressan, A. “Some properties of LR-splines”. In: *Computer Aided Geometric Design* vol. 30, no. 8 (2013), pp. 778–794.
- [3] Bressan, A. and Jüttler, B. “A hierarchical construction of LR meshes in 2D”. In: *Computer Aided Geometric Design* vol. 37 (2015), pp. 9–24.
- [4] Buffa, A., Cho, D., and Sangalli, G. “Linear independence of the T-spline blending functions associated with some particular T-meshes”. In: *Computer Methods in Applied Mechanics and Engineering* vol. 199, no. 23–24 (2010), pp. 1437–1445.
- [5] Cao, J. et al. “A finite element framework based on bivariate simplex splines on triangle configurations”. In: *Computer Methods in Applied Mechanics and Engineering* vol. 357 (2019), p. 112598.
- [6] Cohen, E., Riesenfeld, R. F., and Elber, G. *Geometric Modeling with Splines: An Introduction*. A K Peters, Wellesley, 2001.
- [7] Cottrell, J. A., Hughes, T. J. R., and Bazilevs, Y. *Isogeometric Analysis: Toward Integration of CAD and FEA*. John Wiley & Sons, Chichester, 2009.
- [8] de Boor, C. *A Practical Guide to Splines*. revised. Springer-Verlag New York, 2001.
- [9] Deng, J. et al. “Polynomial splines over hierarchical T-meshes”. In: *Graphical models* vol. 70, no. 4 (2008), pp. 76–86.
- [10] Dokken, T., Lyche, T., and Pettersen, K. F. “Polynomial splines over locally refined box-partitions”. In: *Computer Aided Geometric Design* vol. 30, no. 3 (2013), pp. 331–356.
- [11] Engleitner, N. and Jüttler, B. “Patchwork B-spline refinement”. In: *Computer-Aided Design* vol. 90 (2017), pp. 168–179.
- [12] Forsey, D. R. and Bartels, R. H. “Hierarchical B-spline refinement”. In: *ACM Siggraph Computer Graphics* vol. 22, no. 4 (1988), pp. 205–212.
- [13] Giannelli, C., Jüttler, B., and Speleers, H. “THB-splines: The truncated basis for hierarchical splines”. In: *Computer Aided Geometric Design* vol. 29, no. 7 (2012), pp. 485–498.

- 
- [14] Hughes, T. J. R., Cottrell, J. A., and Bazilevs, Y. “Isogeometric analysis: CAD, finite elements, NURBS, exact geometry and mesh refinement”. In: *Computer Methods in Applied Mechanics and Engineering* vol. 194, no. 39–41 (2005), pp. 4135–4195.
- [15] Johannessen, K. A., Kvamsdal, T., and Dokken, T. “Isogeometric analysis using LR B-splines”. In: *Computer Methods in Applied Mechanics and Engineering* vol. 269 (2014), pp. 471–514.
- [16] Lee, B. G., Lyche, T., and Mørken, K. “Some examples of quasi-interpolants constructed from local spline projectors”. In: *Mathematical Methods in CAGD: Oslo 2000*. Ed. by Lyche, T. and Schumaker, L. L. Vanderbilt University Press, Nashville, 2001, pp. 243–252.
- [17] Lyche, T., Manni, C., and Speleers, H. “Foundations of spline theory: B-splines, spline approximation, and hierarchical refinement”. In: *Splines and PDEs: From Approximation Theory to Numerical Linear Algebra*. Ed. by Lyche, T. et al. Vol. 2219. Lecture Notes in Mathematics. Springer International Publishing AG, 2018, pp. 1–76.
- [18] Manni, C. and Speleers, H. “Standard and non-standard CAGD tools for isogeometric analysis: A tutorial”. In: *IsoGeometric Analysis: A New Paradigm in the Numerical Approximation of PDEs*. Ed. by Buffa, A. and Sangalli, G. Vol. 2161. Lecture Notes in Mathematics. Springer International Publishing AG, 2016, pp. 1–69.
- [19] Mitchell, W. F. and McClain, M. A. “A survey of  $hp$ -adaptive strategies for elliptic partial differential equations”. In: *Recent Advances in Computational and Applied Mathematics*. Ed. by Simos, T. E. Springer Dordrecht, 2011, pp. 227–258.
- [20] Patrizi, F. and Dokken, T. “Linear dependence of bivariate Minimal Support and Locally Refined B-splines over LR-meshes”. In: *Computer Aided Geometric Design* ((2019) In Press).
- [21] Piegl, L. and Tiller, W. *The NURBS Book*. second. Springer-Verlag Berlin, 1997.
- [22] Schumaker, L. L. *Spline Functions: Basic Theory*. third. Cambridge University Press, 2007.
- [23] Sederberg, T. W. et al. “T-splines and T-NURCCs”. In: *ACM Transactions on Graphics* vol. 22, no. 3 (2003), pp. 477–484.
- [24] Speleers, H. “Hierarchical spline spaces: Quasi-interpolants and local approximation estimates”. In: *Advances in Computational Mathematics* vol. 43, no. 2 (2017), pp. 235–255.
- [25] Speleers, H. and Manni, C. “Effortless quasi-interpolation in hierarchical spaces”. In: *Numerische Mathematik* vol. 132, no. 1 (2016), pp. 155–184.



## Paper III

# Transfinite mean value interpolation over polygons

Michael S. Floater, Francesco Patrizi

To appear in *Numerical Algorithms*. arXiv: 1906.08358.

### Abstract

Mean value interpolation is a method for fitting a smooth function to piecewise-linear data prescribed on the boundary of a polygon of arbitrary shape, and has applications in computer graphics and curve and surface modelling. The method generalizes to transfinite interpolation, i.e., to any continuous data on the boundary but a mathematical proof that interpolation always holds has so far been missing. The purpose of this note is to complete this gap in the theory.

### III.1 Introduction

One of the main uses of generalized barycentric coordinates (GBCs) is to interpolate piecewise-linear data prescribed on the boundary of a polygon with a smooth function. This kind of barycentric interpolation has been used, for example, in computer graphics, as the basis for image warping, and in higher dimension, for mesh deformation.

One type of GBCs that is frequently used for this is mean value (MV) coordinates due to a simple closed formula. MV coordinates have been studied extensively in various papers [2] but while they are simple to implement, a mathematical proof of interpolation seems surprisingly difficult. A proof for convex polygons is relatively simple and follows from the fact that MV coordinates are positive in this case. Interpolation for a convex polygon holds in fact for any positive barycentric coordinates; see [4]. For arbitrary polygons, a specific proof of interpolation for MV coordinates was derived in [6].

The MV interpolant to piecewise-linear boundary data is based on integration with respect to angles around each chosen point inside the polygon. This construction extends in a natural way to any continuous boundary data thus providing a transfinite interpolant [1, 7]. Such interpolation could have various applications, one of which is its use as a building block for interpolants of higher order that also match derivative data on the boundary. However, there is currently no mathematical proof of interpolation in the transfinite setting



in all cases, only numerical evidence. Like in the piecewise-linear case, when the polygon is convex, interpolation is easier to establish. In fact it was shown in [1] for more general domains, convex or otherwise, under the condition that the distance between the external medial axis of the domain and the domain boundary is strictly positive. This latter condition trivially holds for convex domains since there is no external medial axis in this case.

This still leaves open the question of whether MV interpolation really interpolates any continuous data on the boundary of an arbitrary polygon, and this is what we establish in this paper. The proof parallels that of [6] in that we treat interpolation at edge points and vertices separately: in Theorems III.3.1 and III.4.1 respectively. At the end of the paper we give two examples that numerically confirm the interpolation property.

Mean value coordinates have been generalized to 3D geometry based on triangular meshes in [5, 7], and the numerical examples in [5] suggest that the interpolation property holds for arbitrary (non-convex) meshes, at least for piecewise-linear boundary data. However, there does not seem to be any straightforward way to prove this based on the proof in the 2D case.

It would also be interesting to establish transfinite interpolation over more general domains with weaker conditions on the shape of the boundary than those used in [1].

## III.2 Definitions

Let  $\Omega \subset \mathbb{R}^2$  be a polygon with vertices  $V$  and edges  $E$ . Suppose that  $f : \partial\Omega \rightarrow \mathbb{R}$  is a continuous function on the boundary  $\partial\Omega$ . We define a function  $g : \Omega \rightarrow \mathbb{R}$  as follows. For each edge  $e \in E$ , let  $\mathbf{n}_e$  denote the outward unit normal to  $e$  with respect to  $\Omega$ , and for each point  $\mathbf{x} \in \Omega$ , let  $h_e(\mathbf{x})$  be the signed distance of  $\mathbf{x}$  to the straight line through  $e$ ,

$$h_e(\mathbf{x}) = (\mathbf{y} - \mathbf{x}) \cdot \mathbf{n}_e,$$

for any  $\mathbf{y} \in e$ . We let  $\tau_e(\mathbf{x}) \in \{-1, 0, 1\}$  be the sign of the distance,

$$\tau_e(\mathbf{x}) = \text{sgn}(h_e(\mathbf{x})).$$

Let  $\mathbb{S}_1$  denote the unit circle in  $\mathbb{R}^2$ . For  $\mathbf{x} \in \Omega$ , let  $\widehat{e}(\mathbf{x}) \subset \mathbb{S}_1$  denote the circular arc on  $\mathbb{S}_1$  formed by projecting  $e$  onto the unit circle centred at  $\mathbf{x}$ ,

$$\widehat{e}(\mathbf{x}) = \left\{ \frac{\mathbf{y} - \mathbf{x}}{\|\mathbf{y} - \mathbf{x}\|} : \mathbf{y} \in e \right\},$$

with  $\|\cdot\|$  the Euclidean norm. This arc is just a point in the case that  $\tau_e(\mathbf{x}) = 0$ . Suppose  $\tau_e(\mathbf{x}) \neq 0$ . Then for each unit vector  $\boldsymbol{\mu} \in \widehat{e}(\mathbf{x})$ , let  $\mathbf{y}_e(\mathbf{x}, \boldsymbol{\mu})$  be the unique point of  $e$  such that

$$\frac{\mathbf{y}_e(\mathbf{x}, \boldsymbol{\mu}) - \mathbf{x}}{\|\mathbf{y}_e(\mathbf{x}, \boldsymbol{\mu}) - \mathbf{x}\|} = \boldsymbol{\mu},$$

and let

$$I_e(\mathbf{x}) = \int_{\widehat{e}(\mathbf{x})} \frac{1}{\|\mathbf{y}_e(\mathbf{x}, \boldsymbol{\mu}) - \mathbf{x}\|} d\boldsymbol{\mu} > 0, \quad I_e(\mathbf{x}; f) = \int_{\widehat{e}(\mathbf{x})} \frac{f(\mathbf{y}_e(\mathbf{x}, \boldsymbol{\mu}))}{\|\mathbf{y}_e(\mathbf{x}, \boldsymbol{\mu}) - \mathbf{x}\|} d\boldsymbol{\mu}.$$

In the case that  $\tau_e(\mathbf{x}) = 0$ , we define  $I_e(\mathbf{x}) = I_e(\mathbf{x}; f) = 0$ .

We now define

$$g(\mathbf{x}) = \mathcal{I}f(\mathbf{x}) = \sum_{e \in E} \tau_e(\mathbf{x}) I_e(\mathbf{x}; f) / \phi(\mathbf{x}), \quad (\text{III.1})$$

where

$$\phi(\mathbf{x}) = \sum_{e \in E} \tau_e(\mathbf{x}) I_e(\mathbf{x}). \quad (\text{III.2})$$

As shown in [3], if  $e = [\mathbf{v}_1, \mathbf{v}_2]$  then

$$I_e(\mathbf{x}) = \tan(\alpha_e(\mathbf{x})/2) \left( \frac{1}{\|\mathbf{v}_1 - \mathbf{x}\|} + \frac{1}{\|\mathbf{v}_2 - \mathbf{x}\|} \right), \quad (\text{III.3})$$

where  $\alpha_e(\mathbf{x}) \in [0, \pi)$  is the angle at  $\mathbf{x}$  of the triangle  $[\mathbf{x}, \mathbf{v}_1, \mathbf{v}_2]$ . It was shown in [6, Theorem 4.3] that  $\phi(\mathbf{x}) > 0$  for all  $\mathbf{x} \in \Omega$ , and therefore  $g$  is well defined. Furthermore, by the results of [6, Section 3], in the case that  $f$  is the restriction of a linear function  $\mathbb{R}^2 \rightarrow \mathbb{R}$  to  $\partial\Omega$ ,  $g$  interpolates  $f$ .

### III.3 Interpolation on an edge

**Theorem III.3.1.** *Let  $\mathbf{y}_*$  be an interior point of some edge of  $\partial\Omega$ . Then  $g(\mathbf{x}) \rightarrow f(\mathbf{y}_*)$  as  $\mathbf{x} \rightarrow \mathbf{y}_*$  for  $\mathbf{x} \in \Omega$ .*

*Proof.* From the form of (III.1),

$$g(\mathbf{x}) - f(\mathbf{y}_*) = \sum_{e \in E} \tau_e(\mathbf{x}) I_e(\mathbf{x}; \tilde{f}) / \phi(\mathbf{x}),$$

where  $\tilde{f}(\mathbf{y}) := f(\mathbf{y}) - f(\mathbf{y}_*)$  and therefore

$$|g(\mathbf{x}) - f(\mathbf{y}_*)| \leq \sum_{e \in E} I_e(\mathbf{x}; |\tilde{f}|) / \phi(\mathbf{x}). \quad (\text{III.4})$$

Let  $[\mathbf{v}_1, \mathbf{v}_2] \in E$  be the edge containing  $\mathbf{y}_*$ , as in Figure III.1. Let  $\epsilon > 0$ . By

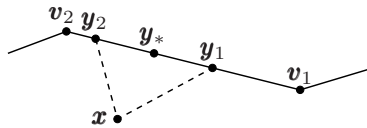


Figure III.1: Interpolation at an edge point  $\mathbf{y}_*$ .

### III. Transfinite mean value interpolation over polygons

---

the continuity of  $f$ , there is some  $\delta$ , where

$$0 < \delta < \min\{\|\mathbf{v}_1 - \mathbf{y}_*\|, \|\mathbf{v}_2 - \mathbf{y}_*\|\},$$

such that if  $\mathbf{y} \in [\mathbf{v}_1, \mathbf{v}_2]$  and  $\|\mathbf{y} - \mathbf{y}_*\| \leq \delta$  then  $|f(\mathbf{y}) - f(\mathbf{y}_*)| < \epsilon$ . Let  $\mathbf{y}_j \in [\mathbf{y}_*, \mathbf{v}_j]$ ,  $j = 1, 2$ , be the point such that  $\|\mathbf{y}_j - \mathbf{y}_*\| = \delta$ , and let  $e_0 = [\mathbf{y}_1, \mathbf{y}_2]$ . Then,

$$\sum_{e \in E} I_e(\mathbf{x}; |\tilde{f}|) = I_{e_0}(\mathbf{x}; |\tilde{f}|) + \sum_{e \in F} I_e(\mathbf{x}; |\tilde{f}|),$$

where

$$F = \{[\mathbf{v}_1, \mathbf{y}_1], [\mathbf{y}_2, \mathbf{v}_2]\} \cup (E \setminus [\mathbf{v}_1, \mathbf{v}_2]),$$

and it follows that  $|g(\mathbf{x}) - f(\mathbf{y}_*)| \leq \gamma(\mathbf{x})/\phi(\mathbf{x})$ , where

$$\gamma(\mathbf{x}) = \epsilon I_{e_0}(\mathbf{x}) + 2M \sum_{e \in F} I_e(\mathbf{x}),$$

and

$$M := \sup_{\mathbf{y} \in \partial\Omega} |f(\mathbf{y})|. \quad (\text{III.5})$$

Similar to  $\gamma(\mathbf{x})$ , we can express  $\phi(\mathbf{x})$  as

$$\phi(\mathbf{x}) = \tau_{e_0}(\mathbf{x}) I_{e_0}(\mathbf{x}) + \sum_{e \in F} \tau_e(\mathbf{x}) I_e(\mathbf{x}).$$

For  $\mathbf{x}$  close enough to  $\mathbf{y}_*$ ,  $\tau_{e_0}(\mathbf{x}) = 1$ , and then

$$\frac{\gamma(\mathbf{x})}{\phi(\mathbf{x})} = \frac{\epsilon + 2M \sum_{e \in F} I_e(\mathbf{x})/I_{e_0}(\mathbf{x})}{1 + \sum_{e \in F} \tau_e(\mathbf{x}) I_e(\mathbf{x})/I_{e_0}(\mathbf{x})}.$$

As  $\mathbf{x} \rightarrow \mathbf{y}_*$ ,  $\alpha_{e_0}(\mathbf{x}) \rightarrow \pi$ , and since  $\mathbf{y}_* \notin e$  for all  $e \in F$ ,

$$\alpha_e(\mathbf{x}) \rightarrow \alpha_e(\mathbf{y}_*) < \pi, \quad e \in F.$$

Therefore, by (III.3), as  $\mathbf{x} \rightarrow \mathbf{y}_*$ ,

$$I_{e_0}(\mathbf{x}) \rightarrow \infty \quad \text{and} \quad I_e(\mathbf{x}) \rightarrow I_e(\mathbf{y}_*) \neq \infty, \quad e \in F.$$

Thus  $\gamma(\mathbf{x})/\phi(\mathbf{x}) \rightarrow \epsilon$  as  $\mathbf{x} \rightarrow \mathbf{y}_*$ . Hence,

$$\limsup_{\mathbf{x} \rightarrow \mathbf{y}_*} |g(\mathbf{x}) - f(\mathbf{y}_*)| \leq \epsilon$$

for any  $\epsilon > 0$  which shows that  $|g(\mathbf{x}) - f(\mathbf{y}_*)| \rightarrow 0$  as  $\mathbf{x} \rightarrow \mathbf{y}_*$ . ■

### III.4 Interpolation at a vertex

**Theorem III.4.1.** For  $\mathbf{v} \in V$ ,  $g(\mathbf{x}) \rightarrow f(\mathbf{v})$  as  $\mathbf{x} \rightarrow \mathbf{v}$  for  $\mathbf{x} \in \Omega$ .

*Proof.* Similar to (III.4), from the form of (III.1),

$$|g(\mathbf{x}) - f(\mathbf{v})| \leq \sum_{e \in E} I_e(\mathbf{x}; |\tilde{f}|) / \phi(\mathbf{x}),$$

where  $\tilde{f}(\mathbf{y}) := f(\mathbf{y}) - f(\mathbf{v})$ .

Let  $\mathbf{v}_1$  and  $\mathbf{v}_2$  be the two neighbouring vertices of  $\mathbf{v}$  with  $\mathbf{v}_1, \mathbf{v}, \mathbf{v}_2$  ordered anticlockwise w.r.t.  $\partial\Omega$  as in Figures III.2 and III.3. Let  $\epsilon > 0$ . By the continuity

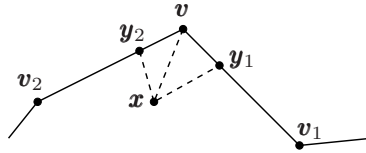


Figure III.2: Interpolation at a convex vertex  $\mathbf{v}$ .

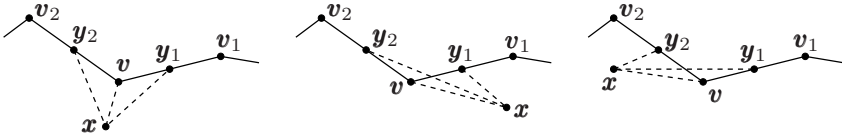


Figure III.3: Interpolation at a concave vertex  $\mathbf{v}$ .

of  $f$ , there is some  $\delta$ , where

$$0 < \delta < \min\{\|\mathbf{v}_1 - \mathbf{v}\|, \|\mathbf{v}_2 - \mathbf{v}\|\},$$

such that if  $\mathbf{y}$  is in  $[\mathbf{v}_1, \mathbf{v}]$  or  $[\mathbf{v}, \mathbf{v}_2]$  and  $\|\mathbf{y} - \mathbf{v}\| \leq \delta$  then  $|f(\mathbf{y}) - f(\mathbf{v})| < \epsilon$ . Let  $\mathbf{y}_j \in [\mathbf{v}, \mathbf{v}_j]$ ,  $j = 1, 2$ , be the point such that  $\|\mathbf{y}_j - \mathbf{v}\| = \delta$ , and define  $e_1 = [\mathbf{y}_1, \mathbf{v}]$  and  $e_2 = [\mathbf{v}, \mathbf{y}_2]$ . Then,

$$\sum_{e \in E} I_e(\mathbf{x}; |\tilde{f}|) = I_{e_1}(\mathbf{x}; |\tilde{f}|) + I_{e_2}(\mathbf{x}; |\tilde{f}|) + \sum_{e \in F} I_e(\mathbf{x}; |\tilde{f}|),$$

where

$$F = \{[\mathbf{v}_1, \mathbf{y}_1], [\mathbf{y}_2, \mathbf{v}_2]\} \cup (E \setminus \{[\mathbf{v}_1, \mathbf{v}], [\mathbf{v}, \mathbf{v}_2]\}).$$

It follows that  $|g(\mathbf{x}) - f(\mathbf{y}_*)| \leq \gamma(\mathbf{x}) / \phi(\mathbf{x})$ , where

$$\gamma(\mathbf{x}) = \epsilon(I_{e_1}(\mathbf{x}) + I_{e_2}(\mathbf{x})) + 2M \sum_{e \in F} I_e(\mathbf{x}),$$

### III. Transfinite mean value interpolation over polygons

---

and  $M$  is as in (III.5). We can similarly express  $\phi(\mathbf{x})$  as

$$\phi(\mathbf{x}) = \tau_{e_1}(\mathbf{x})I_{e_1}(\mathbf{x}) + \tau_{e_2}(\mathbf{x})I_{e_2}(\mathbf{x}) + \sum_{e \in F} \tau_e(\mathbf{x})I_e(\mathbf{x}).$$

Then using (III.3), and multiplying both  $\gamma(\mathbf{x})$  and  $\phi(\mathbf{x})$  by  $\|\mathbf{v} - \mathbf{x}\|$ , we have

$$\frac{\gamma(\mathbf{x})}{\phi(\mathbf{x})} = \frac{\epsilon(\tan(\alpha_{e_1}(\mathbf{x})/2) + \tan(\alpha_{e_2}(\mathbf{x})/2)) + A(\mathbf{x})}{\tau_{e_1}(\mathbf{x})\tan(\alpha_{e_1}(\mathbf{x})/2) + \tau_{e_2}(\mathbf{x})\tan(\alpha_{e_2}(\mathbf{x})/2) + B(\mathbf{x})},$$

where  $A(\mathbf{x}), B(\mathbf{x}) \rightarrow 0$  as  $\mathbf{x} \rightarrow \mathbf{v}$ . Letting  $\tau_j = \tau_{e_j}$  and  $\alpha_j = \alpha_{e_j}$ ,  $j = 1, 2$ , and using the fact that  $-\tan(\beta) = \tan(-\beta)$  for  $\beta \in \mathbb{R}$ , we can rewrite this as

$$\frac{\gamma(\mathbf{x})}{\phi(\mathbf{x})} = \frac{\epsilon(\tan(\alpha_1(\mathbf{x})/2) + \tan(\alpha_2(\mathbf{x})/2)) + A(\mathbf{x})}{\tan(\tau_1(\mathbf{x})\alpha_1(\mathbf{x})/2) + \tan(\tau_2(\mathbf{x})\alpha_2(\mathbf{x})/2) + B(\mathbf{x})}.$$

Next, using the identity

$$\tan(\beta_1) + \tan(\beta_2) = \frac{\sin(\beta_1 + \beta_2)}{\cos(\beta_1)\cos(\beta_2)},$$

and the fact that  $\cos(-\beta) = \cos(\beta)$ , it follows that

$$\frac{\gamma(\mathbf{x})}{\phi(\mathbf{x})} = \frac{\epsilon \sin((\alpha_1(\mathbf{x}) + \alpha_2(\mathbf{x}))/2) + \tilde{A}(\mathbf{x})}{\sin((\tau_1(\mathbf{x})\alpha_1(\mathbf{x}) + \tau_2(\mathbf{x})\alpha_2(\mathbf{x}))/2) + \tilde{B}(\mathbf{x})},$$

where

$$\begin{aligned} \tilde{A}(\mathbf{x}) &= \cos((\alpha_1(\mathbf{x})/2)\cos((\alpha_2(\mathbf{x})/2)A(\mathbf{x}), \\ \tilde{B}(\mathbf{x}) &= \cos((\alpha_1(\mathbf{x})/2)\cos((\alpha_2(\mathbf{x})/2)B(\mathbf{x}), \end{aligned}$$

and so also  $\tilde{A}(\mathbf{x}), \tilde{B}(\mathbf{x}) \rightarrow 0$  as  $\mathbf{x} \rightarrow \mathbf{v}$ .

Finally, we consider the two cases (i)  $\mathbf{v}$  is a convex vertex and (ii)  $\mathbf{v}$  is a concave vertex. In case (i), referring to Figure III.2 we see that for  $\mathbf{x}$  close enough to  $\mathbf{v}$ ,  $\tau_1(\mathbf{x}) = \tau_2(\mathbf{x}) = 1$  and so

$$\lim_{\mathbf{x} \rightarrow \mathbf{v}} \frac{\gamma(\mathbf{x})}{\phi(\mathbf{x})} = \epsilon. \quad (\text{III.6})$$

In case (ii), the values of  $\tau_1(\mathbf{x})$  and  $\tau_2(\mathbf{x})$  depend on the location of  $\mathbf{x}$ , even when  $\mathbf{x}$  is close to  $\mathbf{v}$ . However, for any  $\mathbf{x}$  that is close enough to  $\mathbf{v}$ , we have the identity (observed in [6])

$$\tau_1(\mathbf{x})\alpha_1(\mathbf{x}) + \tau_2(\mathbf{x})\alpha_2(\mathbf{x}) = \alpha_{[\mathbf{y}_1, \mathbf{y}_2]}(\mathbf{x}).$$

This can be verified in the three cases illustrated in Figure III.3. In the three configurations, from left to right, we have, respectively,

$$\alpha_{[\mathbf{y}_1, \mathbf{y}_2]}(\mathbf{x}) = \begin{cases} \alpha_1(\mathbf{x}) + \alpha_2(\mathbf{x}), \\ \alpha_1(\mathbf{x}) - \alpha_2(\mathbf{x}), \\ -\alpha_1(\mathbf{x}) + \alpha_2(\mathbf{x}). \end{cases}$$

Thus,

$$\lim_{\mathbf{x} \rightarrow \mathbf{v}} (\tau_1(\mathbf{x})\alpha_1(\mathbf{x}) + \tau_2(\mathbf{x})\alpha_2(\mathbf{x})) = \alpha_{[\mathbf{y}_1, \mathbf{y}_2]}(\mathbf{v}) = \alpha_{[\mathbf{v}_1, \mathbf{v}_2]}(\mathbf{v}) \in (0, \pi).$$

Since  $\sin((\alpha_1(\mathbf{x}) + \alpha_2(\mathbf{x}))/2) \leq 1$ , it follows that in case (ii),

$$\limsup_{\mathbf{x} \rightarrow \mathbf{v}} \frac{\gamma(\mathbf{x})}{\phi(\mathbf{x})} \leq \frac{\epsilon}{\sin(\alpha_{[\mathbf{v}_1, \mathbf{v}_2]}(\mathbf{v})/2)}. \quad (\text{III.7})$$

From (III.6) and (III.7) we deduce that for any type of vertex  $\mathbf{v}$ ,  $|g(\mathbf{x}) - f(\mathbf{v})| \rightarrow 0$  as  $\mathbf{x} \rightarrow \mathbf{v}$ . ■

### III.5 Numerical examples

In this section we present two examples of transfinite mean value interpolants of different functions over a polygonal-shaped domain in order to confirm the theoretical interpolation property proven in Sections III.3 and III.4. Here, we start with a bivariate function  $f(x, y)$  defined in the entire domain  $\Omega$ . We then compute the mean value interpolant  $g(x, y)$  and compare it with  $f$  on  $\Omega$ . We have used the boundary integral formula of [1] to evaluate  $g$ . This is more efficient than applying the definition, equation (III.1), which would require computing intersection points.

The first function we consider is

$$f(x, y) = x^2 - y^2$$

defined on the non-convex polygon in Figure III.4a. Figures III.4a and III.4b illustrate the exact surface and Figures III.4c and III.4d the corresponding interpolant  $g(x, y)$ . Figure III.4e shows the absolute error  $|f(x, y) - g(x, y)|$ . The darker the colour the smaller the error and, as expected, the error vanishes as we get close to the boundary.

For our second example we chose the function

$$f(x, y) = \frac{1}{9}[\tanh(9x - 9y) + 1].$$

Figures III.5a and III.5b and Figures III.5c and III.5d show the exact surface and the interpolant, respectively, while Figure III.5e shows the absolute error.

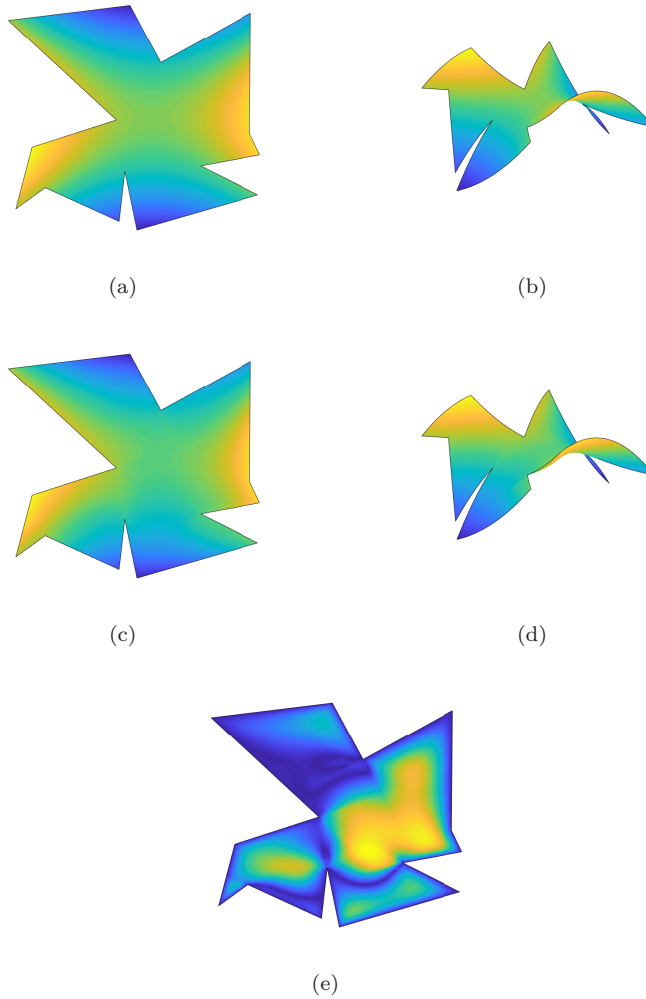


Figure III.4: (a), (b) Exact surface  $f(x, y)$ . (c), (d) Corresponding interpolant  $g(x, y)$ . (e) Absolute error  $|f(x, y) - g(x, y)|$ .

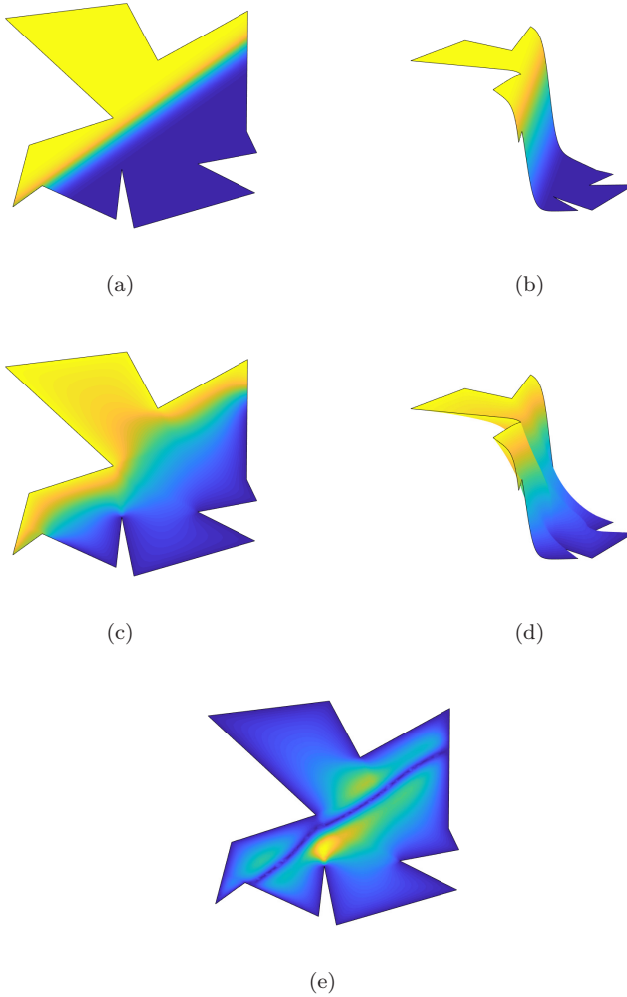


Figure III.5: (a), (b) Exact surface  $f(x, y)$ . (c), (d) Corresponding interpolant  $g(x, y)$ . (e) Absolute error  $|f(x, y) - g(x, y)|$ .

## References

- [1] Dyken, C. and Floater, M. S. “Transfinite mean value interpolation”. In: *Computer Aided Geometric Design* vol. 26 (2009), pp. 117–134.
- [2] Floater, M. S. “Generalized barycentric coordinates and applications”. In: *Acta Numerica* vol. 24 (2015), pp. 161–214.
- [3] Floater, M. S. “Mean value coordinates”. In: *Computer Aided Geometric Design* vol. 20, no. 1 (2003), pp. 19–27.
- [4] Floater, M. S., Hormann, K., and Kós, G. “A general construction of barycentric coordinates over convex polygons”. In: *Advances in Computational Mathematics* vol. 24 (2006), pp. 311–331.
- [5] Floater, M. S., Kós, G., and Reimers, M. “Mean value coordinates in 3D”. In: *Computer Aided Geometric Design* vol. 22, no. 7 (2005), pp. 623–631.
- [6] Hormann, K. and Floater, M. S. “Mean value coordinates for arbitrary planar polygons”. In: *ACM Transactions on Graphics* vol. 25 (2006), pp. 1424–1441.
- [7] Ju, T., Schaefer, S., and Warren, J. “Mean value coordinates for closed triangular meshes”. In: *ACM Transactions on Graphics* vol. 24 (2005), pp. 561–566.

# Appendices



# Appendix A

## Dimension of the spline spaces

The scope of this appendix is to provide a more deep analysis of the dimension of the spline space over a spline mesh and to justify the LR-rules defined at the end of Section 1.1 of the introduction. This is a simplified excerpt for the 2D case of [1], in which the dimension of the spline spaces in  $dD$  is addressed for any  $d \geq 1$ .

**Definition A.0.1.** Given a sequence of vector spaces  $V_i$ ,  $i = n, \dots, m$  for some  $n \leq m$  and linear maps  $\delta_q : V_q \rightarrow V_{q-1}$ , the composition

$$\mathfrak{A} : V_m \xrightarrow{\delta_m} V_{m-1} \xrightarrow{\delta_{m-1}} \dots \xrightarrow{\delta_{n+1}} V_n \quad (\text{A.1})$$

is called **chain complex** if  $\text{Im } \delta_{q+1} \subseteq \text{Ker } \delta_q$  for  $n+1 \leq q \leq m-1$ . For a chain complex of the form (A.1), we define the  **$q$ th homology of  $\mathfrak{A}$**  to be the vector space  $H_q(\mathfrak{A}) = \text{Ker } \delta_q / \text{Im } \delta_{q+1}$ .

As we will see in Theorem A.0.5, in the dimension formula of the spline space  $\mathbb{S}(\mathcal{N})$  over a given spline mesh  $\mathcal{N}$ , there are terms depending on the homologies of a particular chain complex, denoted as  $\mathfrak{S}(\mathcal{N})$ , whose vector spaces and linear maps are defined in what follows.

**Definition A.0.2.** Given a spline mesh  $\mathcal{N} = (\mathcal{M}, \mu, \mathbf{p})$  in  $\mathbb{R}^2$ ,

- for a  $(k, a)$ -meshline  $\gamma \in \mathcal{M}$ , we define

$$P_\gamma(\mathcal{N}) := (x_k - a)^{p_k - \mu(\gamma) + 1} \quad (\text{where } (x_1, x_2) := (x, y)), \quad (\text{A.2})$$

and the vector space of polynomials in  $\Pi_{\mathbf{p}}$  divisible by  $P_\gamma(\mathcal{N})$ ,

$$\Delta_\gamma(\mathcal{N}) := \{F \cdot P_\gamma(\mathcal{N}) : F \in \Pi_{\mathbf{p}\gamma} \text{ with } p_j^\gamma := p_j \text{ for } j \neq k \text{ and } p_k^\gamma := \mu(\gamma) - 1\}, \quad (\text{A.3})$$

- for a vertex  $\mathbf{q}$  in  $\mathcal{V}$ , we define the collection of meshlines

$$\mathcal{D}_{\mathbf{q}}(\mathcal{N}) := \{\gamma \in \mathcal{M} : \mathbf{q} \in \gamma\} \quad (\text{A.4})$$

and the vector space

$$\Delta_{\mathbf{q}}(\mathcal{N}) = \sum_{\gamma \in \mathcal{D}_{\mathbf{q}}(\mathcal{N})} \Delta_\gamma(\mathcal{N}). \quad (\text{A.5})$$

as the smallest vector space including each  $\Delta_\gamma(\mathcal{N})$  for  $\gamma \in \mathcal{D}_{\mathbf{q}}(\mathcal{N})$ .

## A. Dimension of the spline spaces

---

Finally we introduce the spaces

$$\begin{aligned} S_2(\mathcal{N}) &= \bigoplus_{\beta \in \mathcal{E}} [\beta] \Pi_{\mathbf{p}} \\ S_1(\mathcal{N}) &= \bigoplus_{\gamma \in \mathcal{M}} [\gamma] \Pi_{\mathbf{p}} / \Delta_{\gamma}(\mathcal{N}) \\ S_0(\mathcal{N}) &= \bigoplus_{\mathbf{q} \in \mathcal{V}} [\mathbf{q}] \Pi_{\mathbf{p}} / \Delta_{\mathbf{q}}(\mathcal{N}) \end{aligned} \quad (\text{A.6})$$

with  $[\cdot]$  the characteristic function of its argument.

$S_2(\mathcal{N})$  is the space of piecewise polynomials of bidegree  $\mathbf{p}$  over the box-partition elements, and, if  $\mathcal{E} = \{\beta_1, \dots, \beta_{n_{\mathcal{E}}}\}$ , an element in  $S_2(\mathcal{N})$  is expressed as

$$(f_{\beta_1}, \dots, f_{\beta_{n_{\mathcal{E}}}}) = \sum_{i=1}^{n_{\mathcal{E}}} [\beta_i] f_{\beta_i} \text{ with } f_{\beta_i} \in \Pi_{\mathbf{p}},$$

for  $i = 1, \dots, n_{\mathcal{E}}$ .  $S_1(\mathcal{N})$  and  $S_0(\mathcal{N})$  are quotient spaces and therefore their elements are classes of polynomial expressions. However, if  $\mathcal{M} = \{\gamma_1, \dots, \gamma_{n_{\mathcal{M}}}\}$  and  $\mathcal{V} = \{\mathbf{q}_1, \dots, \mathbf{q}_{n_{\mathcal{V}}}\}$ , then, a class representative in  $S_1(\mathcal{N})$  has expression:

$$(f_{\gamma_1}, \dots, f_{\gamma_{n_{\mathcal{M}}}}) = \sum_{i=1}^{n_{\mathcal{M}}} [\gamma_i] f_{\gamma_i}$$

with  $f_{\gamma_i}$ , for  $i = 1, \dots, n_{\mathcal{M}}$ , a polynomial of degree up to  $p_{3-k}$  and  $p_k - \mu(\gamma_i)$  if  $\gamma_i$  is a  $k$ -meshline, and a class representative in  $S_0(\mathcal{N})$  has expression:

$$(f_{\mathbf{q}_1}, \dots, f_{\mathbf{q}_{n_{\mathcal{V}}}}) = \sum_{i=1}^{n_{\mathcal{V}}} [\mathbf{q}_i] f_{\mathbf{q}_i} \text{ with } f_{\mathbf{q}_i} \in \Pi_{(p_1 - \mu_1(\mathbf{q}_i), p_2 - \mu_2(\mathbf{q}_i))}$$

for  $i = 1, \dots, n_{\mathcal{V}}$ .

**Definition A.0.3.** Given a spline mesh  $\mathcal{N} = (\mathcal{M}, \mu, \mathbf{p})$  corresponding to a box-partition  $\mathcal{E}$ , let  $\beta$  be an element of  $\mathcal{E}$ . We define the **positive boundary** of  $\beta$ ,  $B_{\beta}^+$ , as the meshlines of  $\mathcal{M}$  contained in the lower and right edges of  $\beta$  and the **negative boundary** of  $\beta$ ,  $B_{\beta}^-$ , as the meshlines of  $\mathcal{M}$  contained in the left and upper edges of  $\beta$ .

Then, we define the boundary map  $\delta_2 : S_2(\mathcal{N}) \rightarrow S_1(\mathcal{N})$  as the linear map given by

$$\delta_2 \left( \sum_{\beta \in \mathcal{E}} [\beta] f_{\beta} \right) = \sum_{\beta \in \mathcal{E}} \delta_2([\beta]) f_{\beta} \quad \text{with } \delta_2([\beta]) := \sum_{\gamma \in B_{\beta}^+} [\gamma] - \sum_{\gamma \in B_{\beta}^-} [\gamma]. \quad (\text{A.7})$$

Let  $\gamma$  be a meshline of  $\mathcal{M}$  with  $\mathbf{q}_1, \mathbf{q}_2$  its endpoints increasingly ordered. Similarly we define the boundary map  $\delta_1 : S_1(\mathcal{N}) \rightarrow S_0(\mathcal{N})$ , as the linear map given by

$$\delta_1 \left( \sum_{\gamma \in \mathcal{M}} [\gamma] f_{\gamma} \right) = \sum_{\gamma \in \mathcal{M}} \delta_1([\gamma]) f_{\gamma} \quad \text{with } \delta_1([\gamma]) := [\mathbf{q}_2] - [\mathbf{q}_1]. \quad (\text{A.8})$$

---

**Proposition A.0.4** ([1, Lemma 9]). *Given a spline mesh  $\mathcal{N}$  in  $\mathbb{R}^2$ , the following composition is a chain complex*

$$\mathfrak{S}(\mathcal{N}) : 0 \xrightarrow{\delta_3} S_2(\mathcal{N}) \xrightarrow{\delta_2} S_1(\mathcal{N}) \xrightarrow{\delta_1} S_0(\mathcal{N}) \xrightarrow{\delta_0} 0 \quad (\text{A.9})$$

where  $\delta_3, \delta_0$  are the zero mapping while  $\delta_2, \delta_1$  are defined in (A.7) and (A.8) respectively.

The following result is the dimension formula for bivariate spline spaces on arbitrary spline meshes.

**Theorem A.0.5** ([1, Theorem 2]). *Let  $\mathcal{N} = (\mathcal{M}, \mu, \mathbf{p})$  be a spline mesh in  $\mathbb{R}^2$  corresponding to a box-partition  $\mathcal{E}$  and let  $\mathcal{V}$  be the set of vertices of  $\mathcal{E}$ . Moreover, let  $\mathcal{M}^1, \mathcal{M}^2 \subset \mathcal{M}$  be the collections of 1-meshlines and 2-meshlines in  $\mathcal{M}$  respectively. Then the dimension of the spline space  $\mathbb{S}(\mathcal{N})$  is given by*

$$\begin{aligned} \dim \mathbb{S}(\mathcal{N}) &= \sum_{\mathbf{q} \in \mathcal{V}} [(p_1 - \mu_1(\mathbf{q}) + 1)(p_2 - \mu_2(\mathbf{q}) + 1)] \\ &\quad - (p_2 + 1) \sum_{\gamma \in \mathcal{M}^1} (p_1 - \mu(\gamma) + 1) - (p_1 + 1) \sum_{\gamma \in \mathcal{M}^2} (p_2 - \mu(\gamma) + 1) \\ &\quad + |\mathcal{E}|(p_1 + 1)(p_2 + 1) + \dim H_1(\mathfrak{S}(\mathcal{N})) - \dim H_0(\mathfrak{S}(\mathcal{N})), \end{aligned} \quad (\text{A.10})$$

where  $|\mathcal{E}|$  is the cardinality of  $\mathcal{E}$ ,  $\mu_1, \mu_2$  are respectively the vertical and horizontal multiplicities of the box-partition vertices and  $H_1(\mathfrak{S}(\mathcal{N})), H_0(\mathfrak{S}(\mathcal{N}))$  are the 1st and 0th homologies of the chain complex  $\mathfrak{S}(\mathcal{N})$  defined in (A.9).

As we already mentioned in the introduction, the homological part of equation (A.10) makes the dimension of the spline spaces unstable under slight changes of the sizes of the box-partition elements. This implies that two spline spaces of the same bidegree, defined on meshes with the same topological structure and meshlines with the same multiplicities might have different dimensions, as shown in Figure 1.4 in the introduction. In what follows we recall some results from [1] to estimate the homology dimensions and eventually nullify them to reduce the spline dimension only to the combinatorial computation of equation (1.3) in the introduction.

We first present a condition to have zero homology dimensions in the special case of tensor spline meshes.

**Proposition A.0.6** ([1, Corollary 2]). *Suppose  $\mathcal{N} = \mathcal{N}[\boldsymbol{\tau}_{1,p_1}^{\mu_1}, \boldsymbol{\tau}_{2,p_2}^{\mu_2}]$  is a tensor spline mesh generated by the spline sequences  $\boldsymbol{\tau}_{k,p_k}^{\mu_k}$  for  $k = 1, 2$ . Let  $d_k = \dim \mathbb{S}(\boldsymbol{\tau}_{k,p_k}^{\mu_k})$  and let also  $q' \in \{0, 1, 2\}$  be the number of nonzero  $d_k$ . Then*

$$\dim H_q(\mathfrak{S}(\mathcal{N})) = 0 \quad \text{if } q \neq q' \quad (\text{A.11})$$

*Remark A.0.7.* In particular, if  $\mathbb{S}(\mathcal{N}) \neq \{0\}$ , then both  $d_1, d_2 \geq 1$  and  $\dim H_1(\mathfrak{S}(\mathcal{N})) = \dim H_0(\mathfrak{S}(\mathcal{N})) = 0$ .

## A. Dimension of the spline spaces

---

The following result guarantees that the homology term  $H_0(\mathfrak{S}(\mathcal{N}))$  has dimension 0 on any nontrivial spline mesh, i.e., when the spline space  $\mathbb{S}(\mathcal{N}) \neq \{0\}$ .

**Proposition A.0.8** ([1, Lemma 17]). *Given a spline mesh  $\mathcal{N} = (\mathcal{M}, \mu, \mathbf{p})$ , for  $k = 1, 2$  and  $a \in \mathbb{R}$  let  $m_{k,a}$  be the maximum of  $\mu(\gamma)$  over all the  $(k, a)$ -meshlines in  $\mathcal{M}$ , or 0 if no such meshlines exist. Define  $m_k = p_k + 1 - \sum_{a \in \mathbb{R}} m_{k,a}$ . Then*

$$\dim H_0(\mathfrak{S}(\mathcal{N})) = \begin{cases} m_1 \cdot m_2 & \text{if } m_k > 0 \text{ for } k = 1, 2 \\ 0 & \text{if } m_k \leq 0 \text{ for at least one } k \in \{1, 2\}, \end{cases} \quad (\text{A.12})$$

In particular, if  $\dim \mathbb{S}(\mathcal{N}) \neq 0$  then  $\dim H_0(\mathfrak{S}(\mathcal{N})) = 0$ .

*Remark A.0.9.* The sum in the expression of  $m_k$  is a finite sum because  $m_{k,a}$  is different from 0 only for a finite number of  $a$ , i.e., when a  $(k, a)$ -meshline is in the mesh.

The next result provides an estimate of the dimension of the homology term  $H_1(\mathfrak{S}(\mathcal{N}))$  in the special case that the spline mesh  $\mathcal{N}$  is built through a mesh refinement process from a coarse initial tensor spline mesh.

**Theorem A.0.10** ([1, Theorem 6]). *Let  $\mathcal{N}_0$  be a tensor spline mesh in  $\mathbb{R}^2$  and let  $\gamma_1, \gamma_2, \dots$  be a sequence of splits. Define the sequence of spline meshes  $\mathcal{N}_i := \mathcal{N}_{i-1} + \gamma_i$  for  $i = 1, 2, \dots$ . Then,*

$$\dim H_1(\mathfrak{S}(\mathcal{N}_N)) \leq \dim H_1(\mathfrak{S}(\mathcal{N}_0)) + \sum_{i=1}^N \max\{0, -\alpha_i\} \quad \forall N > 0 \quad (\text{A.13})$$

where

$$\alpha_i = \sum_{j=1}^{n_i} \tilde{\mu}_{3-k}(\tau_j) - (p_{3-k} + 1) \quad (\text{A.14})$$

and  $\boldsymbol{\tau}_{i, p_{3-k}}^{\tilde{\mu}_{3-k}} = (\boldsymbol{\tau}_i, \tilde{\mu}_{3-k}, p_{3-k})$ , with  $\boldsymbol{\tau}_i = (\tau_1, \dots, \tau_{n_i})$ , is the expanded knot vector defined on the  $k$ -split  $\gamma_i$ .

*Remark A.0.11.* If the univariate spline space on  $\boldsymbol{\tau}_{p_{3-k}, i}^{\tilde{\mu}_{3-k}}$  is nontrivial, i.e.,  $\mathbb{S}(\boldsymbol{\tau}_{i, p_{3-k}}^{\tilde{\mu}_{3-k}}) \neq \{0\}$ , then, by Theorem 1.1.3,  $\alpha_i > 0$ .

**Example A.0.12.** In this example we estimate the spline space dimension on a spline mesh. Consider bidegree  $\mathbf{p} = (p, p)$  and the mesh  $\mathcal{M}$  with assigned multiplicities reported in Figure A.1(a). The cardinality of the box-partition is  $|\mathcal{E}| = 3$  and, by looking at the meshline multiplicities, one can easily check that

$$\begin{array}{llll} \mu_1(\mathbf{q}_1) = 1, & \mu_2(\mathbf{q}_1) = p + 1, & \mu_1(\mathbf{q}_5) = 1, & \mu_2(\mathbf{q}_5) = 1, \\ \mu_1(\mathbf{q}_2) = 1, & \mu_2(\mathbf{q}_2) = p + 1, & \mu_1(\mathbf{q}_6) = 1, & \mu_2(\mathbf{q}_6) = p + 1, \\ \mu_1(\mathbf{q}_3) = p + 1, & \mu_2(\mathbf{q}_3) = p + 1, & \mu_1(\mathbf{q}_7) = 1, & \mu_2(\mathbf{q}_7) = p + 1, \\ \mu_1(\mathbf{q}_4) = 1, & \mu_2(\mathbf{q}_4) = 1, & \mu_1(\mathbf{q}_8) = p + 1, & \mu_2(\mathbf{q}_8) = p + 1, \end{array}$$

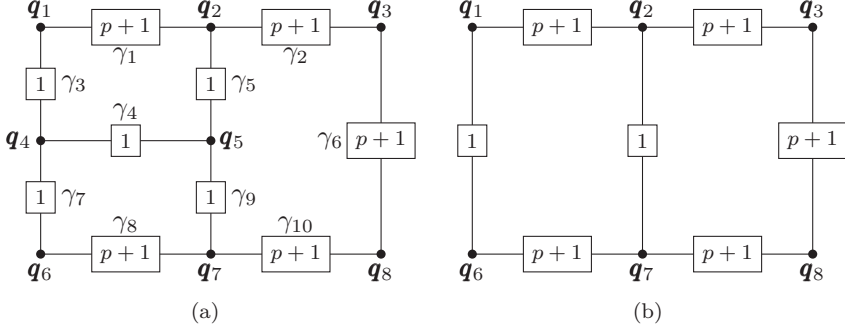


Figure A.1: A spline mesh and the tensor spline mesh in it.

so that

$$\sum_{\mathbf{q} \in \mathcal{V}} [(p - \mu_1(\mathbf{q}) + 1)(p - \mu_2(\mathbf{q}) + 1)] = 2p^2. \quad (\text{A.15})$$

Similarly, one can easily verify that

$$-(p+1) \sum_{\gamma \in \mathcal{M}} (p - \mu(\gamma) + 1) = -5p^2 - 5p. \quad (\text{A.16})$$

Therefore, by Theorem A.0.5, the spline space on the spline mesh  $\mathcal{N}$  depicted in Figure A.1 has dimension

$$\begin{aligned} \dim \mathbb{S}(\mathcal{N}) &= 2p^2 - 5p^2 - 5p + 3(p+1)^2 + \dim H_1(\mathfrak{S}(\mathcal{N})) - \dim H_0(\mathfrak{S}(\mathcal{N})) \\ &= p + 3 + \dim H_1(\mathfrak{S}(\mathcal{N})) - \dim H_0(\mathfrak{S}(\mathcal{N})). \end{aligned} \quad (\text{A.17})$$

Moreover, Proposition A.0.8 ensures that  $\dim H_0(\mathfrak{S}(\mathcal{N})) = 0$  because  $m_1 = -2$  (and  $m_2 = -p-2$ ). Next, we can use Theorem A.0.10 to estimate  $\dim H_1(\mathfrak{S}(\mathcal{N}))$ . Indeed,  $\mathcal{N}$  can be seen as a refined mesh  $\mathcal{N} = \mathcal{N}_1 = \mathcal{N}_0 + \gamma_1$  where  $\mathcal{N}_0 = \mathcal{N}_0[\boldsymbol{\tau}_{1,p}^{\mu_1}, \boldsymbol{\tau}_{2,p}^{\mu_2}]$  is the tensor mesh shown in Figure A.1(b). In  $\boldsymbol{\tau}_{1,p}^{\mu_1}$  and  $\boldsymbol{\tau}_{2,p}^{\mu_2}$ , the two sequences  $\boldsymbol{\tau}_1, \boldsymbol{\tau}_2$  have the  $x$ -coordinates of  $\mathbf{q}_6, \mathbf{q}_7, \mathbf{q}_8$  and the  $y$ -coordinates of  $\mathbf{q}_1, \mathbf{q}_6$  respectively as elements and the multiplicity functions  $\mu_1, \mu_2$  are the vertical and horizontal multiplicities of these vertices. The spline spaces defined on  $\boldsymbol{\tau}_{1,p}^{\mu_1}, \boldsymbol{\tau}_{2,p}^{\mu_2}$  have dimension

$$\begin{aligned} \dim \mathbb{S}(\boldsymbol{\tau}_{1,p}^{\mu_1}) &= d_1 = \sum_{i=6}^8 \mu_1(\mathbf{q}_i) - (p+1) = 2 \\ \dim \mathbb{S}(\boldsymbol{\tau}_{2,p}^{\mu_2}) &= d_2 = \sum_{i=1,6} \mu_2(\mathbf{q}_i) - (p+1) = p+1, \end{aligned} \quad (\text{A.18})$$

so that, by Proposition A.0.6,  $\dim H_0(\mathfrak{S}(\mathcal{N}_0)) = \dim H_1(\mathfrak{S}(\mathcal{N}_0)) = 0$ .

## A. Dimension of the spline spaces

---

The (expanded) spline sequence on  $\gamma_1$  is  $\tau_p^{\mu_1}$  with sequence  $\tau$  given by the  $x$ -coordinates of the vertices  $\mathbf{q}_4, \mathbf{q}_5$  in Figure A.1(a) and multiplicity function equal to the vertical multiplicity of such vertices. Therefore,

$$\alpha_1 = \mu_1(\mathbf{q}_4) + \mu_1(\mathbf{q}_5) - (p + 1) = 1 + 1 - (p + 1) = 1 - p, \quad (\text{A.19})$$

and, by using Theorem A.0.10,

$$\dim H_1(\mathfrak{S}(\mathcal{N})) \leq \dim H_1(\mathfrak{S}(\mathcal{N}_0)) + \max\{0, -\alpha_1\} = \max\{0, p - 1\}. \quad (\text{A.20})$$

For  $p \in \{0, 1\}$ ,  $\dim H_1(\mathfrak{S}(\mathcal{N})) = 0$  so that  $\dim \mathbb{S}(\mathcal{N}) = p + 3$ . If  $p \geq 2$ ,  $\dim H_1(\mathfrak{S}(\mathcal{N})) \leq p - 1$  and  $\dim \mathbb{S}(\mathcal{N}) \leq 2p + 2$ .

By combining the results in Proposition A.0.6, Proposition A.0.8 and Theorem A.0.10, we can state that the LR-rules, defined at the end of Section 1.1, are sufficient conditions for a mesh refinement process to eliminate the homological terms in the spline space dimension formula (A.10).

*Remark A.0.13.* In Example A.0.12, the LR-rule 2 is not verified for  $p \geq 2$  as the spline space on the split to insert in the underlying tensor mesh has dimension zero for  $p \geq 2$ .

## References

- [1] Pettersen, K. F. “On the dimension of multivariate spline spaces”. In: *SINTEF Report A23875* (2013).

# Appendix B

## B-splines

In this appendix we define univariate and bivariate B-splines and their basic properties. We further recall the knot insertion algorithm, which is used for the definition of the LR B-splines, and the Curry-Schoenberg Theorem. This latter guarantees that the B-splines defined on a spline sequence form a basis for the spline space on it. This introduction is far from a complete overview on the B-spline theory. The reader interested in this topic is referred to the classical books [2] and [3].

### B.0.1 Univariate B-splines

**Definition B.0.1.** For a non-decreasing sequence  $\mathbf{t} = (t_1, t_2, \dots, t_{p+2})$  we define a B-spline  $B[\mathbf{t}] : \mathbb{R} \rightarrow \mathbb{R}$  of degree  $p \geq 0$  recursively by

$$B[\mathbf{t}](t) = \frac{t - t_1}{t_{p+1} - t_1} B[t_1, \dots, t_{p+1}](t) + \frac{t_{p+2} - t}{t_{p+2} - t_2} B[t_2, \dots, t_{p+2}](t), \quad (\text{B.1})$$

where each time a fraction with zero denominator appears, it is taken as zero. The initial B-splines of degree 0 on  $\mathbf{t}$  are defined as

$$B[t_i, t_{i+1}](t) := \begin{cases} 1 & \text{if } t_i \leq t < t_{i+1}; \\ 0 & \text{otherwise;} \end{cases} \quad \text{for } i = 1, \dots, p+1. \quad (\text{B.2})$$

The sequence  $\mathbf{t}$  is called knot vector of  $B[\mathbf{t}]$  and its elements are called knots.

By using

$$\omega_{i,p}(t) = \frac{t - t_i}{t_{i+p} - t_i},$$

we can rewrite (B.1) as

$$B[\mathbf{t}](t) = \omega_{1,p}(t) B[t_1, \dots, t_{p+1}](t) + (1 - \omega_{2,p}(t)) B[t_2, \dots, t_{p+2}](t)$$

and by iterating the recurrence relation,

$$\begin{aligned} B[\mathbf{t}] &= \omega_{1,p}(t) \omega_{1,p-1}(t) B[t_1, \dots, t_p](t) + \omega_{1,p}(t) (1 - \omega_{2,p-1}(t)) B[t_2, \dots, t_{p+1}](t) \\ &\quad + (1 - \omega_{2,p}(t)) \omega_{2,p-1}(t) B[t_2, \dots, t_{p+1}](t) \\ &\quad + (1 - \omega_{2,p}(t)) (1 - \omega_{3,p-1}(t)) B[t_3, \dots, t_{p+2}](t) \\ &= \dots = \prod_{j=0}^{p-1} \omega_{1,p-j}(t) B[t_1, t_2](t) + \prod_{j=0}^{p-1} (1 - \omega_{j+2,p-j}(t)) B[t_{p+1}, t_{p+2}](t) \end{aligned}$$

Therefore, the coefficient of every  $B[t_i, t_{i+1}](t)$  is a polynomial in  $\Pi_p$  and it is positive on  $[t_i, t_{i+1})$ . From the above expansion we derive the following basic B-splines properties:

## B. B-splines

---

- $B[\mathbf{t}]$  restricted to any non-empty interval  $[t_i, t_{i+1})$  is a polynomial in  $\Pi_p$ ,
- $B[\mathbf{t}]$  is nonnegative,
- $B[\mathbf{t}]$  has compact (or local) support,  $\text{supp } B[\mathbf{t}] = [t_1, t_{p+2}]$ .

Given a B-spline  $B[\mathbf{t}]$  of degree  $p$ , we say that a knot  $t_j \in \mathbf{t}$  has multiplicity  $\mu(t_j)$  if it appears  $\mu(t_j)$  times in  $\mathbf{t}$ . We always assume that  $\mu(t_j) \leq p + 1$  for every  $j$  to ensure that the B-spline support is non-empty.

The next results yield two other fundamental B-splines properties: the polynomial reproduction and the partition of unity. These are guaranteed for the B-splines defined on open spline sequences.

**Definition B.0.2.** Given a spline sequence,  $\mathbf{t}_p = (t_1, \dots, t_{p+r+1})$ , for some  $r \geq 1$ , the **B-splines of degree  $p$  defined on  $\mathbf{t}_p$**  are the B-splines defined on the  $r$  knot vectors provided by taking subcollections of  $p + 2$  consecutive elements in  $\mathbf{t}_p$ ,  $B[\mathbf{t}_p^i]$  with  $\mathbf{t}_p^i = (t_i, \dots, t_{i+p+1}) \subseteq \mathbf{t}_p$ , for  $i = 1, \dots, r$ .

**Lemma B.0.3** ([2, page 95]). *Let  $\mathbf{t}_p = (t_1, \dots, t_{p+r+1})$  for  $r \geq 1$  be an open spline sequence and let  $B[\mathbf{t}_p^i]$  for  $i = 1, \dots, r$  be the B-splines of degree  $p$  defined on  $\mathbf{t}_p$ . Then*

$$(t - a)^p = \sum_{i=1}^r \psi_{i,p}(a) B[\mathbf{t}_p^i](t) \quad a \in \mathbb{R}, t \in \bigcup_{i=1}^r \text{supp } B[\mathbf{t}_p^i] \quad (\text{B.3})$$

where  $\psi_{i,0}(a) := 1$  and  $\psi_{i,p}(a) := (t_{i+1} - a) \cdots (t_{i+p} - a)$ , for  $p \geq 1$ .

The polynomial  $\psi_{i,p}$  is sometimes called dual polynomial of the B-spline  $B[\mathbf{t}_p^i]$ . By dividing by  $p!$  and deriving  $m$  times  $\psi_{i,p}$ , from (B.3) we get

$$(-1)^m \frac{(t - a)^{p-m}}{(p - m)!} = \sum_{i=1}^r D^m \psi_{i,p}(a) \frac{1}{p!} B[\mathbf{t}_p^i](t). \quad (\text{B.4})$$

Equation (B.4) is called Marsden's identity. Let  $q \in \Pi_p$ . Then the Taylor expansion of it at  $a$  is

$$q(t) = \sum_{m=0}^p \frac{(t - a)^{p-m}}{(p - m)!} D^{p-m} q(a) = \sum_{m=0}^p \sum_{i=1}^r D^m \psi_{i,p}(a) \frac{(-1)^m}{p!} D^{p-m} q(a) B[\mathbf{t}_p^i](t)$$

and therefore

$$q(t) = \sum_{i=1}^r \Lambda_{i,p}(q) B[\mathbf{t}_p^i](t) \quad t \in \bigcup_{i=1}^r \text{supp } B[\mathbf{t}_p^i] \quad (\text{B.5})$$

where

$$\Lambda_{i,p}(q) = \sum_{m=0}^p \frac{(-1)^m}{p!} D^m \psi_{i,p}(a) D^{p-m} q(a).$$

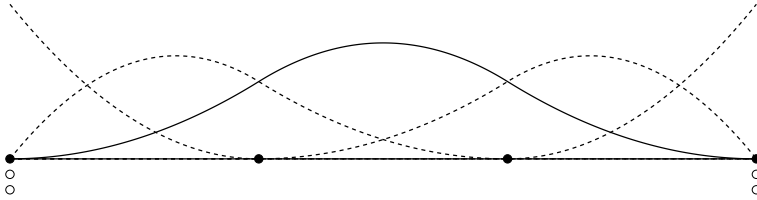


Figure B.1: The B-spline basis of  $\mathbb{S}(\mathbf{t}_2)$  (solid) and of  $\mathbb{S}(\tilde{\mathbf{t}}_2)$  (solid and dashed).

Equation (B.5) provides the representation of any polynomial in  $\Pi_p$  in terms of B-splines of degree  $p$ . In particular, by considering  $q(t) \equiv 1$  and observing that  $\Lambda_{i,p}(1) = 1$  for all  $i$ , we get the following partition of unity:

$$1 = \sum_{i=1}^r B[\mathbf{t}_p^i](t) \quad t \in \bigcup_{i=1}^r \text{supp } B[\mathbf{t}_p^i]. \quad (\text{B.6})$$

The next result is the Curry-Schoenberg Theorem. It guarantees that the B-splines defined on an open spline sequence  $\mathbf{t}_p$  form a basis of the spline space  $\mathbb{S}(\mathbf{t}_p)$ .

**Theorem B.0.4** (Curry-Schoenberg [2, page 97]). *Let  $\mathbf{t}_p = (t_1, \dots, t_{p+r+1})$  for  $r \geq 1$  be an open spline sequence. Then the B-splines of degree  $p$  on  $\mathbf{t}_p$ ,  $\{B[\mathbf{t}_p^i]\}_{i=1}^r$  with  $\mathbf{t}_p^i = (t_i, \dots, t_{i+p+1}) \subseteq \mathbf{t}_p$ , form a basis for the spline space  $\mathbb{S}(\mathbf{t}_p)$ .*

This theorem can be extended to general spline sequences, not necessarily open. Let  $\mathbf{t}_p$  be a spline sequence and let  $\tilde{\mathbf{t}}_p$  be the corresponding open spline sequence given by duplicating the first and last element of  $\mathbf{t}_p$  enough times. Since  $\mathbf{t}_p \subseteq \tilde{\mathbf{t}}_p$ , we have  $\mathbb{S}(\mathbf{t}_p) \subseteq \mathbb{S}(\tilde{\mathbf{t}}_p)$ . Let  $\mathcal{B} = \{B[\tilde{\mathbf{t}}_p^i]\}_i$  be the B-spline basis of  $\mathbb{S}(\tilde{\mathbf{t}}_p)$ . Then a basis for  $\mathbb{S}(\mathbf{t}_p)$  is composed by the B-splines in  $\mathcal{B}$  that have knot vector in  $\mathbf{t}_p$ . Indeed, such B-splines are contained in  $\mathbb{S}(\mathbf{t}_p)$  and are linearly independent because they are elements of the basis  $\mathcal{B}$  and their number is equal to  $\dim \mathbb{S}(\mathbf{t}_p)$ , by definition of the knot vectors  $\mathbf{t}_p^i \subseteq \mathbf{t}_p$ . This procedure is illustrated in Figure B.1. Here we consider degree  $p = 2$  and a spline sequence  $\mathbf{t}_2$  of 4 elements (black dots). By Theorem 1.1.3,  $\dim \mathbb{S}(\mathbf{t}_2) = 4 - (2 + 1) = 1$ . The corresponding open spline sequence  $\tilde{\mathbf{t}}_2$  is composed of 8 elements: the four of  $\mathbf{t}_2$  with the first and the last repeated  $p + 1 = 3$  times (black and white dots). The dimension of  $\mathbb{S}(\tilde{\mathbf{t}}_2)$  is equal to 5 and its B-spline basis  $\mathcal{B}$  is represented in the figure (both the dashed and solid B-spline plots). The B-spline spanning the spline space on the original spline sequence  $\mathbf{t}_2$  is the B-spline drawn with a solid line.

Given a spline sequence  $\mathbf{t}_p = (t_1, \dots, t_{p+r+1})$ , let  $\{B[\mathbf{t}_p^i]\}_{i=1}^r$  be the B-splines of degree  $p$  defined on  $\mathbf{t}_p$ . They are basis for  $\mathbb{S}(\mathbf{t}_p)$  by the Curry-Schoenberg Theorem. In particular, on any non-empty interval  $[t_\ell, t_{\ell+1})$  we have

$$\text{span} \{B_{\ell-p}, \dots, B_\ell\}_{|[t_\ell, t_{\ell+1})} \equiv \Pi_p|_{|[t_\ell, t_{\ell+1})},$$

and so all non-vanishing B-splines defined on  $[t_\ell, t_{\ell+1})$  are linearly independent. This is enough to state that the B-splines on  $\mathbf{t}_p$  are locally linearly independent.

**Corollary B.0.5.** *Given a spline sequence  $\mathbf{t}_p$ , the B-splines of degree  $p$  defined on  $\mathbf{t}_p$  are locally linearly independent.*

Furthermore, given the knot vector  $\mathbf{t} = (t_1, \dots, t_{p+2})$  of a B-spline  $B[\mathbf{t}]$  of degree  $p$ , let  $t_{i_1}, \dots, t_{i_r}$  be the distinct knots in  $\mathbf{t}$ . Define the spline sequence  $\boldsymbol{\tau}_p^\mu$  by setting  $\boldsymbol{\tau} = (\tau_1 = t_{i_1}, \dots, \tau_r = t_{i_r})$  and the multiplicities  $\mu(\tau_\ell)$  equal to the number of times  $t_{i_\ell}$  appears in  $\mathbf{t}$ , for  $\ell = 1, \dots, r$ . Then the Curry-Schoenberg Theorem shows that  $B[\mathbf{t}]$  is  $C^{p-\mu(t_{i_\ell})}$ -continuous at  $t_{i_\ell}$  for  $\ell = 1, \dots, r$ .

We conclude this section by recalling knot insertion. Given a spline sequence  $\mathbf{t}_p = (t_1, \dots, t_{p+r+1})$  and a value  $\hat{t} \in (t_1, t_{p+r+1})$ , consider the refined spline sequence  $\mathbf{t}_p \cup \{\hat{t}\} = \hat{\mathbf{t}}_p$ . This is a sequence of  $p + r + 2$  elements. Let  $\mathcal{B}$  and  $\hat{\mathcal{B}}$  be the B-spline bases of  $\mathbb{S}(\mathbf{t}_p)$  and  $\mathbb{S}(\hat{\mathbf{t}}_p)$  respectively. Since  $\mathbf{t}_p \subseteq \hat{\mathbf{t}}_p$ , we have  $\mathbb{S}(\mathbf{t}_p) \subseteq \mathbb{S}(\hat{\mathbf{t}}_p)$  and in particular all the B-splines in  $\mathcal{B}$  can be expressed as a linear combination of the B-splines in  $\hat{\mathcal{B}}$ . Knot insertion provides the coefficients for these expressions.

**Theorem B.0.6** (knot insertion, [1, page 200]). *Given a B-spline of degree  $p$ ,  $B[\mathbf{t}]$ , defined on the knot vector  $\mathbf{t} = (t_1, \dots, t_{p+2})$ , and a value  $\hat{t} \in (t_1, t_{p+2})$ , suppose we insert  $\hat{t}$  in  $\mathbf{t}$ . Then, we obtain two knot vectors  $\mathbf{t}_1$  and  $\mathbf{t}_2$  considering the first and last  $p + 2$  consecutive elements in the non-decreasing sequence  $\hat{\mathbf{t}} = \mathbf{t} \cup \{\hat{t}\}$ . Then*

$$B[\mathbf{t}] = \alpha_1 B[\mathbf{t}_1] + \alpha_2 B[\mathbf{t}_2]$$

with  $\alpha_1, \alpha_2 \in (0, 1]$  provided by

$$\alpha_1 = \begin{cases} 1, & \hat{t} \in [t_{p+1}, t_{p+2}) \\ t - t_1 / t_{p+1} - t_1, & \hat{t} \in (t_1, t_{p+1}) \end{cases} \quad \alpha_2 = \begin{cases} 1, & \hat{t} \in (t_1, t_2] \\ t_{p+2} - t / t_{p+2} - t_2, & \hat{t} \in (t_2, t_{p+2}). \end{cases} \quad (\text{B.7})$$

## B.0.2 Bivariate B-splines

**Definition B.0.7.** Consider a bidegree  $\mathbf{p} = (p_1, p_2)$  and let  $\mathbf{x} = (x_1, \dots, x_{p_1+2})$  and  $\mathbf{y} = (y_1, \dots, y_{p_2+2})$  be nondecreasing sequences. We define the **bivariate B-spline**  $B[\mathbf{x}, \mathbf{y}] : \mathbb{R}^2 \rightarrow \mathbb{R}$  by

$$B[\mathbf{x}, \mathbf{y}](x, y) := B[\mathbf{x}](x)B[\mathbf{y}](y), \quad (\text{B.8})$$

where  $B[\mathbf{x}]$  and  $B[\mathbf{y}]$  are the univariate B-splines defined on  $\mathbf{x}$  and  $\mathbf{y}$  respectively.

By their definition, the properties of the univariate B-splines are conserved by the bivariate B-splines:

- $B[\mathbf{x}, \mathbf{y}]$  is a piecewise bivariate polynomial of bidegree  $\mathbf{p}$ ,
- $B[\mathbf{x}, \mathbf{y}]$  is nonnegative,
- $B[\mathbf{x}, \mathbf{y}]$  has compact (local) support,  $\text{supp } B[\mathbf{x}, \mathbf{y}] = [x_1, x_{p_1+2}] \times [y_1, y_{p_2+2}]$ .

**Definition B.0.8.** Given a tensor spline mesh  $\mathcal{N} = \mathcal{N}[\mathbf{x}_{p_1}, \mathbf{y}_{p_2}]$ , with  $\mathbf{x}_{p_1} = (x_1, \dots, x_{p_1+r_1+1})$  and  $\mathbf{y} = (y_1, \dots, y_{p_2+r_2+1})$ , the **B-splines defined on  $\mathcal{N}$**  are the bivariate B-splines

$$\{B[\mathbf{x}_{p_1}^i, \mathbf{y}_{p_2}^j]\}_{i,j} \quad \text{with } i = 1, \dots, r_1 \text{ and } j = 1, \dots, r_2,$$

where  $\mathbf{x}_{p_1}^i = (x_i, \dots, x_{i+p_1+1}) \subseteq \mathbf{x}_{p_1}$  and  $\mathbf{y}_{p_2}^j = (y_j, \dots, y_{j+p_2+1}) \subseteq \mathbf{y}_{p_2}$ .

It is then clear, by applying equations (B.5) and (B.6) respectively, that, given an open tensor spline mesh  $\mathcal{N}$ , the bivariate B-splines defined on  $\mathcal{N}$  reproduce the polynomials in  $\Pi_{\mathbf{p}}$  and sum to one.

Furthermore, by the Curry-Schoenberg Theorem, given any tensor spline mesh  $\mathcal{N} = (\mathcal{M}, \mu, \mathbf{p})$ , the B-splines defined on  $\mathcal{N}$  form a basis of  $\mathbb{S}(\mathcal{N})$  and are locally linearly independent. Moreover, we recall that, given a bivariate B-spline  $B[\mathbf{x}, \mathbf{y}]$ , its knot vectors  $\mathbf{x}, \mathbf{y}$  identify a tensor spline mesh  $\mathcal{N}[\mathbf{x}, \mathbf{y}] = (\mathcal{M}[\mathbf{x}, \mathbf{y}], \mu[\mathbf{x}, \mathbf{y}], \mathbf{p})$  where the splits of  $\mathcal{M}[\mathbf{x}, \mathbf{y}]$  are defined by the distinct knots in  $\mathbf{x}$  and  $\mathbf{y}$  and the multiplicity function  $\mu[\mathbf{x}, \mathbf{y}]$  by the times these distinct knots appear in the sequences, see the beginning of Section 1.2 in the Introduction. Then, again by the Curry-Schoenberg Theorem,  $B[\mathbf{x}, \mathbf{y}]$  is  $C^{p_k - \mu(\gamma)}$ -continuous across any  $k$ -meshline  $\gamma$  in  $\mathcal{M}[\mathbf{x}, \mathbf{y}]$ .

Finally, as in the univariate case, after the insertion of a knot  $\hat{x}$  in  $\mathbf{x}$ , we define  $\mathbf{x}_1$  and  $\mathbf{x}_2$  considering in  $(x_1, \dots, \hat{x}, \dots, x_{p_1+2})$  the first and last  $p_1 + 2$  knots respectively, and we can write  $B[\mathbf{x}, \mathbf{y}]$  in terms of the two B-splines defined on the two new pairs of knot vectors

$$B[\mathbf{x}, \mathbf{y}] = \alpha_1 B[\mathbf{x}_1, \mathbf{y}] + \alpha_2 B[\mathbf{x}_2, \mathbf{y}] \quad (\text{B.9})$$

with  $\alpha_1, \alpha_2 \in (0, 1]$  provided by (B.7). The same holds when inserting a knot  $\hat{y}$  in  $\mathbf{y}$ .

## References

- [1] Boehm, W. "Inserting new knots into B-spline curves". In: *Computer-Aided Design* vol. 12, no. 4 (1980), pp. 199–201.
- [2] de Boor, C. *A Practical Guide to Splines*. revised. Springer-Verlag New York, 2001.
- [3] Schumaker, L. L. *Spline Functions: Basic Theory*. third. Cambridge University Press, 2007.